FINAL REPORT

SOLAR CELL CONTACT DEVELOPMENT

Contract No. NAS 5-11595

Prepared by:

Space and Defense Products Department
3M Company
St. Paul, Minnesota 55101

for

Goddard Space Flight Center

Greenbelt, Maryland

FINAL REPORT
SOLAR CELL CONTACT DEVELOPMENT
28 June 1968 - 28 June 1969

and

1 January 1970 - 1 March 1970

Contract No.: NAS 5-11595
Goddard Space Flight Center

Prepared by:

Space and Defense Products Department
3M Company
St. Paul, Minnesota 55101
Project Manager: Richard Jacobson

Authors:

R. L. Jacobson
G. S. Anderson

for

Goddard Space Flight Center
Greenbelt, Maryland

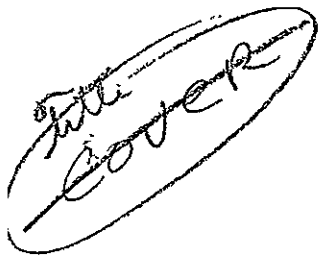

SUMMARY

This report presents the results of work performed under research contract No. NAS 5-11595 during the period 28 June 1968 through 28 June 1969 and during a 2-month extension of this contract from 1 January 1970 through 1 March 1970 for NASA-Goddard Space Flight Center, Greenbelt, Maryland. Contract objectives were twofold: (1) to identify the cause of Ti/Ag contact degradation as observed on Si solar cells currently in use, and (2) to determine whether contact deposition by sputtering is compatible with present solar cell configurations.

Contract work during the first and second quarters was directed at the problem of contact degradation. Degradation was characterized by examining a number of degraded cells. The results of this study strongly suggested that contacts degrade by diffusion of corrosive species through the Ag overlayer with the eventual corrosion of the underlying layer of Ti. The general porosity of thin Ag films was demonstrated by exposing Ti/Ag contacts to various corrosive environments. Also, the effectiveness of various environments in producing contact degradation was qualitatively evaluated. In addition to water vapor, which was previously known to degrade contacts, environments included oxygen at elevated temperatures, electrolytes of NaOH, KOH, and NaCl, and vapors of HCl, HF, and Cl_2. This work clearly demonstrated that these corrosive species are capable of penetrating through thin Ag films at normal temperatures and, furthermore, Ti/Ag contact degradation proceeds rapidly when their concentration is high.

In a later phase of this contract, sputtering was applied to the deposition of Ti/Ag and Ti-Pt/Ag contacts onto Si wafers and the properties of these contacts were evaluated. Finally, Ti/Ag and Ti-Pt/Ag contacts were sputter deposited onto Si solar cell blanks. Initial attempts were unsuccessful in preparing durable contacts. However, modifications in cell blank cleaning procedures resulted in the successful preparation of 40 cells for evaluation by NASA-Goddard. Limited tests conducted in our laboratory have indicated the importance of prefiring cell blanks in forming gas just prior to the deposition of cell contacts. This predeposition treatment gave highly durable contacts by sputtering and were significantly more resistant to degradation in a high humidity/temperature environment. Prefiring apparently removes residual impurities which otherwise remain on the cell blank and subsequently enhance the degradation process. Sputtered contacts are believed to be at least equal to, if not better than, conventional evaporated contacts in regard to degradation in a high humidity/temperature environment.

TABLE OF CONTENTS

LIST OF ILLUSTRATIONS

SECTION I

Introduction

A serious problem currently experienced with conventional Si solar cells which use vacuum evaporated Ti/Ag contacts is the degradation in power output with storage time. Degradation has been attributed to a deterioration of the Ti/Ag contacts. Contacts frequently lose their initially high bond strength and electrical continuity to the cell with the result that the internal resistance of the cell is increased. Catastrophic failure has at times occurred when contacts literally separate from the cell. This problem is aggravated by stresses exerted by cell interconnections and thermal cycling. Degradation generally is found to be a slow process under normal environmental conditions and not all cells degrade to the same extent. An accelerated degradation test, developed at Goddard Space Flight Center, consists of exposing cells to a high humidity and temperature environment. This environment can produce contact degradation in a period of several weeks. Significantly, degradation is known to be much more pronounced for the solderless Ti/Ag cell than for the solder-coated Ti/Ag cell.[1] Yet, the solderless cell has several advantages over the solder-coated cell such as a wider temperature excursion capability and lower weight. Hence, it is important to understand the physical or chemical mechanism of contact degradation with the goal of reducing or possibly eliminating the degradation problem altogether. This was one of the objectives of this research program. A second objective was to prepare Ti/Ag and possibly other contact systems by sputtering the contact material in a noble gas discharge of argon. The purpose of this work was to develop an improved contact. It was important in this connection to determine whether or not sputtering is a feasible process for applying contacts to Si solar cells using established solar cell fabrication procedures.

Recent work was directed at sputter depositing contacts to Si and this subject is treated in Section II. Here, the physical properties, electrical characteristics, and corrosion behavior of these contacts are given. Sputtering was later applied to the fabrication of Si solar cells and the results are given in Section III. Serious problems were encountered in our initial attempts to prepare durable contacts and our approach to solve these problems is described. Also, typical I-V characteristics and contact degradation results in a water vapor environment are presented. Section IV summarizes

the main findings of our degradation studies on evaporated Ti/Ag contacts and these results are discussed in terms of various degradation mechanisms. Finally, the main results of this program are summarized in Section V and some recommendations in regard to solutions to contact degradation are given.

SECTION II

Contact Deposition by Sputtering

Introduction

Our approach to the deposition of contacts by sputtering consisted of first depositing Ti/Ag and Ti-Pt/Ag contacts onto n- and p-type Si wafers having resistivities similar to those used for Si solar cells. These contacts were subsequently characterized before solar cells were fabricated using sputtering. It should be noted that the limited time precluded a detailed investigation various sputtering parameters have on contact properties and the eventual optimization of the sputtering process.

The "triode" system of sputtering was used throughout this work. A schematic of the initial 8 in. system is given in Figure 1. Ti/Ag contacts were prepared by sequentially sputtering Ti and Ag in an Ar plasma supported by a tungsten thermionic cathode as described previously.(2) Ar pressure was in the 2 to 3 micron range. Ti-Pt/Ag contacts were similarly prepared except for the addition of approximately 1% Pt to Ti. Pt was simultaneously sputtered with Ti by winding a Pt wire around the Ti target. The purpose of adding Pt was to note its effect on contact corrosion since even small quantities are known to substantially reduce the reactivity of Ti.(3)

The sputtering procedure consisted of first exposing the Si substrates and targets to a general plasma scrub for times ranging from several minutes to one hour. Next, with the shutter protecting the substrates, each target was given a 5 to 10 min sputter cleaning treatment for the purpose of removing strongly adherent surface impurities. The shutter was then removed and a Ti film of from 500 to 1000 Å thick was deposited at a rate of ∿40 Å/min. Without interrupting the discharge, the target assembly was rotated 180° and an overlayer film of Ag was sputtered at a rate of ∿400 Å/min. No attempt was made to blend these two materials. Typical background pressure during sputtering was in the low 10^{-6} Torr range. The partial pressure of reactive gases such as oxygen is believed to be much less due to the strong gettering action of the discharge.

Initial Deposition Study

Contacts were initially deposited onto 1-1/4 in. diameter Si wafers and these contacts were evaluated in regard to adhesion, electrical characteristics, and corrosion behavior. Resistivity of the n-type wafers was ∿$10^{-3}\Omega$ -cm

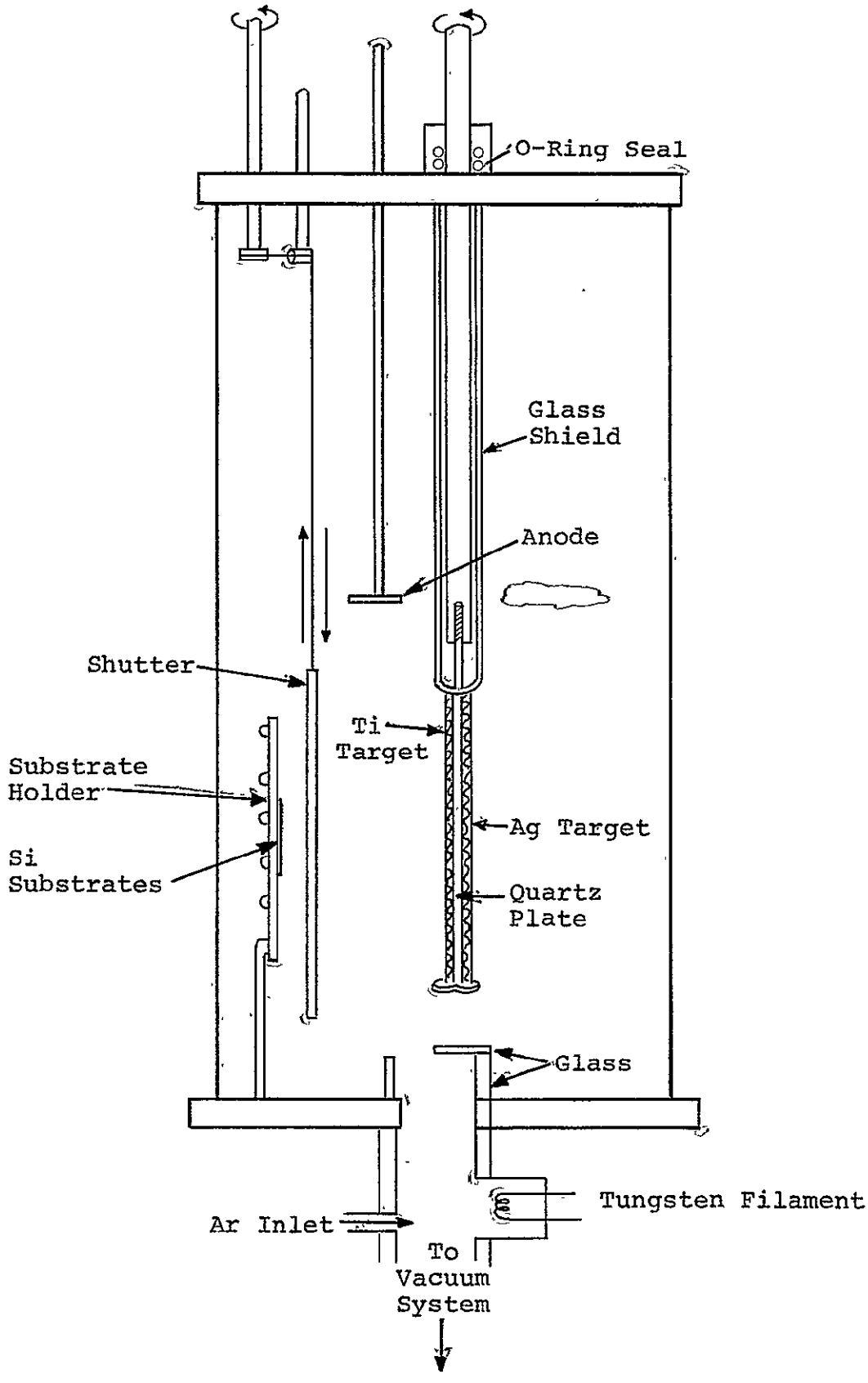

Figure 1 A schematic of the sputtering system

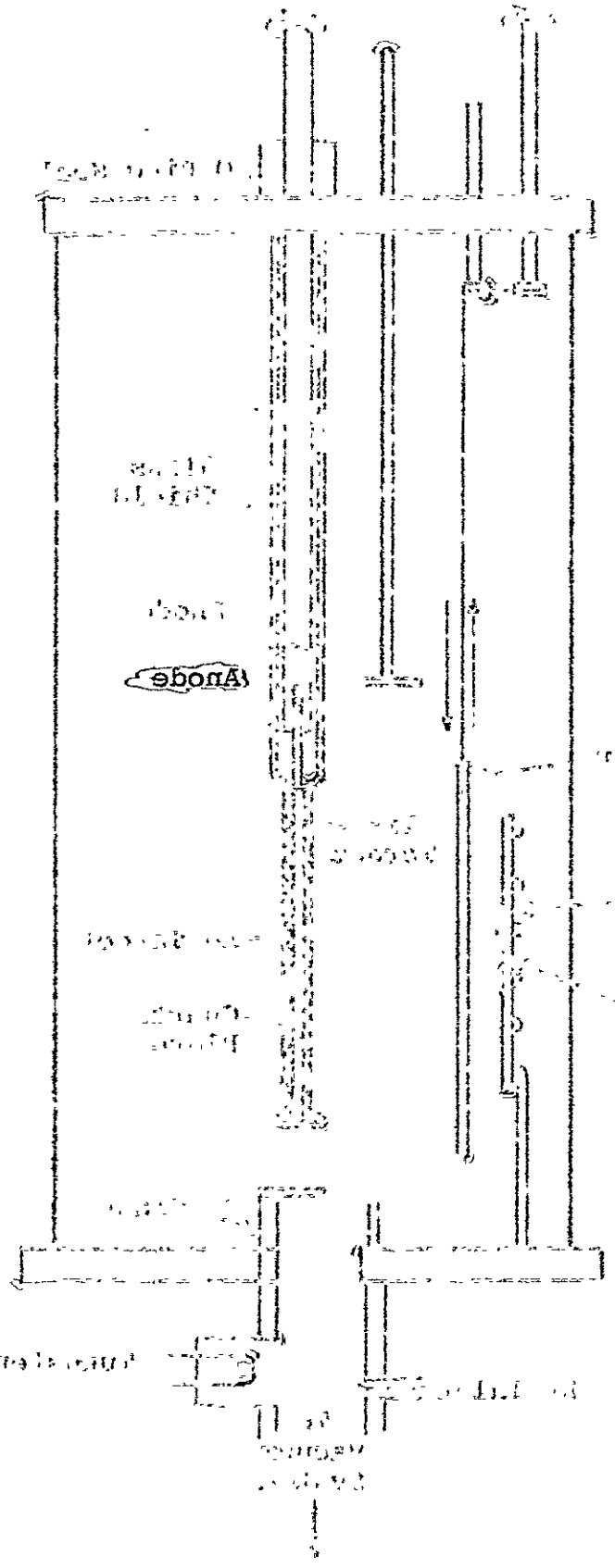
Anode

and p-type wafers, $\sim 1\ \Omega$-cm. Wafers were generally etched in concentrated HF acid, rinsed in distilled water, and blown dry with N_2 gas before mounting in the sputtering system. A tantalum mask was used to give approximately one dozen small area contacts in addition to one large area contact on each wafer as shown in Figure 2. It can be seen here that the nominally 3 mm diameter small area contacts were not always well-defined. Poor definiition results from material deposited under the mask and occurred when the mask was not in intimate contact with the Si wafer. Two factors are known to contribute to poor contact definition. First, the relatively large angle subtended by the sputtering target on the substrate produces a wide angular distribution of incident Ti and Ag atoms. Second, sputtered atoms have a certain probability of being scattered by the Ar plasma gas and results in further broadening the angular distribution. Gas scattering was evident from thin coatings that developed on surfaces not facing the target. Good contact definition was observed only when the mask made good contact to the Si wafers such as at the edge of the large area contact.

Current-voltage characteristics were measured between the large area contact and one of the various small area contacts. Two probes were placed on each contact, one carried the current while the second sampled the potential of the contact. This was done in order to exclude the resistance of probe wires and resistance appearing between the probe and contact. Voltage applied across the contacts was displayed on the x-axis of an x-y recorder and current on the y-axis. Typical I-V characteristics of contacts sputtered onto n- and p-type Si are shown in Figure 3. Both characteristics are non-ohmic or rectifying. Rectification is particularly strong in the case of p-type Si.

The d.c. equivalent circuit for the I-V characteristics is given by three resistance elements in series: namely, the resistance of the small area contact, the large area contact, and the resistance of the bulk Si separating the two contacts. Generally the bulk resistance was very small in comparison to contact resistance. The resistance of the large area contact can be neglected to a first approximation because its contact area is roughly 20 times greater than the small area contacts. Hence, the measured I-V characteristics principally reflect the electrical characteristics of small area contacts.

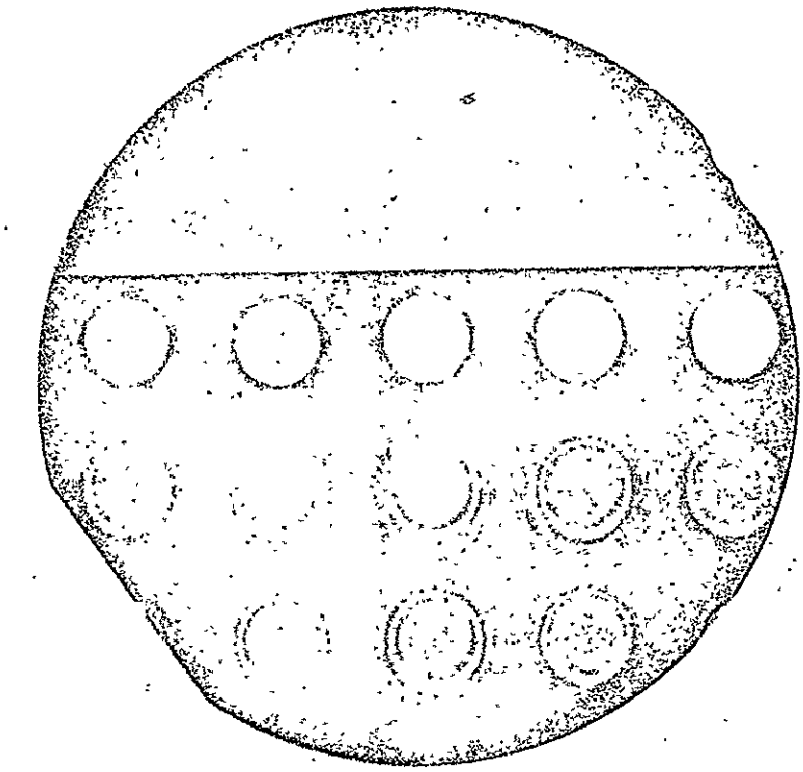

Figure 2 Si wafer with sputtered contacts

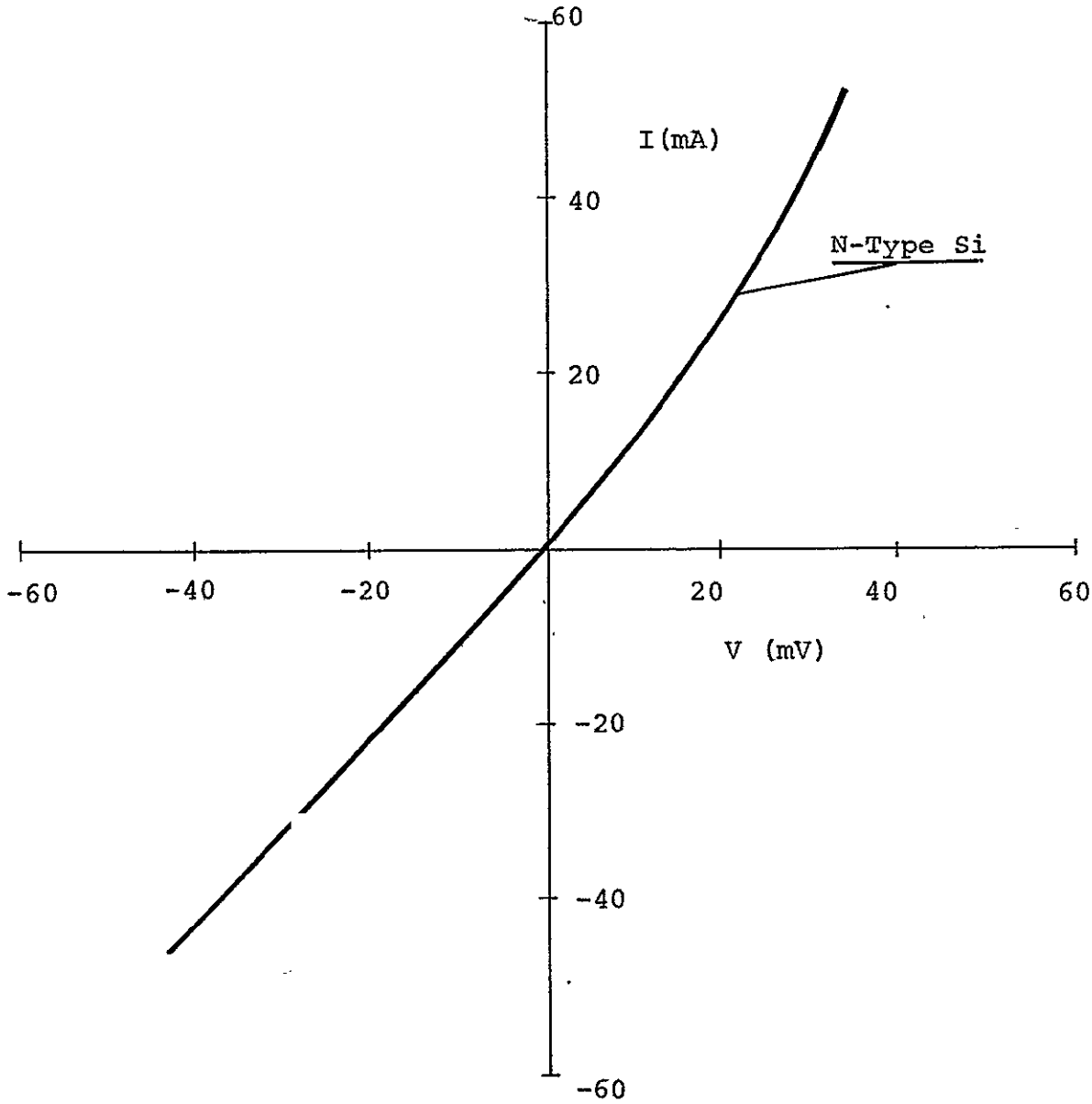

Figure 3 (a) Typical I-V characteristics of Ti/Ag contacts on n-type Si

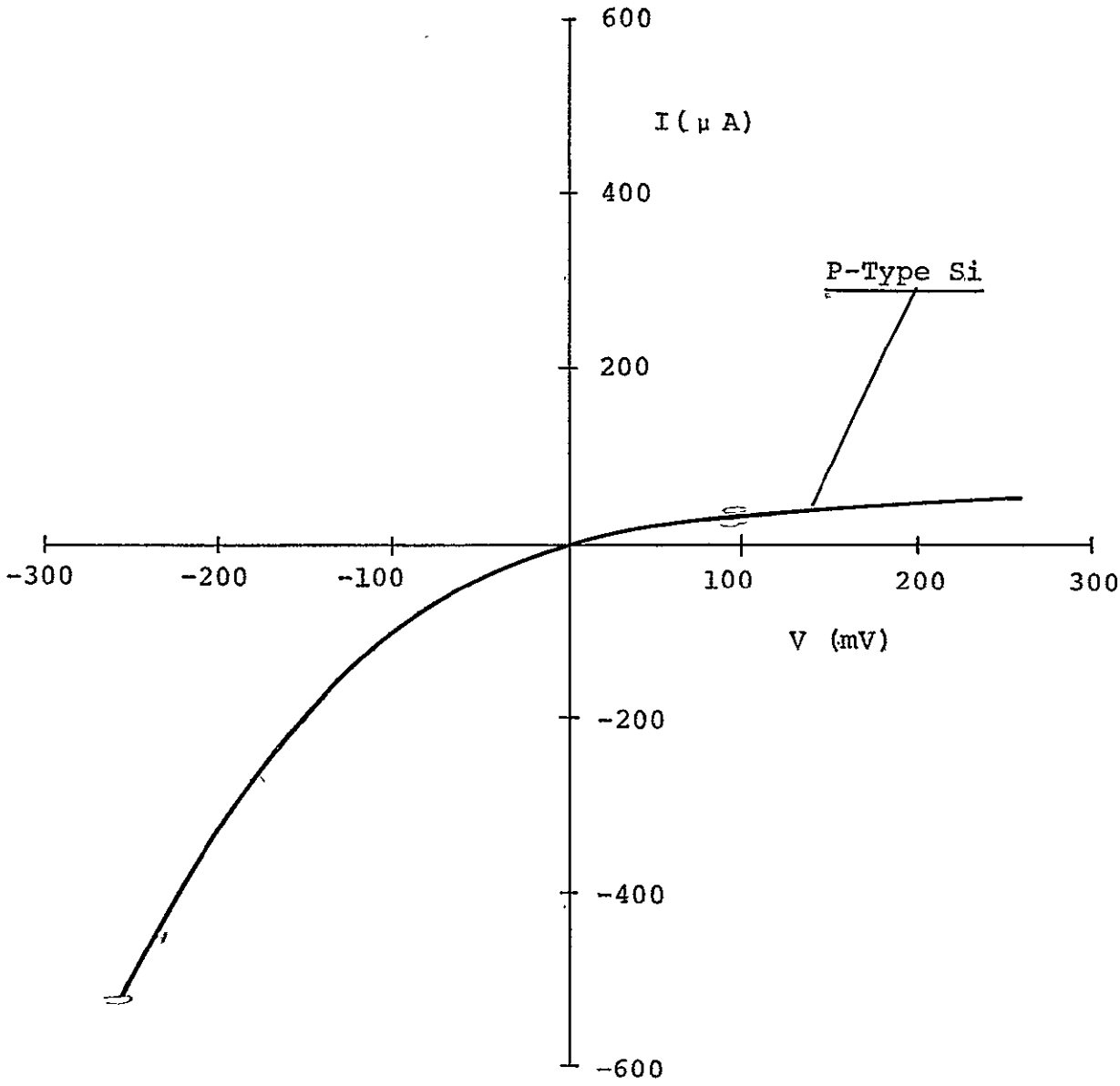

Figure 3 (b) Typical I-V characteristics of Ti/Ag contacts on p-type Si

Contact resistance in Ω cm^2 was derived from the slope of I-V characteristics at V = 0. These are listed in Table I along with other data of the various sputtering runs. Resistance values were obtained by averaging over a number of the small area contacts and normalizing to 1 cm^2.

It was assumed in these calculations that all contacts were 3 mm in diameter because of the inability to precisely measure contact area (due to poor contact definition). Resistance values of Table I then represent a lower limit of contact resistance while corrected values probably lie 20 to 30% higher. It is noted that resistance to n-type Si is generally in the 10^{-2} Ω cm^2 range while tens of ohm cm^2 for p-type material. Some consistent dependence of contact resistance on plasma scrub time for HF etched n-type wafers was observed and this is plotted in Figure 4. A long plasma exposure has the beneficial effect of reducing contact resistance to n-type Si. Although the data is limited, plasma exposure appears to have the opposite effect for p-type Si. These data suggest that plasma treatment has the effect of cleaning the Si surface by partially removing the ever-present Si oxide layer, in addition to weakly absorbed gases. It also suggests that even lower contact resistance values to n-type Si might result if the Si substrates were intentionally sputter cleaned just prior to contact deposition. Si wafers which were not precleaned by HF etching gave, with one exception, higher resistance values when compared to etched wafers of the same run.

Contact adhesion was checked by tape testing. Good adhesion was almost invariably observed except for some peeling at the periphery of some of the more poorly defined contacts. This region was just outside the area defined by the mask. Also, contact peeling occurred on several solar cell blanks which were included in Runs 5-22 and 6-10. This observation was not fully appreciated at the time, as will become evident below. More quantitative measurements of adhesion were attempted by soldering wires to contacts and measuring the tensile force required to remove the contact. Each time the Si substrate fractured before the Si contact interface failed. This occurred at a tensile force of approximately 20 kg/cm^2 and hence this value represents a lower limit to the actual adhesive strength of these contacts.

Some sputtered contacts on Si were heat treated in forming gas (85% N_2, 15% H_2) and also in Ar at 605°C for 10 min. These sintering treatments always reduced contact resistance to both n- and p-type Si and the I-V characteristics became

Table I

Contact Deposition Data and Contact Resistance Values

Run No.	Contact System	Si Resistivity and Type	Predeposition Treatment	Plasma Scrub Time	Contact Resistance Ω cm^2
5-12	Ti/Ag	0.001 Ω cm-N	HF Etched	20 min.	3.3×10^{-2} 3.5×10^{-2}
			None		2.7×10^{-2} 6.0×10^{-2}
5-13	Ti/Ag	0.001 Ω cm-N	HF Etched	14 min.	4.7×10^{-2} 5.8×10^{-2}
			None		2.3×10^{-1} 7.6×10^{-2}
5-22	Ti/Ag	0.001 Ω cm-N	HF Etched	10 min.	2.0×10^{-1} 9.4×10^{-2}
		1 Ω cm-P	HF Etched		2.8×10^{1}
6-7	Ti-Pt/Ag	0.001 Ω cm-N	HF Etched	14 min.	6.0×10^{-2} 2.1×10^{-2}
6-10	Ti-Pt/Ag	0.001 Ω cm-N	HF Etched	67 min.	5.2×10^{-3} 7.7×10^{-3}
		1 Ωcm-P	HF Etched		1.4×10^{2}

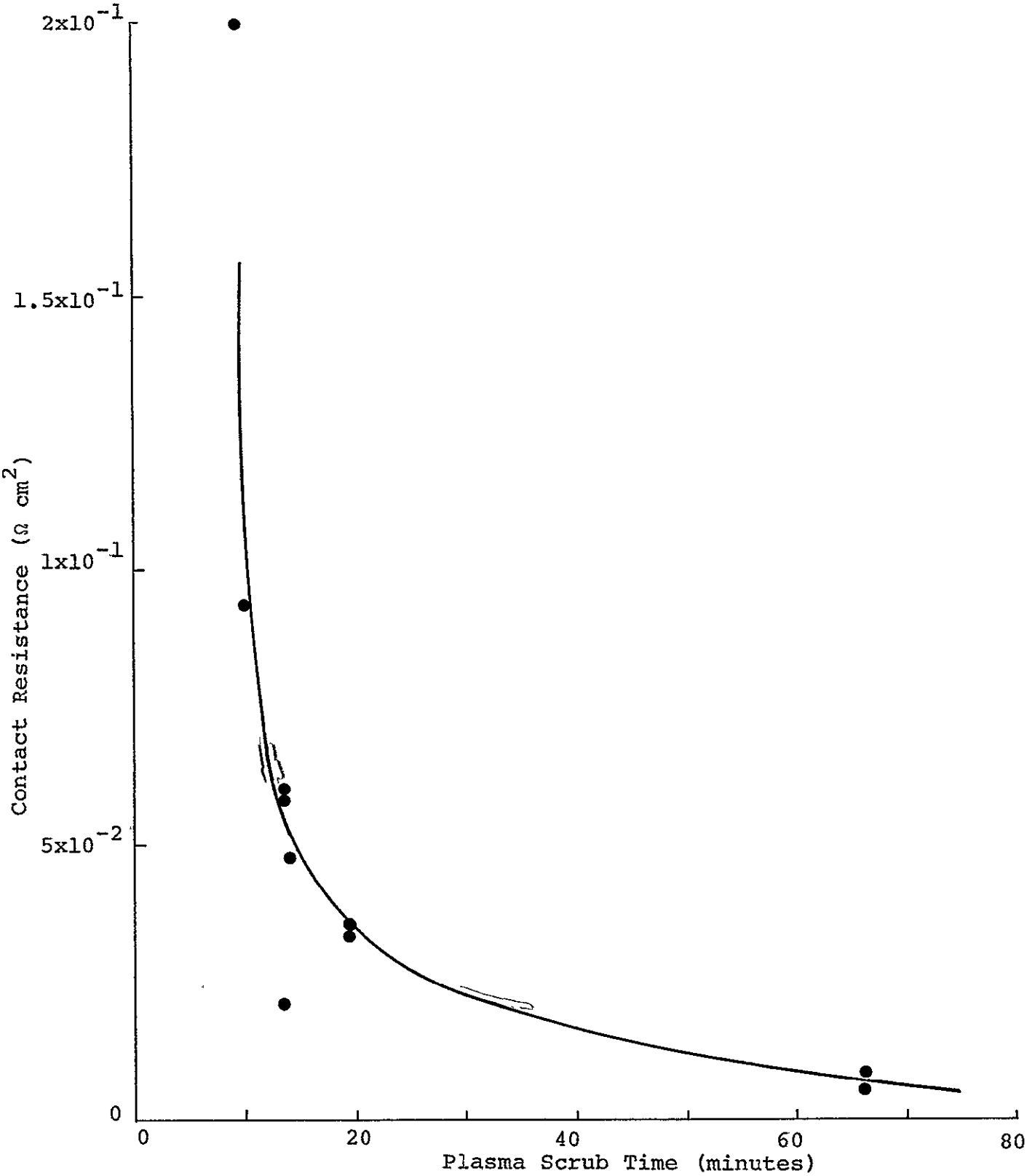

Figure 4 Dependence of contact resistance on plasma exposure time for n-type Si

linear. For n-type material, the contact resistance became negligible in comparison to the resistance of the bulk Si separating the contacts. It can therefore be concluded that contact resistance to n-type Si became substantially less than 2.5×10^{-3} Ω cm^2. Resistance to p-type material of Run 6-10 decreased on sintering to 9 Ω cm^2. This is roughly a factor of 20 less than the unsintered contacts.

Sintering had, on the other hand, a detrimental effect. Blisters frequently developed during the sintering process and occurred mainly at the periphery of some of the more poorly defined contacts. Some blisters nevertheless developed in the central region of contacts and these could not be attributed to poor contact definition. Also, some discoloration developed at the edge of poorly defined contacts. We suspected that some impurities in the sintering gas, such as oxygen or water vapor, produced these undesirable results. Yet, bulk Ti did not develop a visible oxide film under similar sintering conditions. Hence the discoloration is believed to be due to the reaction of Ti with the Si substrate, i.e., through the dissolution of a thin Si oxide layer.

Some sputtered contacts were exposed to water vapor at 70°C for the purpose of evaluating their susceptibility to degradation. Smaller samples were preparing having three small area contacts and a larger area end contact by scribing the above Si wafers. Contact resistance was determined from I-V characteristics after various exposure times. Results of water vapor exposure for an unsintered Ti/Ag contact of Run 5-12 are shown in Figure 5. Degradation is expressed by the ratio R_o/R where R_o is the contact resistance at t = o. The other two contacts from the same sample degraded similarly. It is evident that a one-week exposure seriously degraded these contacts.

Similar measurements were made for three samples prepared from one wafer of Run 5-13. In this case one sample each was placed in separate beakers containing ordinary tap water, distilled water, and high purity deionized water at 70°C. The degradation results are given in Table II. R_o is again the initial contact resistance and R_t is the resistance when the humidity tests were terminated after 3 weeks. The percentage increase in contact resistance is indicated in the right column and ranges from 5.6 to 16%. Note that the degradation was not as severe for these samples and that the amount of degradation depended, to some extent, on the purity of the water. This finding is believed to reflect the effect of impurities in the water on contact degradation since all samples were taken from the same wafer.

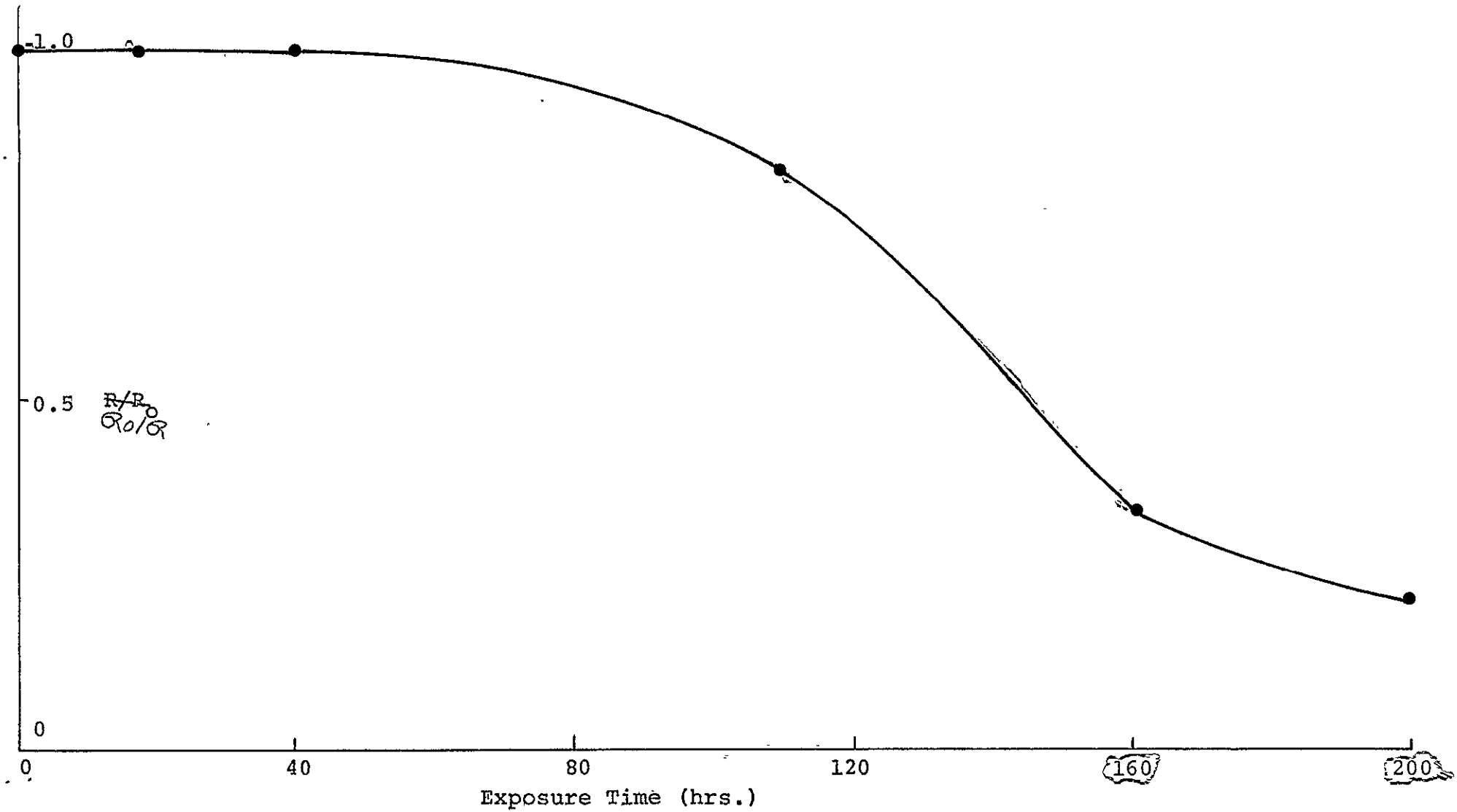

Figure 5 Degradation in contact resistance by high humidity/70°C temperature environment

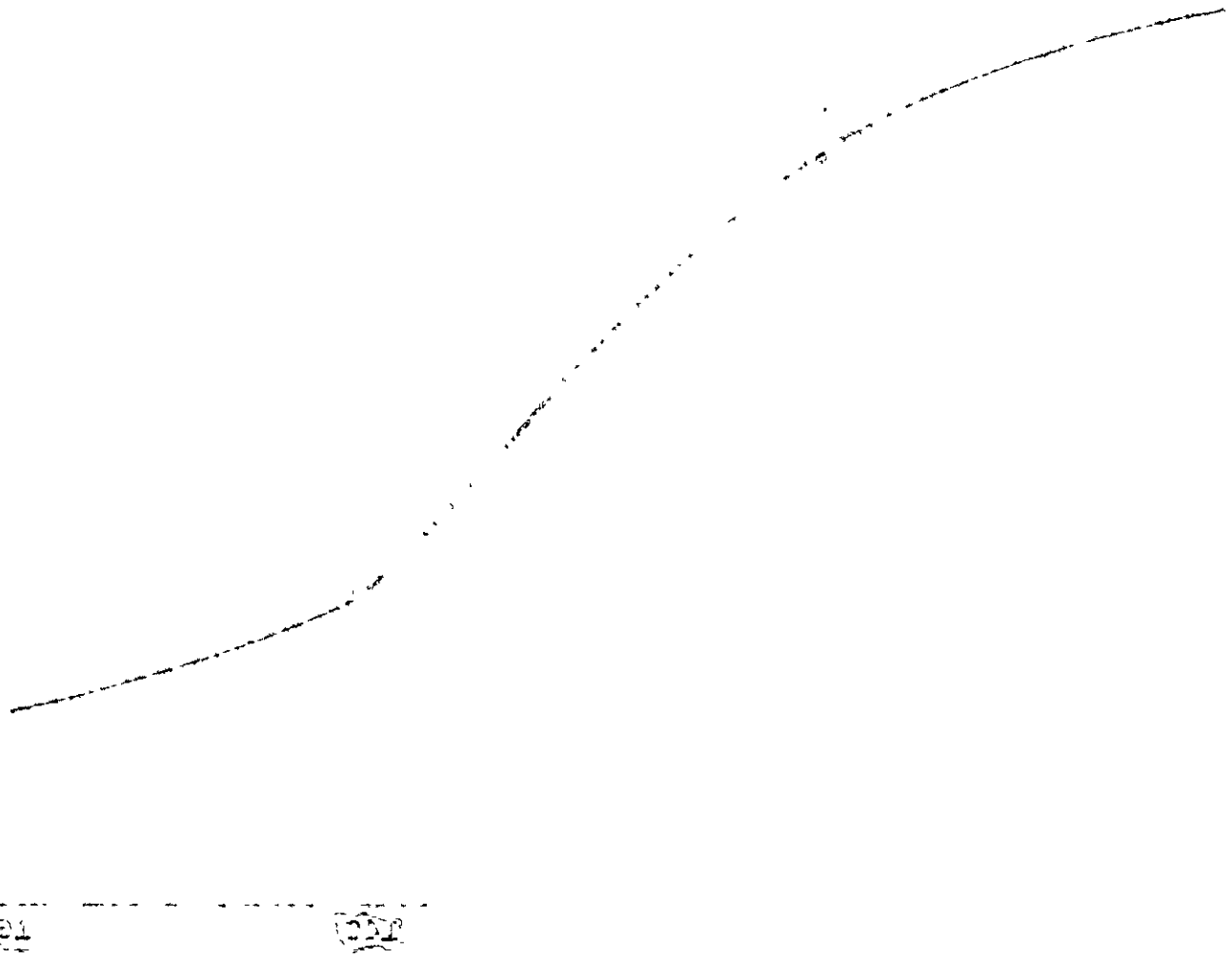

Table II

Ti/Ag Contact Degradation by Tap Water, Distilled Water, and Deionized Water

Environment	Contact No.	R_o (Ω)	R_t (Ω)	$\frac{(R_t-R_o)}{R_o} \times 100\%$
Tap Water Vapors	1	0.88	0.96	9%
	2	0.72	0.87	16%
	3	1.01	1.15	14%
Distilled Water Vapors	1	0.90	0.95	5.6%
	2	0.73	0.81	11%
	3	1.13	1.25	11%
Deionized Water Vapors	1	0.84	0.91	7.7%
	2	0.74	0.80	8.1%
	3	1.15	1.25	8.7%

One sample each from Runs 5-12, 5-13, 6-7, and 6-10 were sintered in forming gas and, afterwards, were placed in HCl vapors in a covered beaker. This environment is known to cause a rapid degradation of Ti/Ag contacts when prepared by vacuum evaporation.[2] Consequently, it was of interest to note its effect on sputtered contacts. We expected to find Ti-Pt/Ag contacts more resistant to HCl vapors;[3] however, the data of Figure 6 show the opposite result, i.e., Ti-Pt/Ag contacts degraded more rapidly than Ti/Ag contacts in HCl vapors.

Sputtered contacts were also observed to develop blisters during water vapor and HCl exposure. Blistering was generally more severe for contacts whose electrical characteristics showed the most pronounced degradation. Some contacts actually lifted off the Si when exposed to HCl vapors.

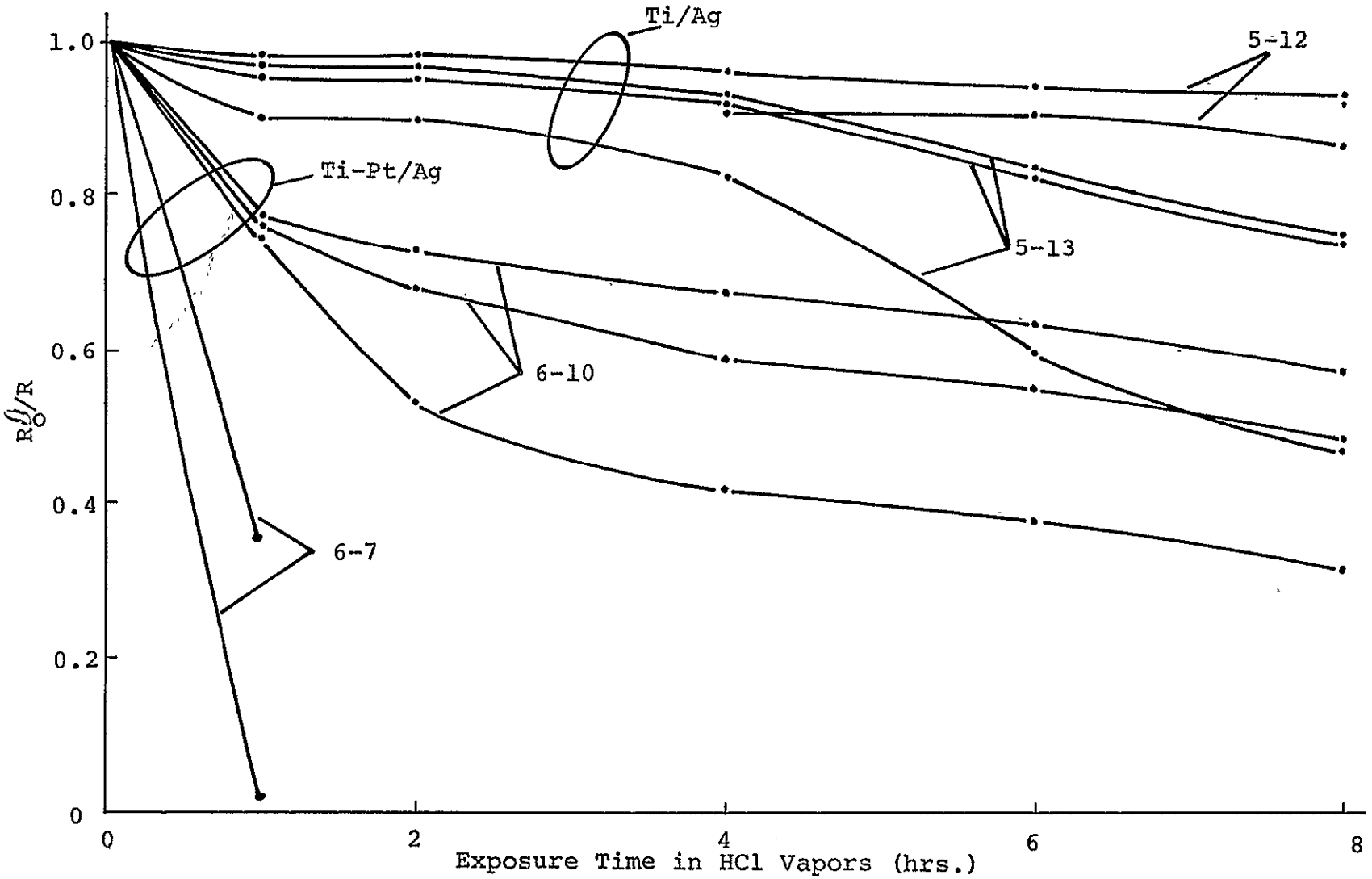

Figure 6 Degradation in contact resistance by HCl vapors

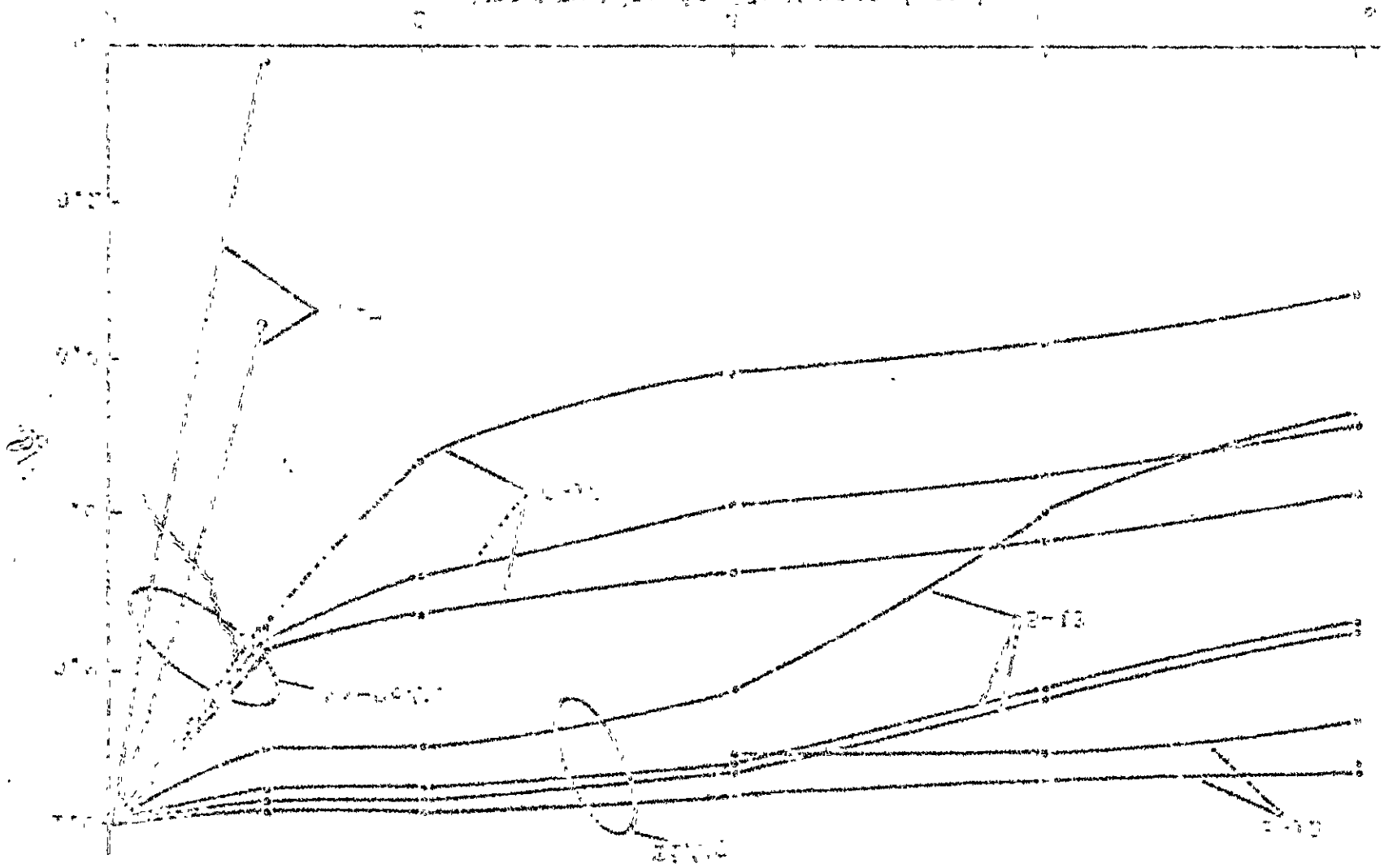

SECTION III

Fabrication of Si Solar Cells with Sputtered Contacts

The objective of this effort was to determine the feasibility of fabricating Si solar cells using sputtering to apply cell contacts and, if successful, to prepare 40 cells for evaluation by NASA-Goddard. Before this task was undertaken, the original 8 in. diameter sputtering system was increased to 18 in. in order to accommodate the mask fixture used for defining cell contacts.* A different target support arrangement was later installed and the final system is illustrated in Figure 7. Ti and Ag targets were rotated into position using a bellow-type rotary feedthrough. An O-ring seal was used in initial cell fabrication runs, but problems were sometimes encountered with electrical shorting. We also suspected a small air leak at the O-ring.

Phosphorus diffused 2 x 2 cm cell blanks were processed according to the following procedure:

1) Washed in near boiling distilled water for 1/2 min and subsequently dried.

2) Etched in concentrated HF acid for 2 min, repeatedly rinsed in distilled water, and dried with N_2 gas.

3) Mounted in a fixture for deposition of the ohmic strip contact and grid lines.

4) Ti and Ag were sequentially sputter deposited onto the active cell face.

5) Removed from the fixture and waxed cells to an Al plate with the active face protected.

6) Etched in CP_4 for 15 sec to remove the diffused n-type layer from the back face.

7) Repeatedly washed in distilled water, dried, and removed from the Al plate with moderate heating.

8) Dissolved wax in benzene using repeated solutions and then dried with N_2.

9) Mounted in fixture for deposition of back contact.

*Mask fixtures were kindly furnished by Centralab Semiconductor Division and Texas Instruments, Inc.

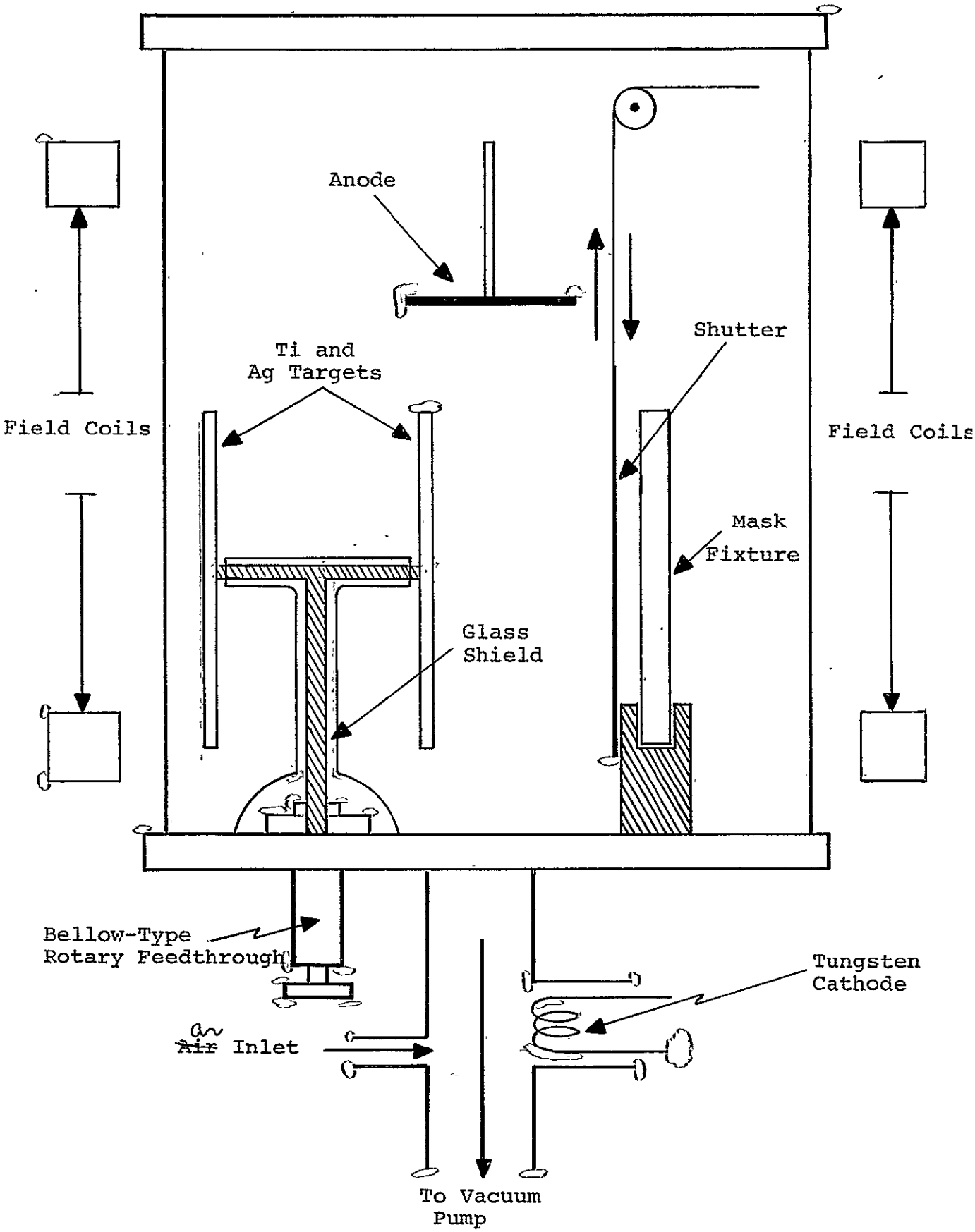

Figure 7 Sputtering system used in the fabrication of Si solar cells

System used in the fabrication
of solar cells

10) Sputtered Ti and Ag to the back face.

11) Sintered in forming gas at 605°C for 10 min.

12) Finally, cells were inspected and I-V characteristics were recorded.

Approximately 20 cells were prepared in each of 3 runs. Ti was deposited to a thickness of ∿500 Å and Ag to 5 to 8 μ. The results of the first three runs were discouraging. Contacts frequently lifted in Steps 5 and 8. Only 2 out of some 60 cells exhibited I-V characteristics typical of Si solar cells. Characteristics of one of these cells are shown in Figure 8a.* Most cells gave characteristics of Figure 8b which indicated a high series resistance. A few cells were shorted and exhibited characteristics of Figure 8c.

Again sintering had a detrimental effect on contacts. Besides blistering, some contacts actually lifted from the cell. The extreme ends of the ohmic strip contact were particularly affected. Also, poor definition of contacts was observed for many cells. The mask was not making good contact with cell blanks.

At this point in the program it appeared questionable whether sputtering was a technically feasible method of applying contacts to solar cells. Yet, it was felt that better contacts could be made by modifying certain process steps and improving the sputtering system.

Six additional fabrication runs were made in the two-month contract extension and led eventually to the fulfillment of the contract objectives. Forty cells were delivered to NASA-Goddard for evaluation, 20 had Ti/Ag contacts, the remainder, Ti-Pt/Ag. Six cells were subjected to high humidity-temperature tests in our laboratory, the results of which are given below.

The first two runs employed basically the same cell process steps as previously noted. They differed from previous runs in that the new target support arrangement with the metal bellow rotary feedthrough and an improved front mask fixture were used.** Also, Al was first sputter deposited

---

*All I-V characteristics were taken by adjusting the light level of a W lamp to give approximately 100 mA short circuit current. No significance should therefore be placed on variations in the circuit current among the different cells.

**The mask fixture was kindly furnished by Centralab Semiconductor Division.

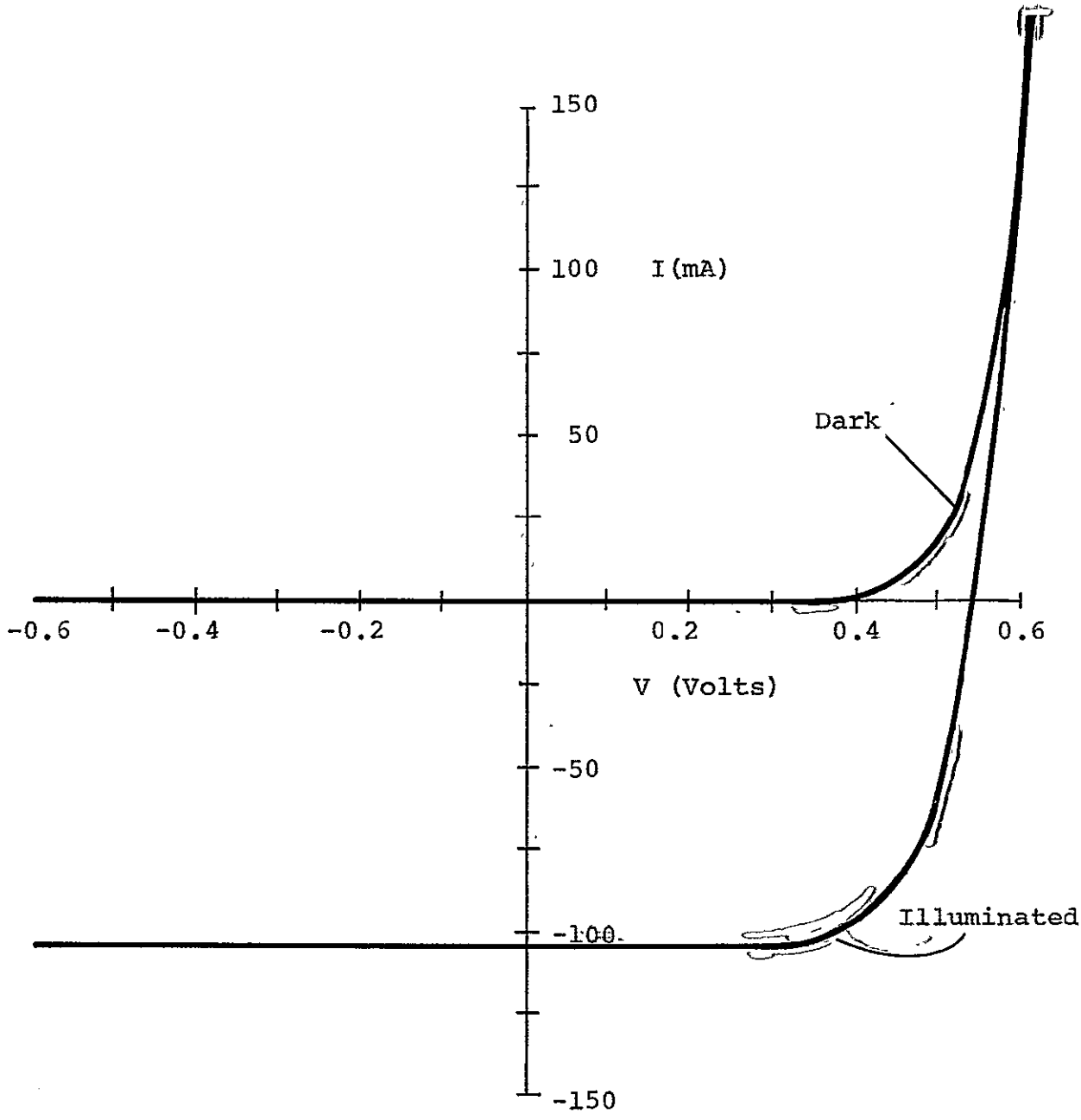

Figure 8 (a) I-V characteristics of a solar cell prepared in initial sputter-deposition runs

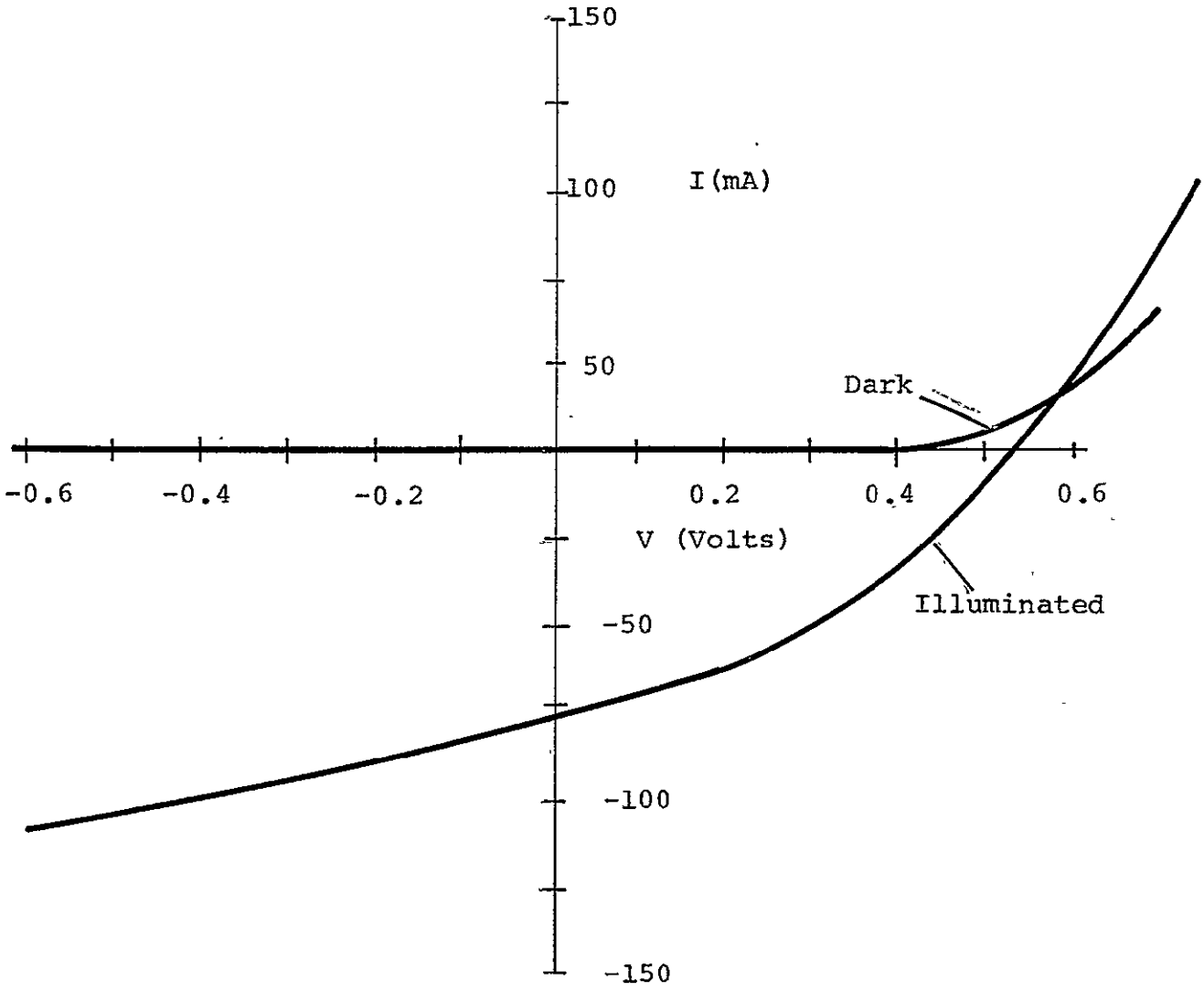

Figure 8 (b) I-V characteristics of a solar cell prepared in initial sputter-deposition runs

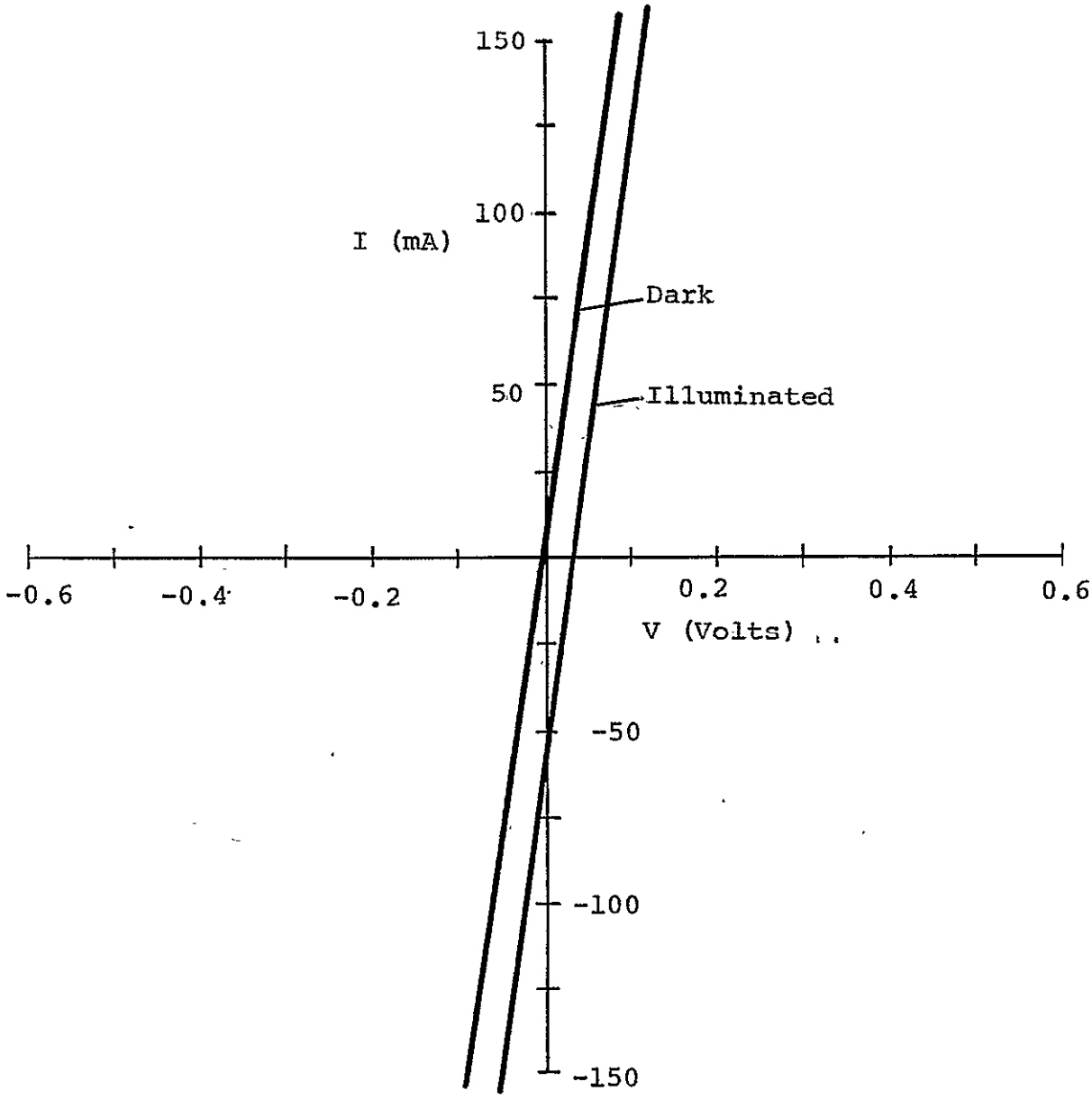

Figure 8 (c) I-V characteristics of a solar cell prepared in initial sputter-deposition runs

in situ on the back face of cell blanks before Ti and Ag were sputtered in order to reduce contact resistance to p-type Si. The new mask gave good contact definition. Sintering nevertheless produced blisters as before and the back contact lifted on all but a few cells when they were removed from the sintering furnace.

The effect of various pretreatments given to cell blanks just prior to contact deposition was investigated in the third run. It was suspected that some residual impurities remaining on the cell blanks after chemical cleaning were causing the contacts to blister. Pretreatment followed Process Step 2 above and included:

1) O_2 glow discharge for 15 min.

2) Ar glow discharge for 30 min.

3) 150°C in air for 30 min.

4) HF:HNO_3 etch for 2 sec.

5) 600°C in forming gas for 15 min.

6) 800°C in forming gas for 15 min.

7) HF etch for 15 min.

8) NaOH etch for 5 min.

9) NaOH etch for 5 min. followed by HF for 2 min.

10) No pretreatment.

Cell blanks were processed as before except that the diffused n-layer on the back face was removed by sandblasting instead of etching. Etching was omitted in order to avoid contaminants from the etchant and the wax used in masking.

The above pretreatment had strikingly different results on the durability of sintered contacts. Some contact lifting and/or blistering was noted for pretreatments 1, 2, 7, 8, and 10. Also, pretreatments 1, 3, 4, 7, 8, 9, and 10 produced some non-uniformity in contact appearance. Often areas of the contact on the outer periphery of the cell blank looked more reflecting than areas in the interior. It was mainly these outer areas that had blistered and peeled previously. Additionally, I-V characteristics of unsintered

and sintered cells found that pretreatments 7, 8, and 9 produced much more leakage currents than the average cell and, in fact, increased on sintering for 7 and 9. Pretreatment 4 produced a shorted cell, undoubtedly because the $HF:HNO_3$ etchant removed the diffused n-layer from the cell blank. These observations, together with adhesion tests, indicated that preheating cell blanks in forming gas at 600° to 800°C gave the most durable contacts and therefore this procedure was adopted in following runs. Also, the n-skin was removed by sandblasting instead of masking and etching in CP4.

The final three runs, which included both Ti/Ag and Ti-Pt/Ag sputtered contacts, were highly successful. Blistering or peeling was not observed on any of the 36 cells fabricated. All but three cells gave acceptable I-V characteristics. All three cells were sintered at the same time and were believed to be sintered at a temperature somewhat above 605°C.

Most cells exhibited some excess leakage current; this was particularly apparent for cells in the unsintered condition. Sintering had the effect of reducing the leakage and the series (contact) resistance. This tendency is shown in one extreme case in Figures 9a and 9b. Cell series resistance decreased from approximately 0.45Ω to 0.18Ω on sintering. Other cells initially exhibited a relatively low series resistance in the unsintered condition and sintering mainly reduced the leakage current. Figures 10a and 10b give an example of this. Series resistance in this case is around 0.23 Ω.

It is not surprising that some leakage currents were noted for these cells because they were not chemically etched to remove the surface damage produced by sandblasting. Yet it was of interest to find that edge leakage was substantially reduced by sintering.

Figure 11 is an enlarged photograph of a cell with sputtered contacts. Good contact definition is noted.

A photomicrograph of a sputtered contact is shown in Figure 12. Single crystalline grains or grain boundaries are not evident, although the surface is very rough in appearance. Surface roughness is not caused by the sputtering process but is due to the original roughness of the Si blank.

X-ray diffraction of sputtered Ti/Ag and Ti-Pt/Ag contacts shows that the Ag layer is fine grained and has only a small degree of preferred orientation. In contrast, the evaporated Ag layer on commercial solar cells invariably

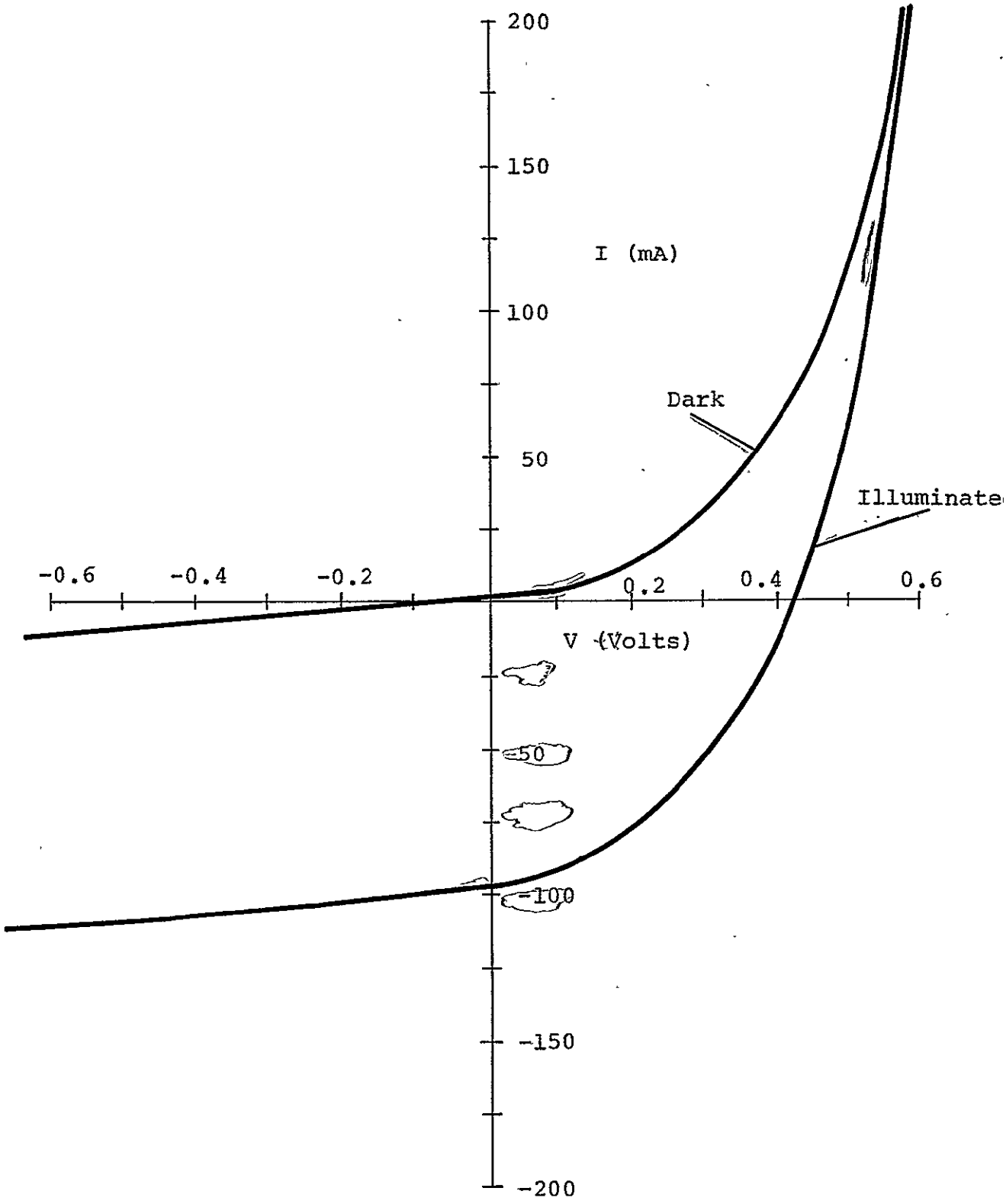

Figure 9 (a) I-V characteristics of a cell before sintering

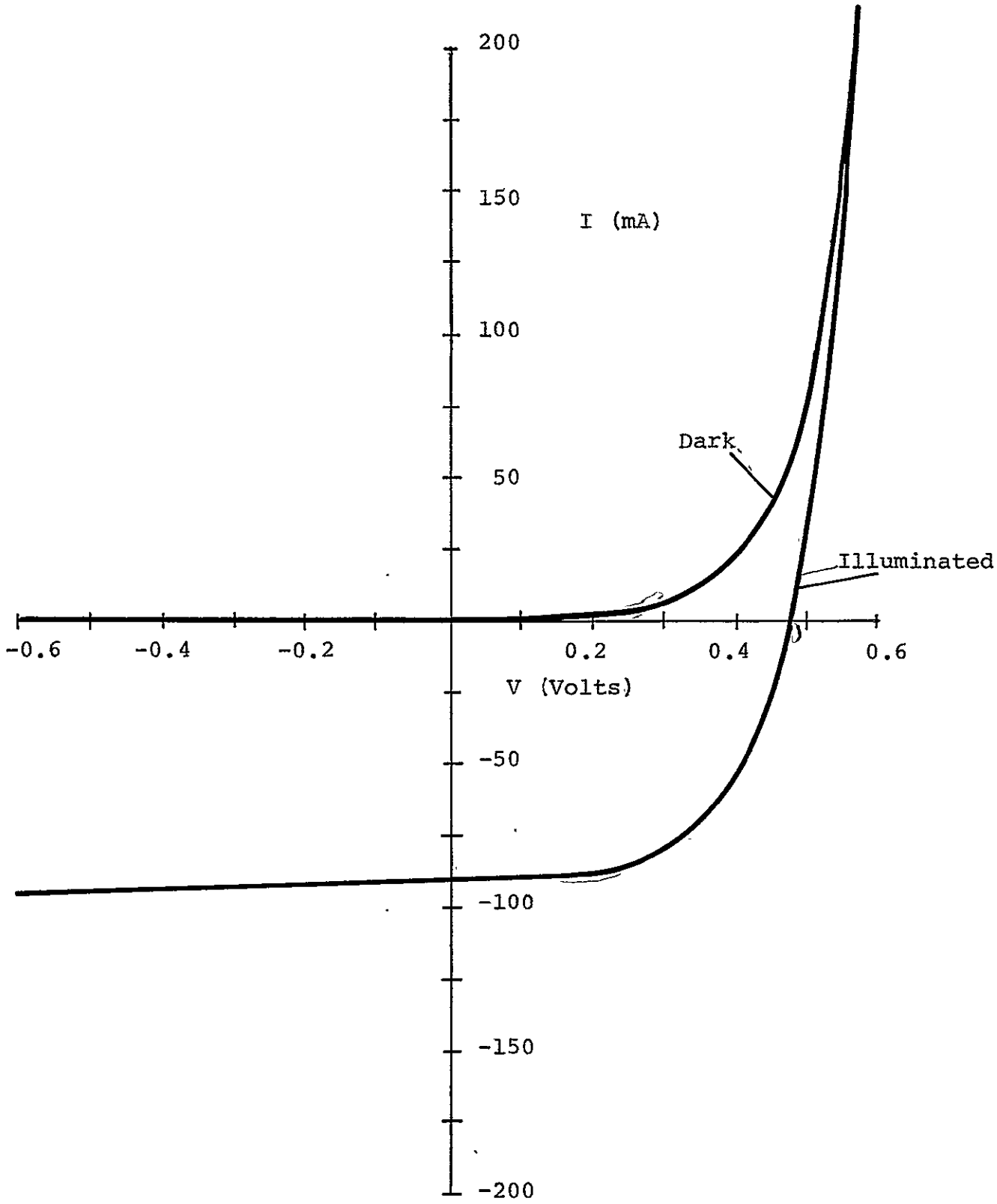

Figure 9 (b) I-V characteristics of a
cell after sintering

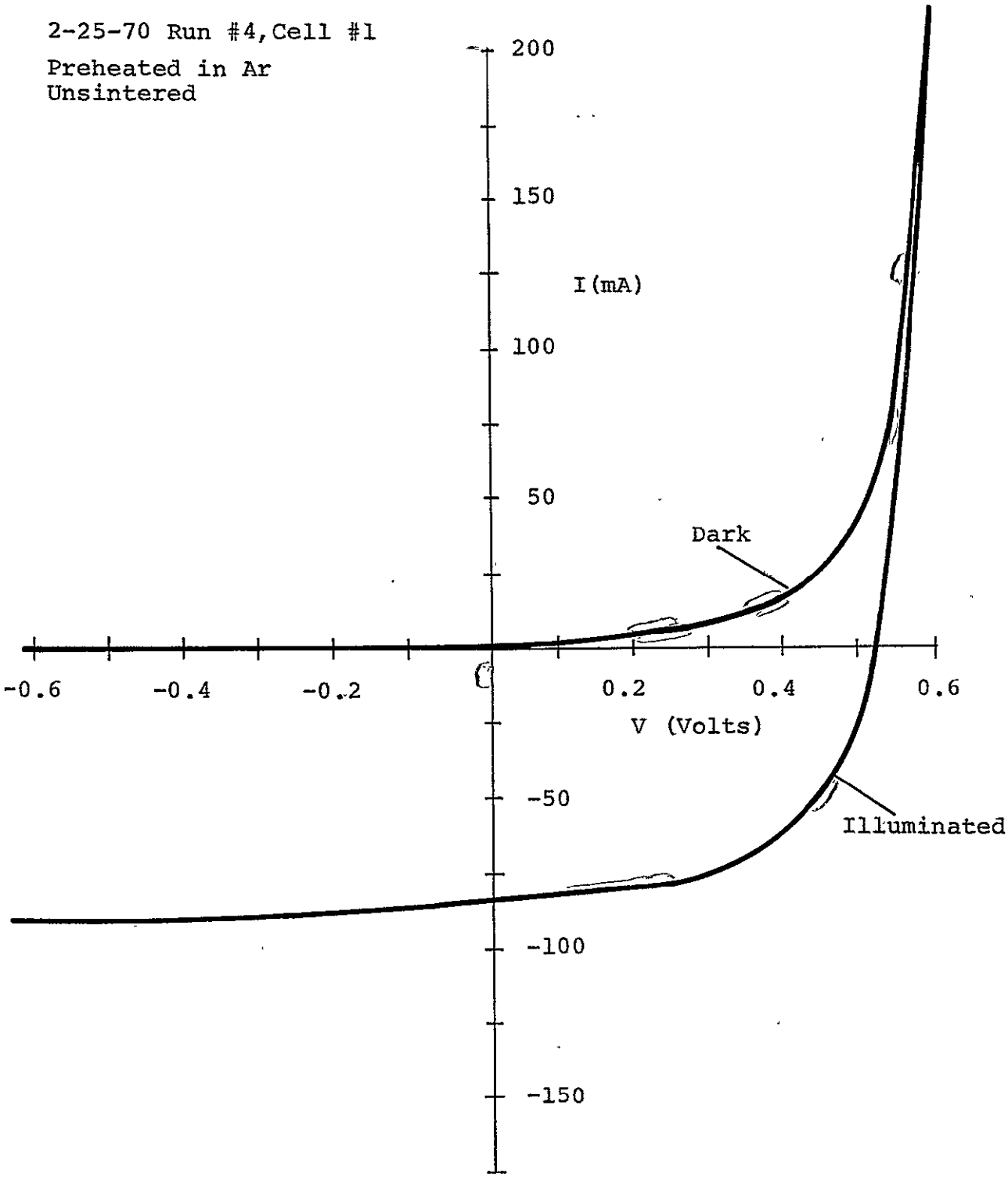

Figure 10 (a) I-V characteristics of a cell before sintering

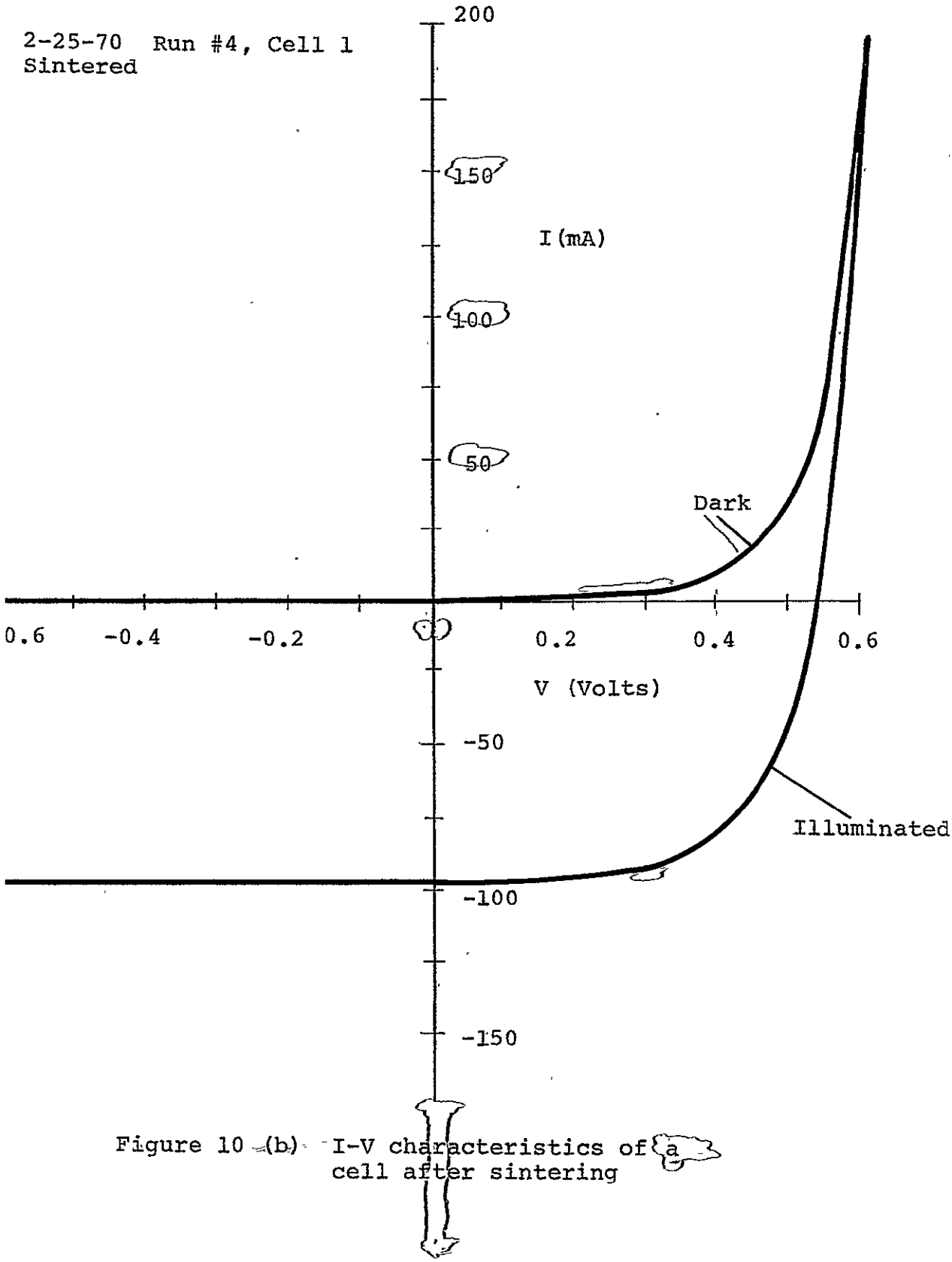

Figure 10 (b) I-V characteristics of a cell after sintering

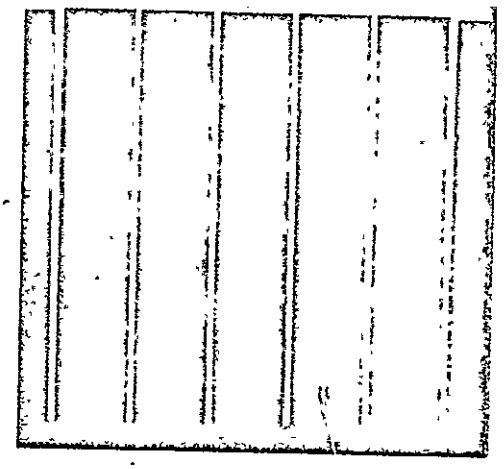

Figure 11 Photograph of a sputter-coated cell

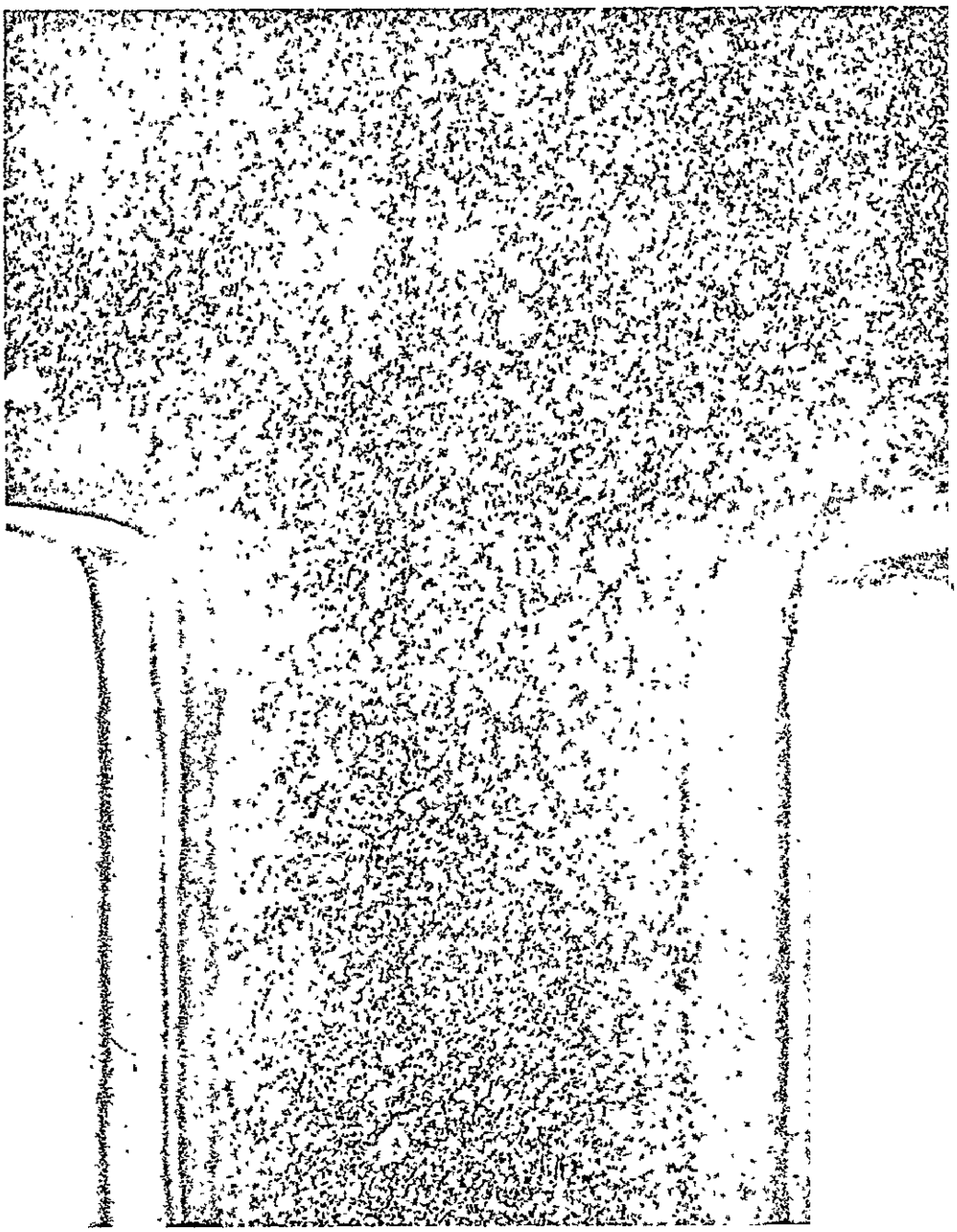

Figure 12 Photomicrograph of a Ti/Ag contact (320X)

exhibits a relatively large grain size of the order of 50 microns in lateral dimensions and a high degree of preferred orientation. This can be seen from typical forward scattering x-ray diffraction patterns shown in Figure 13. The grain size can be estimated from the nature of the diffraction arcs. For sputtered Ag, the grain size is believed to be in the 0.1 to 1.0 micron range.

Six cells with sputtered contacts were simultaneously subjected to a high humidity, 80°C temperature environment. Contact degradation was studied by recording dark current I-V characteristics under forward bias conditions. Data on the four cells with Ti/Ag contacts and two with Ti-Pt/Ag contacts are given in Table III. Here predeposition treatment and initial series resistance are shown for each cell. Included in this group are three cells which were not prefired in forming gas prior to contact deposition and therefore are not the most durable sputtered cells. Also, cell 5 which exhibited excessive leakage current was included.

I-V characteristics were recorded initially and at various times during humidity exposure. Figure 14 shows initial dark characteristics (curve i) and characteristics after 1224 hr in the high humidity environment (curve f).

In Figure 15 the resistance ratio R_o/R is plotted as a function of exposure time where R_o is the initial series resistance and R the resistance at a given exposure. Resistance values were determined from the maximum slope of I-V characteristics at around 0.7 V forward bias.

It is evident from Figure 15 that cells 1 and 2, which were not given a special predeposition treatment after etching in HF, degraded rapidly over the first one to two-hundred hours of humiditiy exposure whereas cells 4 and 6 did not. Cell 5, which was sintered at a higher than normal temperature, degraded most seriously. Cell 6, with Ti-Pt/Ag contacts, was particularly stable and degraded at most by 10% over the long exposure time. Many small blisters were observed to develop on cells 2 and 5 during humidity tests; i.e., on the two most seriously degraded cells. A few small blisters developed on cells 1 and 3. No blisters developed on cells 4 and 6.

Two "aged" commercial cells with evaporated Ti/Ag contacts were included in the humidity tests for the purpose of comparing degradation results. Both cells developed blisters soon after exposure and contact resistance on one cell seriously degraded. Contact resistance on the second cell was essentially unaffected by humidity, at least for an exposure time of 400 hr.

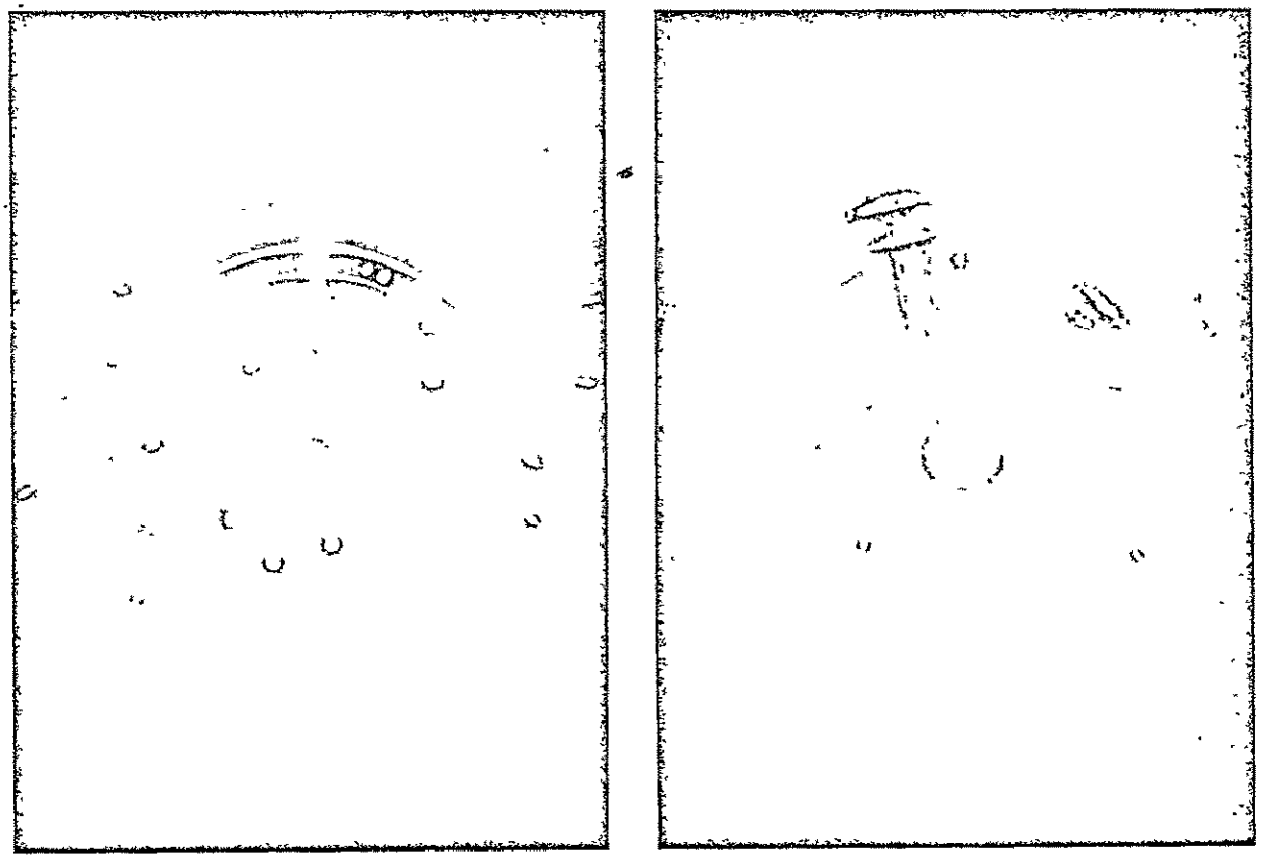

(a) (b)

Figure 13 Typical x-ray diffraction pattern of (a) sputtered contact and (b) evaporated tact

Table III

Data of Cells Exposed to High Humidity/Temperature Testing

Cell No.	Contact System	Predeposition Treatment	Initial Series Resistance
1	Ti/Ag	2 min HF	0.142
2	Ti/Ag	15 min HF	0.197
3	Ti/Ag	2 min HF, prefired in forming gas	0.155
4	Ti/Ag	2 min HF, 1/2 hr Ar glow*	0.145
5	Ti-Pt/Ag	2 min HF, prefired in forming gas	0.209
6	Ti-Pt/Ag	2 min HF, prefired in forming gas	0.138

*This cell blank was exposed to an rf excited glow discharge of Ar.

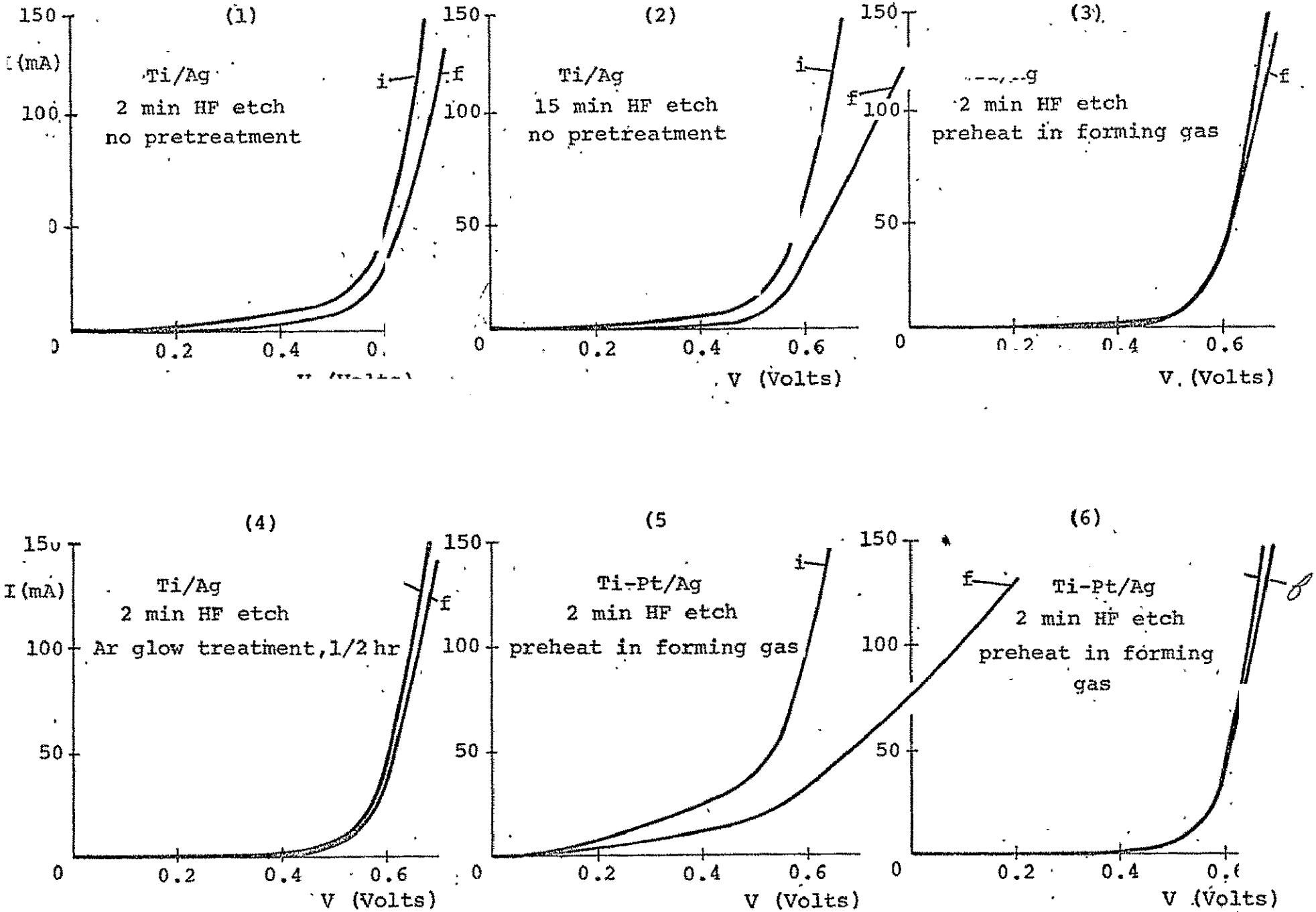

Figure 14 Cell I-V characteristics recorded initially (i) and after 1224 hr (f) in a high humidity/80°C

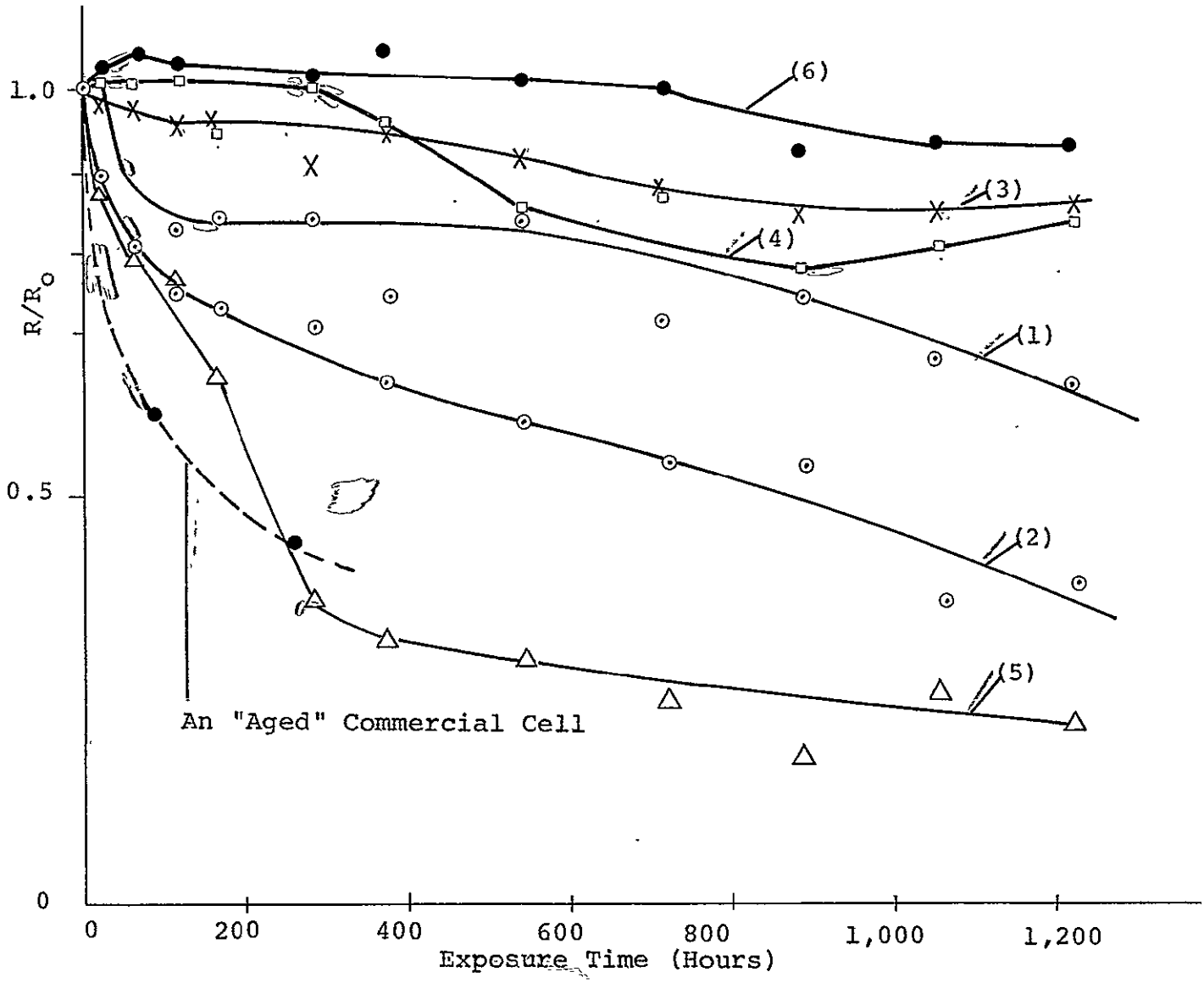

Figure 15 Degradation in series resistance as a function of humidity exposure time

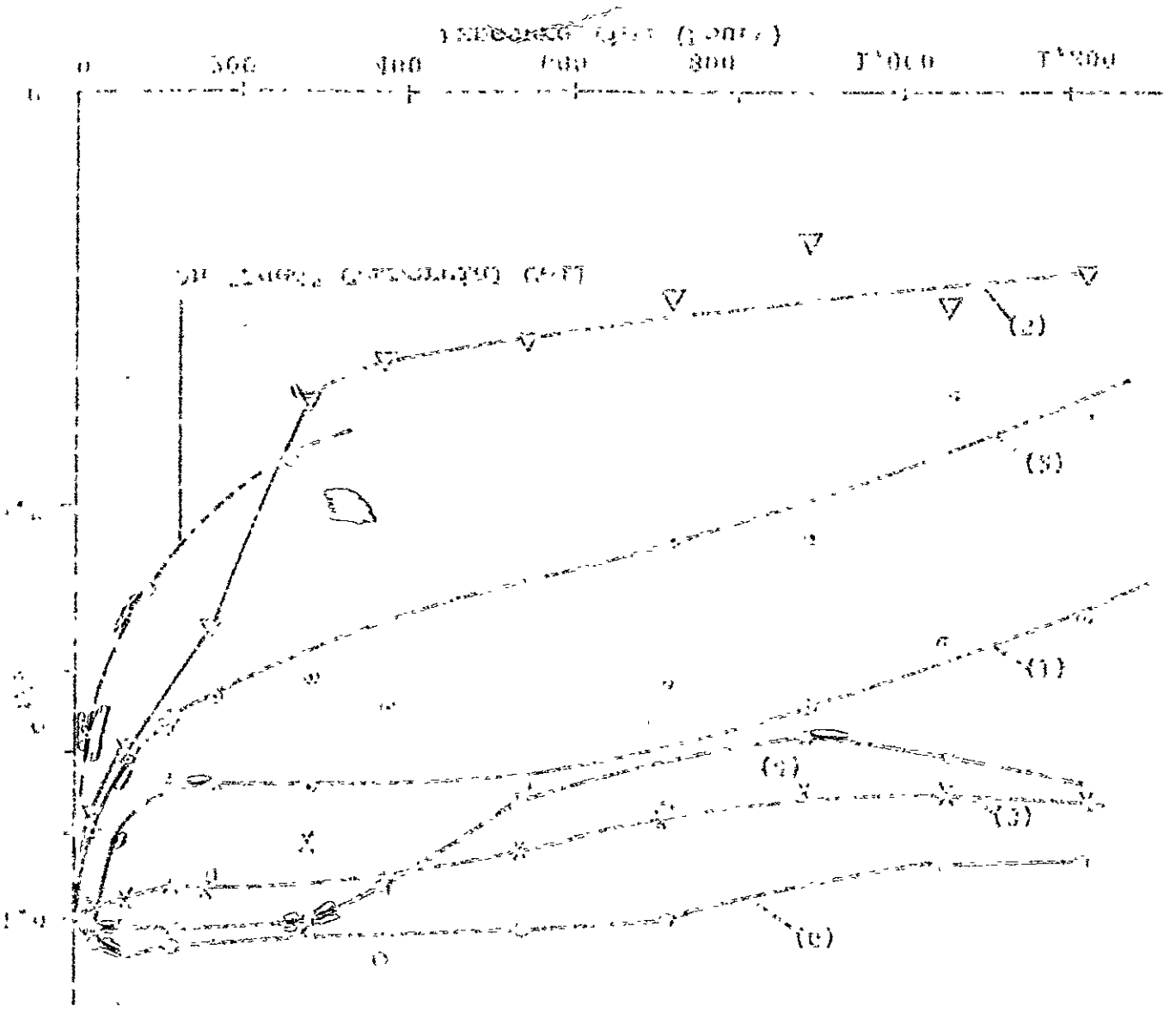
(1)
(2)
(3)
(4)
(5)

The above findings, although limited in extent, clearly demonstrate the importance of predeposition treatment of cell blanks on the quality of sputtered Ti/Ag and Ti-Pt/Ag contacts. In addition, this fabrication step has a significant effect on the degradation of contacts in humid environments. The exact reason for this is not known although we believe it is due to an effect of impurities remaining on or in the cell blank after HF etching, even though cell blanks were thoroughly washed in deionized water after etching. Some insoluble phosphide or fluoride compounds may possibly remain on the surface after etching. Or, HF or F may penetrate into a thin surface layer of Si and later diffuse to the surface and attack the Ti layer. In any event, heat treating cell blanks in forming gas in the 600° to 800°C temperature range just prior to contact deposition gave much improved contacts. Additionally, an Ar glow discharge pretreatment also appears reasonably effective as seen in Figure 15.

Although cell 6 was superior to other cells in respect to degradation, the limited data is insufficient to conclude that Ti-Pt/Ag contacts are superior to Ti/Ag contacts. Also, it is not clear that sputtered contacts are superior to evaporated contacts from the limited data. More extensive examination of cells with sputtered contacts are being conducted by NASA-Goddard.

SECTION IV

Ti/Ag Contact Degradation

Experimental

The objective of this study was to determine the cause or origin of contact degradation as it has been frequently observed on Si solar cells with evaporated Ti/Ag contacts. Solderless-type contacts have been found to be particularly susceptible to degradation whereas solder-coated contacts are not noticeably affected.(1) While degradation proceeds at a slow rate under normal environmental conditions, it is greatly accelerated in a high humidity temperature environment. Degraded contacts generally result in a reduction in contact adhesion and cell efficiency. Contacts frequently develop blisters when exposed to high humidity and, at times, partially or wholly separate from the cell. Stress exerted by cell interconnections and thermal cycling is furthermore known to aggravate the problem. Cell efficiency is affected because degraded contacts almost invariably produce a higher internal series resistance. And, of course, a catastrophic loss of efficiency occurs when a contact separates from a cell.

The main results of our contact characterization study(2,4,5) are briefly summarized. Most cells supplied to us by NASA-Goddard were degraded and exhibited poor contact adhesion. Adhesion was checked by tape testing or by physically peeling contacts with a tweezer. Sometimes the entire ohmic strip contact with grid lines was removed from the cell intact. A few cells had good adhesion; i.e., their contacts could not be removed.

Examination of cells with an optical microscope revealed that evaporated Ag films possess a large grain size, typically in the 30 to 60 micron size. Single crystal grains could be inferred from ridges that develop at grain boundaries. The silicon monoxide antireflection coating used on these cells was readily detected on the active face, but it does not generally cover the Ti/Ag grid lines uniformly and, at times, not at all. In some cases, the coating appeared to have chipped off the contacts while in others a web structure of SiO was evident. Some stress release was also evident at the edge of some contacts where characteristic snake features were noted. The first batch of degraded cells, which were removed from RAE flight panels, did not show blisters, although subsequent cells which were subjected to the accelerated humidity test chamber almost always exhibited some blisters.

The interface exposed by peeling contacts from cells invariably exhibited profuse colors. A wide variation was observed among cells, some showing predominantly one color while others showed a variety of colors. Colors included various shades of black, brown, blue, green, yellow, and red. These findings suggested that Ti exists in a chemically combined state. Ti oxides are known to exhibit many of these colors.

X-ray diffraction analysis of Ti/Ag contacts showed Ag is in its normal crystalline state and has a large grain size of around 50 microns. Some streaking was also observed in the pattern and suggests that the contact is under stress. However, streaks may also arise from other effects. Diffraction lines characteristic of metallic Ti were not observed, apparently because sufficient Ti does not exist in its elemental state.

Electron microprobe analysis of the peeled interface revealed that contact failure generally occurs within the metallized contact and in the vicinity of the Ti/Ag transition region. Some variations in the amount of Ti and Ag remaining on cells were observed and indicates that contact separation is not always limited to the thin transition region.

Electron mirror microscopy examination revealed a dielectric charging behavior on the surface of the Ag film. This unexpected result was later traced to the SiO antireflecting coating which partially coated the contact. Contact discontinuities, due to grain boundary or physical cracks, were not detected.

Potential probing of contacts when cells were biased in the forward direction also did not reveal any gross potential discontinuities along Ti/Ag contacts. Additionally, these measurements showed that the resistivity of the Ag overlayer is not substantially different from bulk Ag.

Auger spectroscopy measurements detected several impurities in Ti/Ag contacts. In one case, a significant quantity of Cl was noted and, in another, oxygen. The unexplained Auger peak at ~127 eV is very likely due to phosphorus, the n-type dopant material. Other impurities, such as hydrogen or fluorine, could not be detected by our Auger system.

The above finding clearly suggests that Ti/Ag contacts degrade by a corrosion or oxidation process and that Ti is the element that corrodes. Studies were subsequently directed at determining what possible agents, besides high humidity, cause contact degradation. Also, it was of importance to determine the means by which corrosive agents attack the Ti. For example, do they diffuse through the Ag layer or do they propagate from the edge of the contact?

The reactive nature of Ti and the porosity of Ag were investigated by exposing test samples to various gaseous environments and aqueous media. It is not surprising that oxygen and water vapor were found effective in producing visible oxide films on Ti at elevated temperatures. Additionally, it was observed that evaporated films of Ag on Ti do not adequately protect Ti from oxidation. This was concluded by noting that interference colors on the front and back face of a Ti test sample were similar even though one face was coated with a Ag film. However, oxygen and water vapor (at low concentrations) do not produce visible oxide films on Ti at temperatures of less than several hundred degrees centigrade. Yet, high humidity tests on solar cells definitely show Ti/Ag contacts degrade at temperatures less than 100°C.

Oxide growth on Ti was subsequently found to proceed at room temperature when Ti was immersed in aqueous solutions of NaOH and KOH. In concentrated solutions, oxidation occurs at a high rate and thick oxide films develop. Lower concentrations also produce an oxide but the oxidation rate is less and the final film thickness is less. Ordinary tap water and seawater at 80° to 90°C were also found effective in producing visible films on Ti. NaCl solutions did not, on the other hand, form a visible surface film.

Concentrated solutions of NaCl, NaOH, and KOH were found to degrade Ti/Ag contacts at room temperature on specially prepared test specimens and also on solar cells. Blisters generally developed over the contact and adhesion was seriously impaired. Degradation was particularly rapid for the test specimens, apparently because the thickness of the Ag film in this case was around one micron and compares to around ten microns on solar cells. Hence thick Ag coatings on solar cells appear to provide some protection but, even at room temperature, is far from complete. In one experiment the edges of a large area Ti/Ag contact were masked with Apiezon wax and, after exposure to KOH, it was observed that the contact degraded only in the unmasked region. Hence the corroding species must have diffused through the Ag film.

Ti and also Ti/Ag contacts were also found to be highly susceptible to an additional number of corrosive environments at room temperature. Among these include vapors of HF, HCl, wet Cl_2, and wet CO_2. Again these findings reaffirm the general porosity of Ag films and the reactivity of Ti.

Discussion of Results

We have seen that electrical contacts on Si solar cells often undergo degradation. This degradation manifests itself by an increased contact resistance, which results in reduced efficiency, and/or actual physical separation of contacts from solar cells.

The process which causes the degradation has not been definitely established. It does appear that there may be more than one mechanism which can lead to unsatisfactory cell performance.

There are strong indications that the degradation mechanism is chemical in nature. Furthermore, an external agent generally appears necessary for the resulting cell failure. A standard accelerated degradation test is to expose cells to elevated temperatures in a high humidity environment. It has also been found that cells heated in vacuum or by nitrogen do not appear to undergo degradation.(6) This suggests that an external agent, such as water, is instrumental in the degradation process. However, not all cells degrade under this treatment. In those cases either the water is not able to reach a contact interface, or another essential ingredient within the cell is missing. For example, undesirable residue may remain from a faulty cleaning procedure. In fact, the deleterious effects of impurities on contacts is demonstrated in Section II.

Our studies on contact degradation, described earlier in this section, also demonstrated that other external agents can cause contact degradation. These studies plus the high humidity tests raise two questions: (1) How can the external agent reach one of the interfaces? and (2) What effect could the agent have once it reached an interface? These points will be considered in the following discussion.

Initially, it seems somewhat surprising that a chemical agent can penetrate the relatively thick silver coating at low temperatures. However, as noted earlier in this section, various chemical agents readily penetrate evaporated Ag films of these thicknesses. Burns and Bradley state that commercial Ag plates are porous for coating thicknesses less than one mil.(7) The porosity of Ag films can also explain why solder-coated cells are less susceptible to degradation when compared to solderless cells.

Consider the means by which a chemical agent can penetrate Ag films. Possible processes include bulk diffusion, grain boundary diffusion, and microcrack conductance. These processes will be generally described first and then discussed in terms of the Ag films used for contacts on solar cells.

Bulk diffusion through Ag appears to be much too slow at 100°C to account for the observed effects. For example, consider the diffusion of oxygen through Ag. Even by assuming that the diffusion constants at higher temperatures are applicable at lower temperatures, a simple calculation shows that, at 100°C, it would take about two years to get an equivalent monolayer of oxygen through an Ag film one micron thick. If the coating was 5 microns thick, it would take ten years. Thus it appears that bulk diffusion can be ruled out.

It is well-known that grain boundary diffusion can in some cases proceed much more readily than bulk diffusion. However, this does not always appear to be the case. LeClaire, for instance, suggested that activation energies for grain boundary and volume diffusion may not differ appreciably.(8) Others, however, have found higher diffusion rates along grain boundaries.(9) Such experiments are difficult to perform. The diffusion of Th in W has been utilized for such experiments.(10) Th is essentially insoluble in W, except along grain boundaries. A W filament containing Th was first flashed to rid the surface of Th. Then the filament was maintained at a lower temperature and the thermionic emission was used to detect the Th which had diffused to the filament surface. The diffusion rate (the diffusion constant, actually, and not the activation energy) was shown to be dependent on grain size. The rate was lower for W composed of large grains. Fine grains resulted in more grain boundary surface area and hence higher rates. This would suggest that fine-grained Ag should be more porous than coarse-grained Ag.

Diffusion through thin films could obviously proceed even more rapidly if microcracks occurred in the films. Microcracks in films would most likely tend to develop in films which were deposited under tensile stress.

Now let us consider the evaporated Ag films used for solar cell contacts. These films, as normally deposited, have a typical grain size of about 50 microns. For most metals the grain size is usually smaller. The relatively large grain size for Ag is probably a consequence of the high mobility of deposited Ag atoms. The films show some fiber texture (preferred

orientation). The intrinsic stress of the deposited films has not been measured, but it is typically tensional for evaporated Ag.(11) Furthermore, it should be realized that evaporated films usually exhibit a pronounced columnar growth generally in the direction of atom deposition. In fact, Wade and Silcox suggested that films grown at low deposition rates at normal incidence (∿ 1 Å/sec) consist of separated parallel rods with their long axis perpendicular to the film.(12) Such a structure would suggest a strong anisotropy in diffusion rates, with the highest rate being parallel to the rod axes. At higher deposition rates this effect was less pronounced. Furthermore, this effect is less important when deposited atoms have higher mobility. For instance, Ag films deposited at elevated temperature show little anisotropic growth.

The growth conditions just discussed are concerned basically with amorphous substrates. In the solar cell contact, however, this is not the case. The Ag is deposited onto a polycrystalline Ti film of some preferred orientation. The structure of the Ag film would be expected to be influenced by the Ti. For instance, Ag coatings for the protection of steel must be at least 1 mil thick before they are pore free. The quality of the Ag coating, however, is strongly influenced by the initial layers, which are often applied over an intermediate film of a material like Ni.(7)

Another possibility for enhanced diffusion through Ag films could be the existence of microcracks. We have already indicated that evaporated Ag films have an intrinsic tensile stress. Conceivably, these stresses could cause the films to crack. This could be more pronounced when the Ag is heated above the recrystallization temperature, as it is during the sintering process. In fact, grain growth in Ag has been observed above ∿ 100°C. The possibility of microcracks causing the Ag film porosity was suggested by Morrison.(13)

At this time it is not possible to state unequivocably what mechanism is responsible for the porosity of Ag films. It would appear, however, that the high room temperature porosity of the films is probably due to film defects. A more perfect film would be expected to be more protective. Morrison, et al., for example, have reported that Ag films evaporated onto solar cells maintained at 0°C have superior properties to those deposited on substrates at 100°C.(13) Generally speaking, films deposited at higher substrate temperatures have larger grains and therefore less grain boundary area. Since grain boundary diffusion would be

expected to increase with decreasing grain size, these results suggest that the porosity is not simply a matter of grain boundary diffusion. Furthermore, the columnar growth discussed earlier should also be less pronounced at higher temperatures, especially for Ag at these deposition temperatures. This would leave microcracks as being the predominant likely cause of the porosity. It has already been indicated that evaporated Ag films typically have a tensile intrinsic stress. This would tend to result in film cracking. The effect of a cooler substrate during deposition is not known. However, the difference in thermal expansion coefficients between Ag and Si is such as to put the Ag in tensile stress. Even for the same tensile stress, it would seem that larger grains might result in wider cracks, since there are fewer boundary regions available for stress relief. Again, as mentioned earlier, grains are larger for higher deposition temperatures. These considerations suggest that microcracks are responsible for the observed porosity.

Ag films deposited by means other than evaporation would be expected to have quite different properties. For instance, it appears that sputtering may have certain advantages. One advantage is that sputtered films typically have compressive intrinsic stress. This would act to retard the formation of microcracks. Furthermore, the grain size for sputtered films is much less than for evaporated films. A careful study of the porosity of sputtered Ag films compared with evaporated Ag films could be very informative.

Now consider what effect a chemical agent could have on the electrical contact. Studies performed in this program have demonstrated that considerable oxidation of Ti is observed generally in regions of contact failure.

Ti is chemically a highly reactive metal. It is extremely resistant to corrosion by most solutions because of a thin, inert, protective oxide film which forms on its surface. When this film has formed, the Ti is said to be passive. An oxide film of sufficient thickness to exhibit interference colors does not form in air unless the Ti temperature is raised above ~300°C. In fact, at 300°C the oxide film which forms is just 100 Å. (14)

Some substances, such as hydrofluoric, hydrochloric, and sulphuric acid, severely attack Ti. The reason is that these substances can break down the protective oxide film. The resulting dissolution of Ti is electrochemical in nature.

The rate of attack is determined by the activity of localized cells on the metal surface.(15)

Galvanic corrosion of an electrically conductive material can occur when it is in electrical contact with another conductive material in the presence of an electrolyte which allows current to flow. When Ti is coupled to Ag, the corrosion rate of Ti is quite high. However, when Ti is coupled with Pt, the corrosion rate of Ti is dramatically reduced.(16,17) The Ti corrosion for this couple is reduced since the Pt promotes the formation of a protective oxide film on the Ti surface.(17,18) In fact, it has been shown that alloying small amounts (< 1%) of noble metals like Pt to Ti is also very effective in reducing the corrosion rate of Ti.(3) Alloying of Ag with Ti is very detrimental.(19)

The relatively low temperature (< 100°C) involved in the deterioration of the solar cell contacts suggests an electrochemical mechanism. Furthermore, dry chemical gases generally do no cause contact deterioration, whereas wet chemicals do. However, for such a process to occur, an electrolyte must be in the reaction zone. We have already suggested how an electrolyte could penetrate porous Ag. If certain ions, such as Cl^-, are added to water, the reaction proceeds more rapidly. It has also been shown that contact degradation on expsoure to water depends on the water used. The degradation process decrease in the order tap water, distilled water, and deionized water (see Section II). It is significant, however, that the degradation does not cease with deionized water. This suggests that some impurity atoms, which could become ionized in water, are already present in the contact region. This could be material present from the dopant diffusion process or residue from cell cleaning.

If an electrolyte is able to reach the interface, quite active corrosion of Ti would be expected to occur. If galvanic corrosion in an aqueous media occurs, hydrogen gas would be expected to be released at the cathode. Hydrogen gas has been observed in the blisters commonly observed.(20) As the reaction proceeds, the hydrogen pressure would build up and eventually could lead to blistering of the film. This could expose more Ag-Ti interface with further corrosion. Since Pt is known to reduce the corrosion of Ti, Telefunken proposed adding a layer of Pt (or Pd) between the Ti and Ag.(21) This contact is still being investigated. Some studies have indicated that this combination is superior to the Ti/Ag contact. It is interesting to note that Pt layers have been used between Ti and Au layers for contacts to Si for a long time.(22) The purpose of the Pt layer

in this case is to separate Ti and Au, which react chemically at relatively low temperatures to form undesirable compounds.(23)

An interesting and relevant study on contact adhesion was recently made by Haq, et al.(24) It is well-known that Au and Ag do not bond well to oxides. Therefore, metallic underlayers which do bond well to oxides are often used. They studied intermediate layers of Ta, Cr, Ge, and Si to bond Au to oxides. For Au-Si and Au-Ge, alloying and diffusion problems result in unsatisfactory contacts. For Ta, exposure of the combination to air resulted in oxidation of the Ta with the resulting lifting of Au. The Au was obviously not able to protect the Ta. The Cr underlayer behaved completely differently. Even exposure of the combination to high temperatures in air did not result in oxidation of the Cr. Apparently the affinity of Cr for oxygen is not sufficient to replace the metal-metal bond by a metal-oxide bond. Cr alone, of course, would have readily formed an oxide surface.

SECTION V

Conclusions and Recommendations

We conclude that sputtering can be successfully employed in the deposition of electrical contacts to Si solar cells and that durable contacts result with proper cell fabrication procedures. Most important is the cleaning procedure of the cell blank prior to contact deposition. Heat treating in forming gas after etching in HF was very beneficial. It was also desirable, but perhaps not essential, to exclude chemical etching in subsequent fabrication steps. Apparently residues remaining on the cell blank after etching had a detrimental effect on cell contacts.

Long-term exposure of several sputter coated cells to high humidity at 80°C showed that cells can be quite resistant to contact degradation provided that a proper cell blank cleaning procedure is used. However, the limited data precludes any conclusion concerning whether sputtered contacts are, in general, an improvement over evaporated contacts in regard to contact degradation. A distinguishing feature of sputtered Ti/Ag contacts is the fine grain size of the Ag film and this might be advantageous insofar as film porosity is concerned.

One likely contact degradation mechanism is the penetration of water vapor through the Ag film and an electrolyte, formed by foreign impurities, attacks the underlying layer of Ti. Hydroxyl ions may possibly form at the Ti/Ag interface by dissociation and these ions have been shown to readily oxidize Ti. Furthermore, the adhesion of the Ag film is at the same time reduced because the chemical bond strength of Ag to a metal oxide is known to be substantially less than to the metal itself. Blisters develop from the generation of H_2 gas and contacts lift or separate from the solar cell when adhesion is impaired.

There are also indications that chemical impurities originating within the cell can promote degradation. These impurities can be removed by adequate cleaning procedures, which may not be presently established. The most reliable surface cleaning procedure would be sputtering, which acts like a universal etchant since all materials can be sputtered.

It is apparent that one solution to the degradation problem is to develop a relatively non-porous Ag coating since the coating would prevent water vapor and/or other corrosive species from reaching the Ti/Ag interface. The success of producing such a coating does not appear likely unless, for example, a much greater film thickness is used or if sputter coatings are substantially less porous.

A second solution is to add an additional layer either on top or intermediate the Ti and Ag. Both approaches have been used with some success, i.e., solder-coated contacts and the Ti/Pd/Ag (or Ti/Pt/Ag) contact system, respectively.

If the existing contact cannot be improved by these means, then other contacts become necessary. Other contact systems could be considered, such as Cr underlayers. This could be of value if Ag-Cr behaves as Au-Cr does. Sputtering might also be used to remove the natural oxide layer from the Si immediately prior to contact deposition. This could eliminate the necessity of using a material like Ti, which is used to reduce the silicon oxide.

SECTION VI

New Technology

All the research tools and techniques employed in this study program are not new technology developed under this contract and therefore there is none to report here.

SECTION VII

References

1. W. Luft, et al. Temperature and Humidity Effects on Si Solar Cells. Seventh Photovoltaic Specialist Conference Proceedings, Pasadena, California, Nov. 1968.

2. R. Jacobson. Solar Cell Contact Development. Third Quarterly Report, Contract No. NAS 5-11595, Goddard Space Flight Center, March 1969.

3. M. Stern and H. Wissenberg. The Influence of Noble Metal Alloy Additions on the Electrochemical and Corrosion Behavior of Titanium. J. Electrochem. Soc. 106: 759-764 (1959).

4. R. Jacobson. Solar Cell Contact Development. First Quarterly Report, Contract No. NAS 5-11595, Goddard Space Flight Center, Sept. 1968.

5. R. Jacobson. Solar Cell Contact Development. Second Quarterly Report, Contract No. NAS 5-11595, Goddard Space Flight Center, Dec. 1968.

6. Private Communication with John Fairbanks, Goddard Space Flight Center.

7. R. M. Burns and W. W. Bradley. Protective Coatings for Metals, 3rd ed., Reinhold Publ. Corp., N.Y., 1967. p. 304.

8. A. D. LeClaire. Grain Boundary Diffusion in Metals. Phil. Mag. 42: 468 (1961).

9. R. E. Hoffman and D. Turnbull. Lattice and Grain Boundary Self-Diffusion in Silver. J. Appl. Phys. 22: 634 (1951) and

   P. J. Fensham. Self Diffusion in Polycrystalline Tin. Austral. J. Sci. Res. 3: 105 (1950).

10. Gv. Henesy. Z. Elektrochem. 39: 490 (1933), and

    G. Fonda, A. Young, and A. Walker. Physics 4 (1933).

11. H. P. Murbach and H. Wilman. Proc. Phys. Soc. London B66: 905 (1953), and

    H. Blackburn and D. S. Campbell. Trans. 8th Natl. Vacuum Symp., Pergamon Press, N.Y., 1961. p. 943.

12. R. H. Wade and J. Silcox. Appl. Phys. Letters 8: 7 (1966).

13. G. Morrison. Solar Cell Contact Deposition Parameter Study. First Quarterly Report, Contract No. NAS 5-11612 Goddard Space Flight Center, Nov. 1968.

14. L. Holland. Vacuum Deposition of Thin Films. John Wiley and Sons Inc., N.Y., 1960. p. 469.

15. A. D. McQuillan and M. K. McQuillan. Titanium. Butterworth's Scientific Publications, London,1956. p. 438 ff.

16. W. Roger Buck, III and Henry Leidheiser, Jr. Nature 181: 1681 (1958).

17. W. Roger Buck, III, Billy W. Sloope, and Henry Leidheiser, Jr. Corrosion 15: 26 (1959).

18. Milton Stern and Herman Wissenberg. Journ. Electrochem. Soc. 106: 755 (1959).

19. Milton Stern and Herman Wissenberg. Journ. Electrochem. Sox. 106: 759 (1959).

20. W. F. Springgate. Investigation into the Mechanism of Degradation of Solar Cells with Silver-Titanium Contacts First Quarterly Report, Contract No. NASW-1859, NASA Headquarters, June 1969.

21. H. Fisher and R. Gereth. New Aspects for the Choice of Contact Materials for Silicon Solar Cells. Seventh Voltaic Specialists Conference, Pasadena, Calif., Nov. 1968.

22. M. P. Lepselter. Bell Lab. Record 44: 298 (1966).

23. Lewis E. Terry and Richard W. Wilson, Proc. IEEE 57: 1580 (1969).

24. K. E. Haq, R. H. Behrndt, and Ilse Kobin. Journ. Vac. Sci. and Tech. 6: 148 (1969).

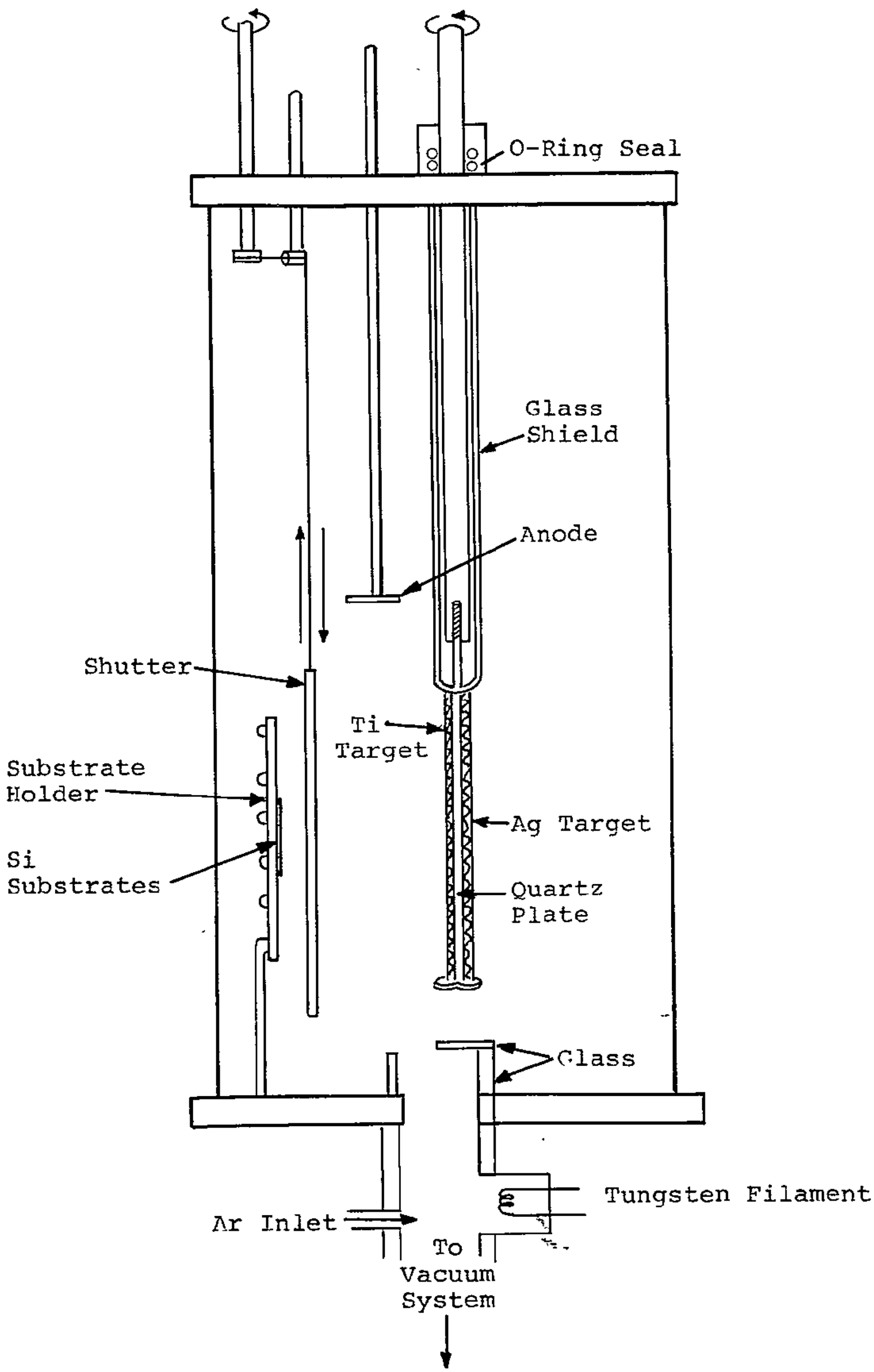

CONTRACT # NAS 5-11595 FINAL REPORT FIG. #1

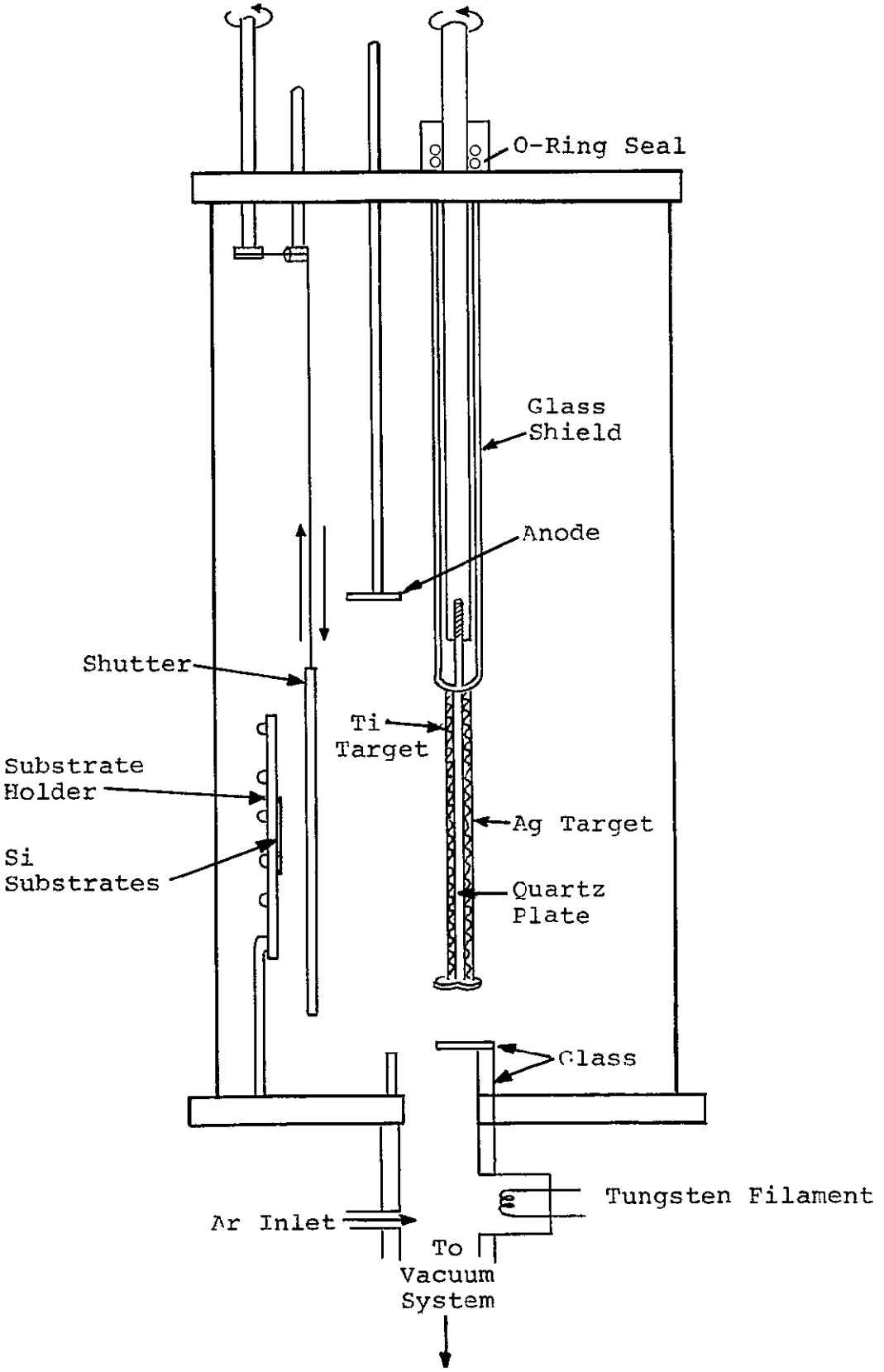
O-Ring Seal
Glass
Shield
Anode
Shutter
Ti
Target
Substrate
Holder
Si
Substrates
Ag Target
Quartz
Plate
Glass
Tungsten Filament
Ar Inlet
To
Vacuum
System

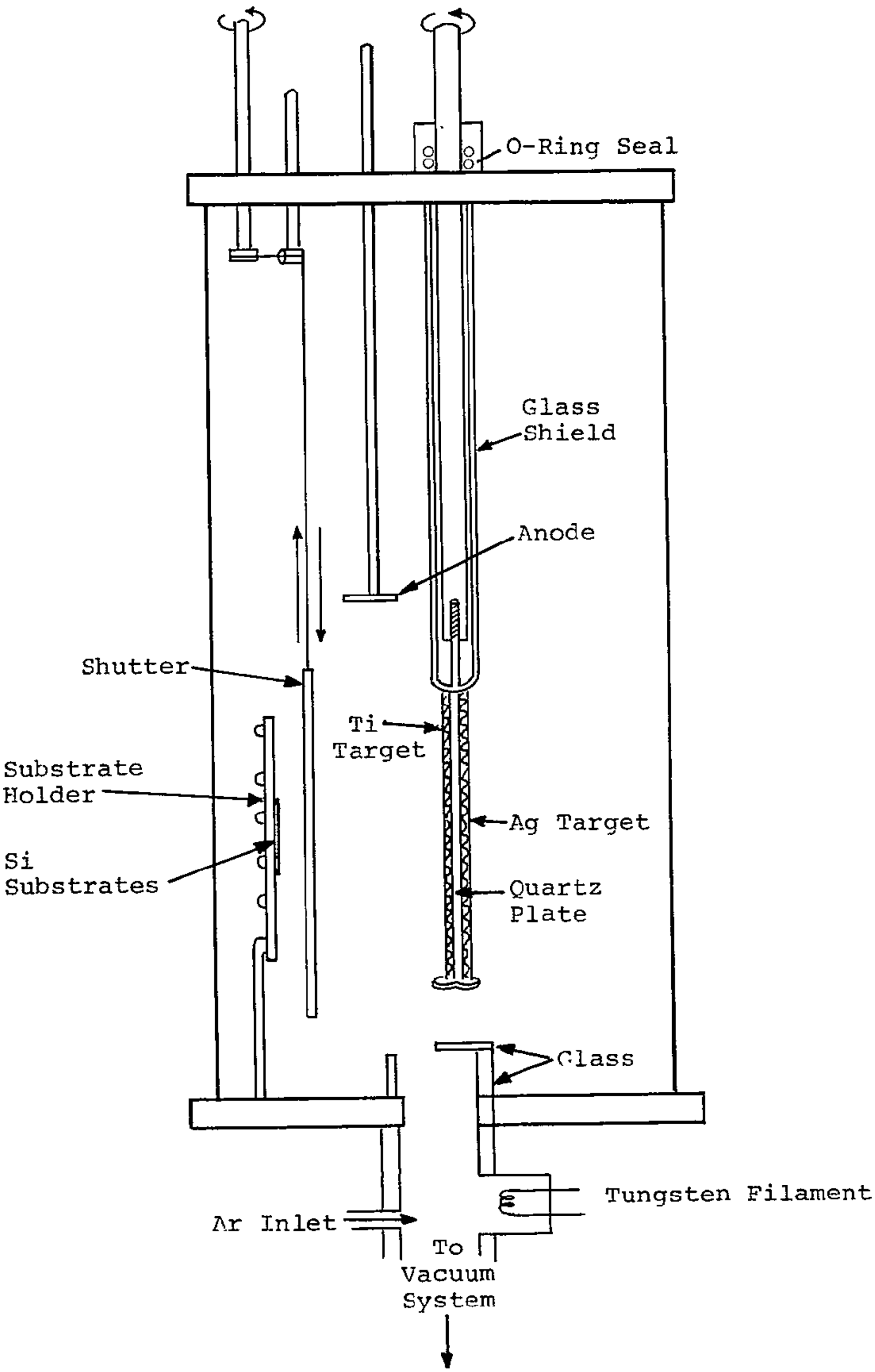

CONTRACT #NAS 5-11595 FINAL REPORT FIG #1

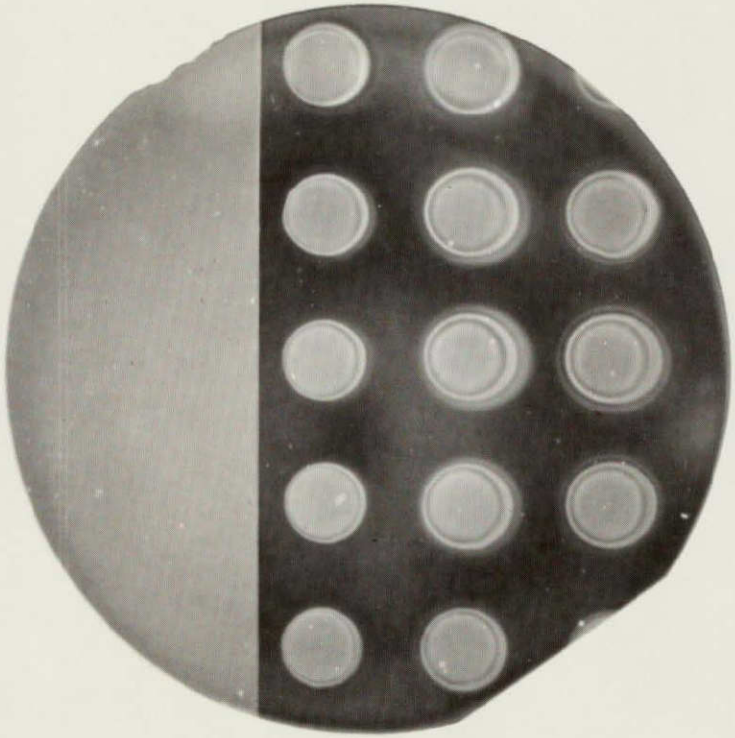

CONTRACT # NAS 5-11595 FINAL REPORT FIG # 2

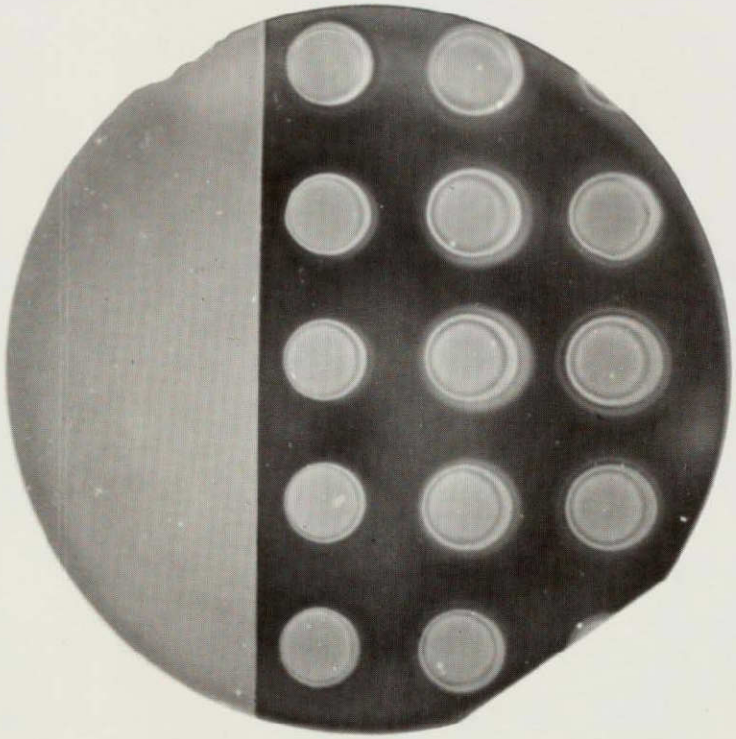

CONTRACT # NAS 5-11595 FINAL REPORT FIG # 2

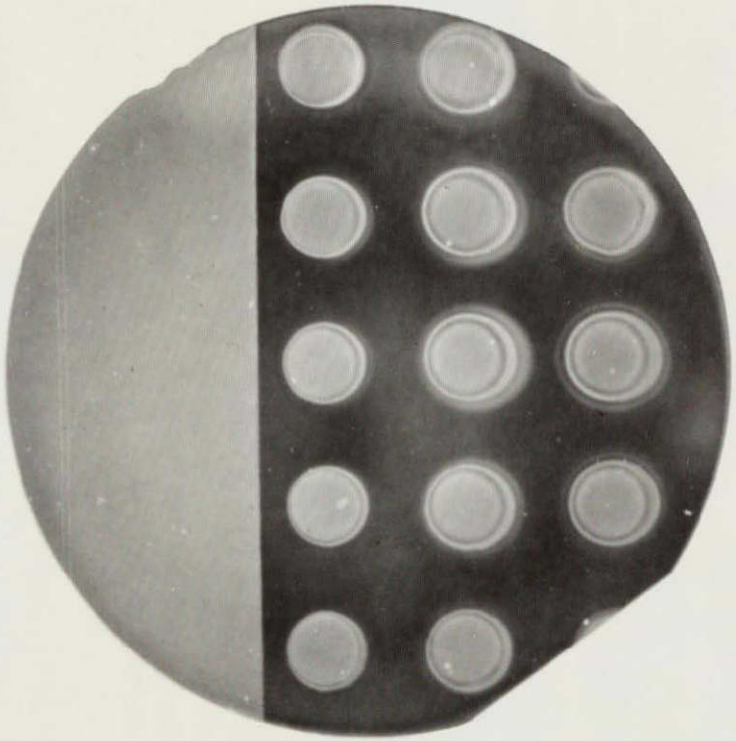

CONTRACT # NAS 5-11595 FINAL REPORT FIG # 2

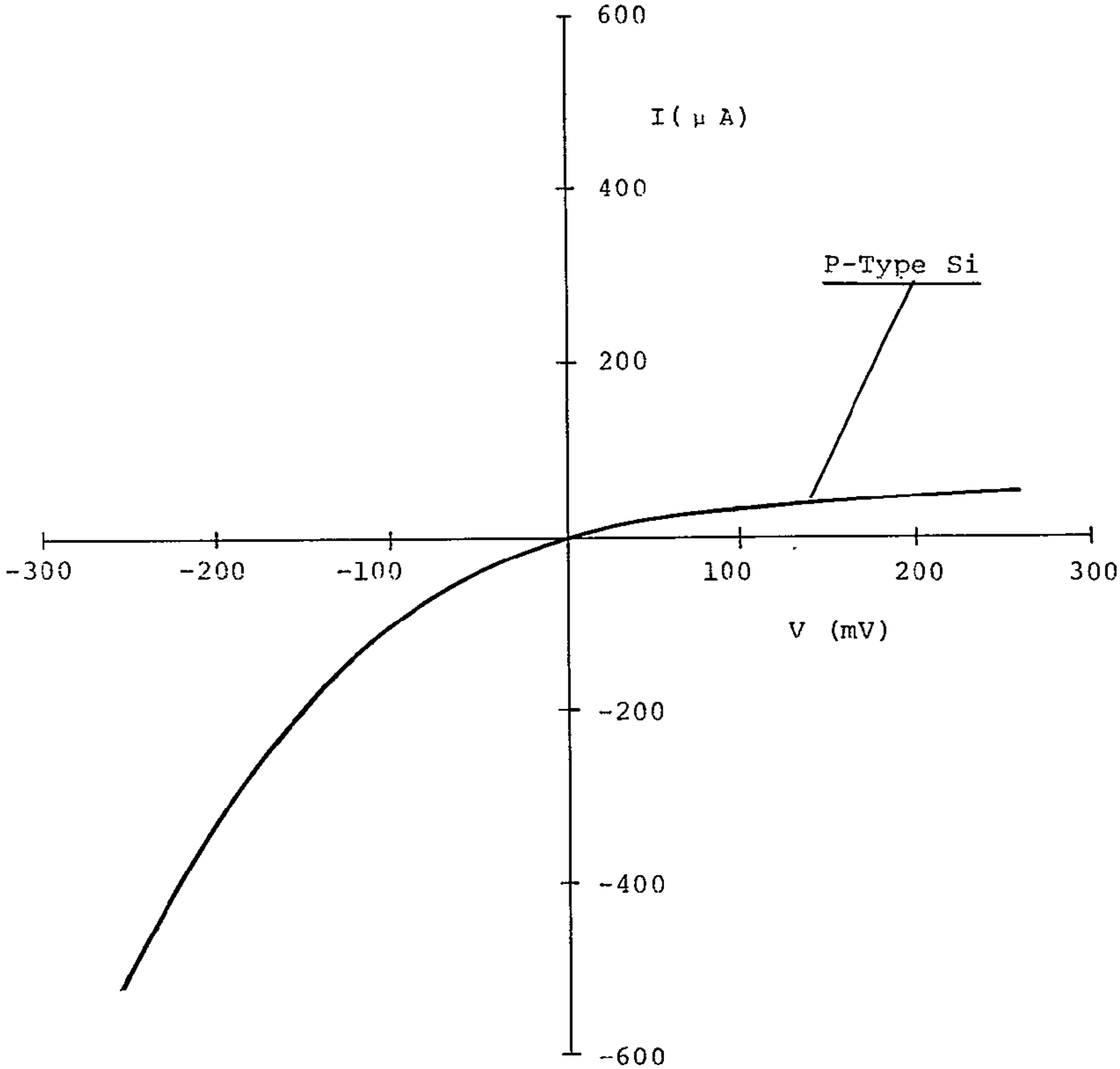

CONTRACT #NAS 5-11585 FINAL REPORT FIG. #3

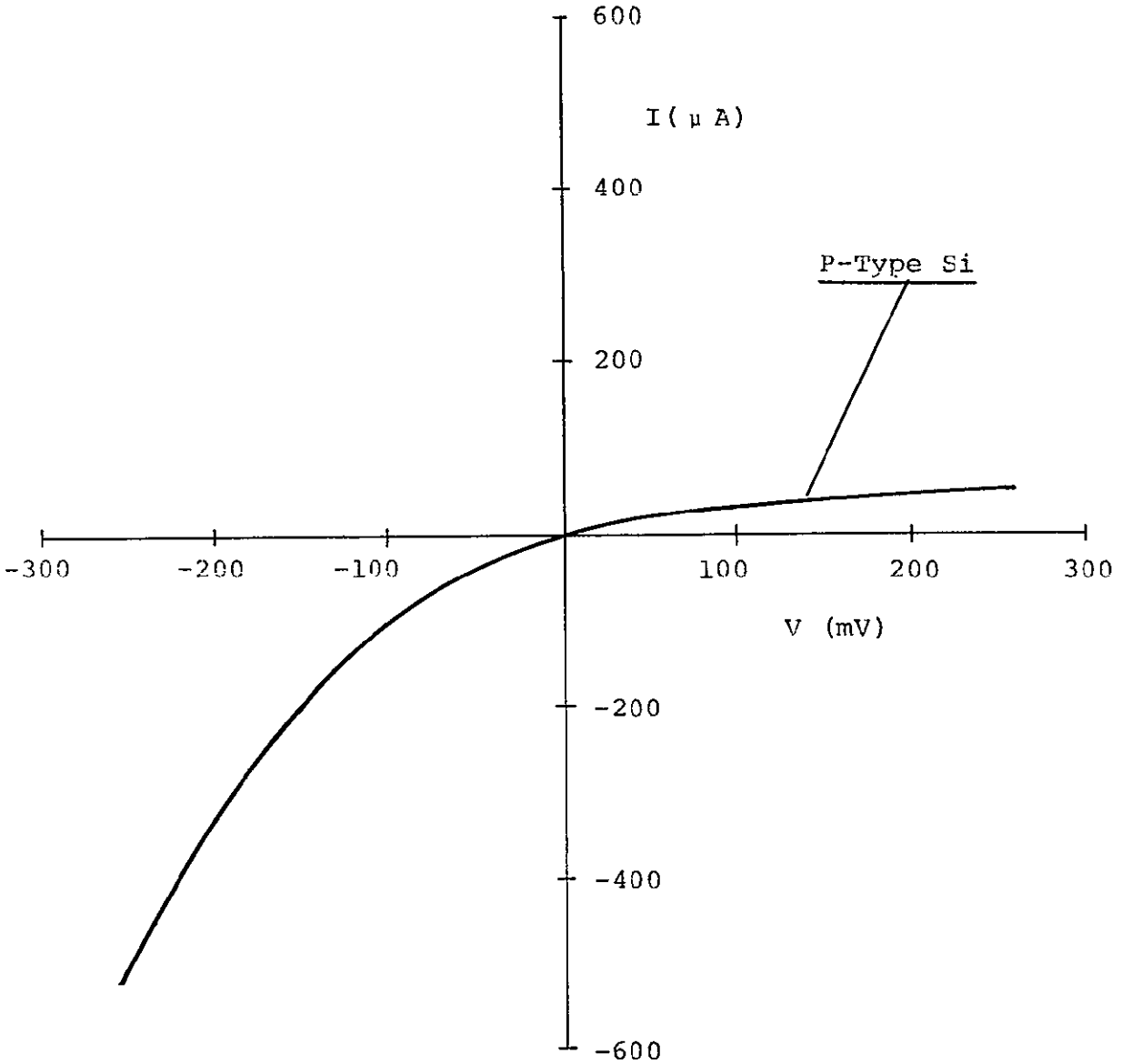

CONTRACT #NAS5-11595 FINAL REPORT FIG #3

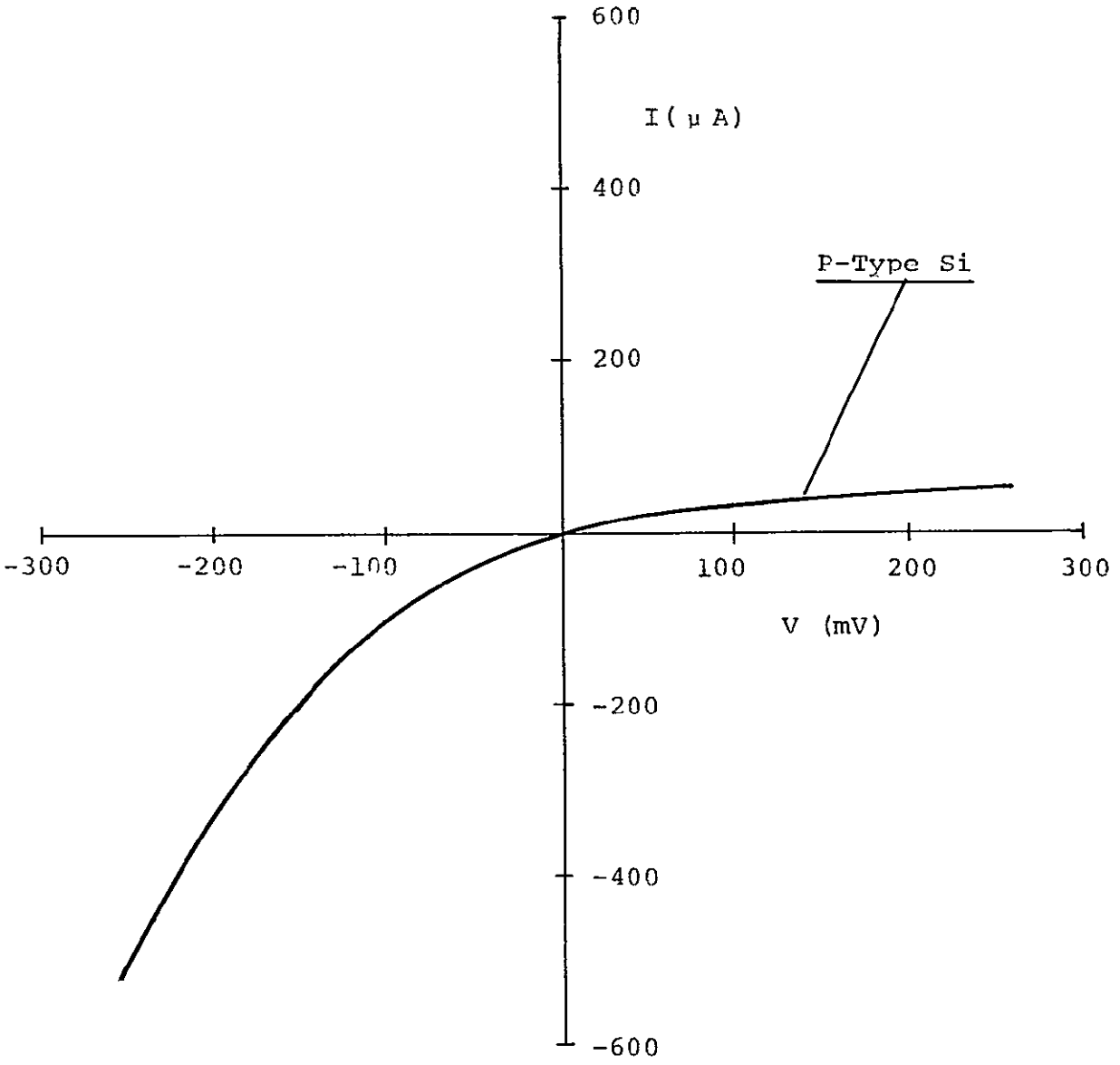

Contract #NAS 5-11545 Final Report Fig. 3

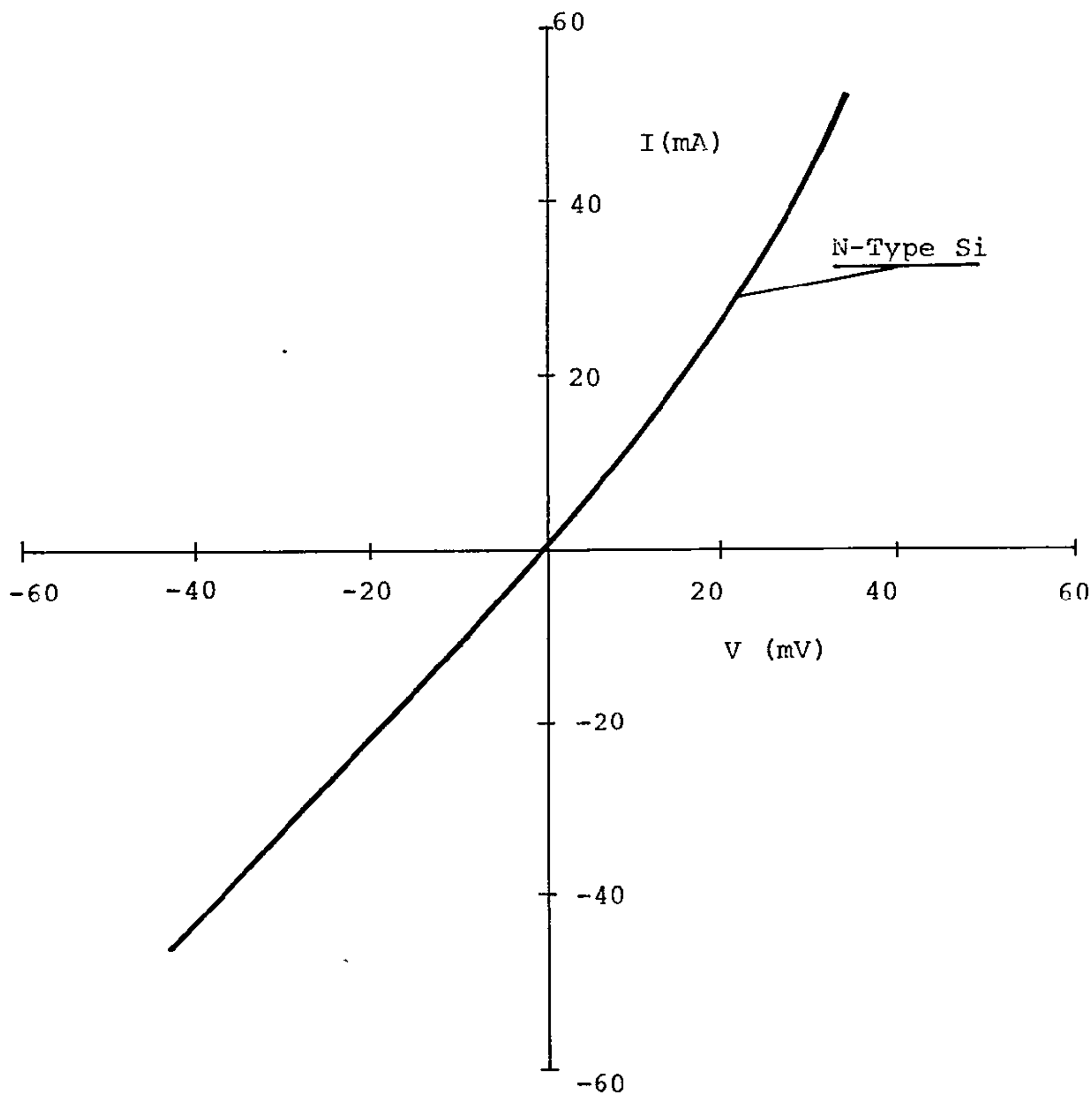

CONTRACT #NAS 5-11595 FINAL REPORT FIG #3A

60
I(mA)
40
N-Type Si
20
-60
-40
-20
20
40
60
V (mV)
-20
-40
-60

Contract #NAS 5-11585 Final Report Fig. #3a

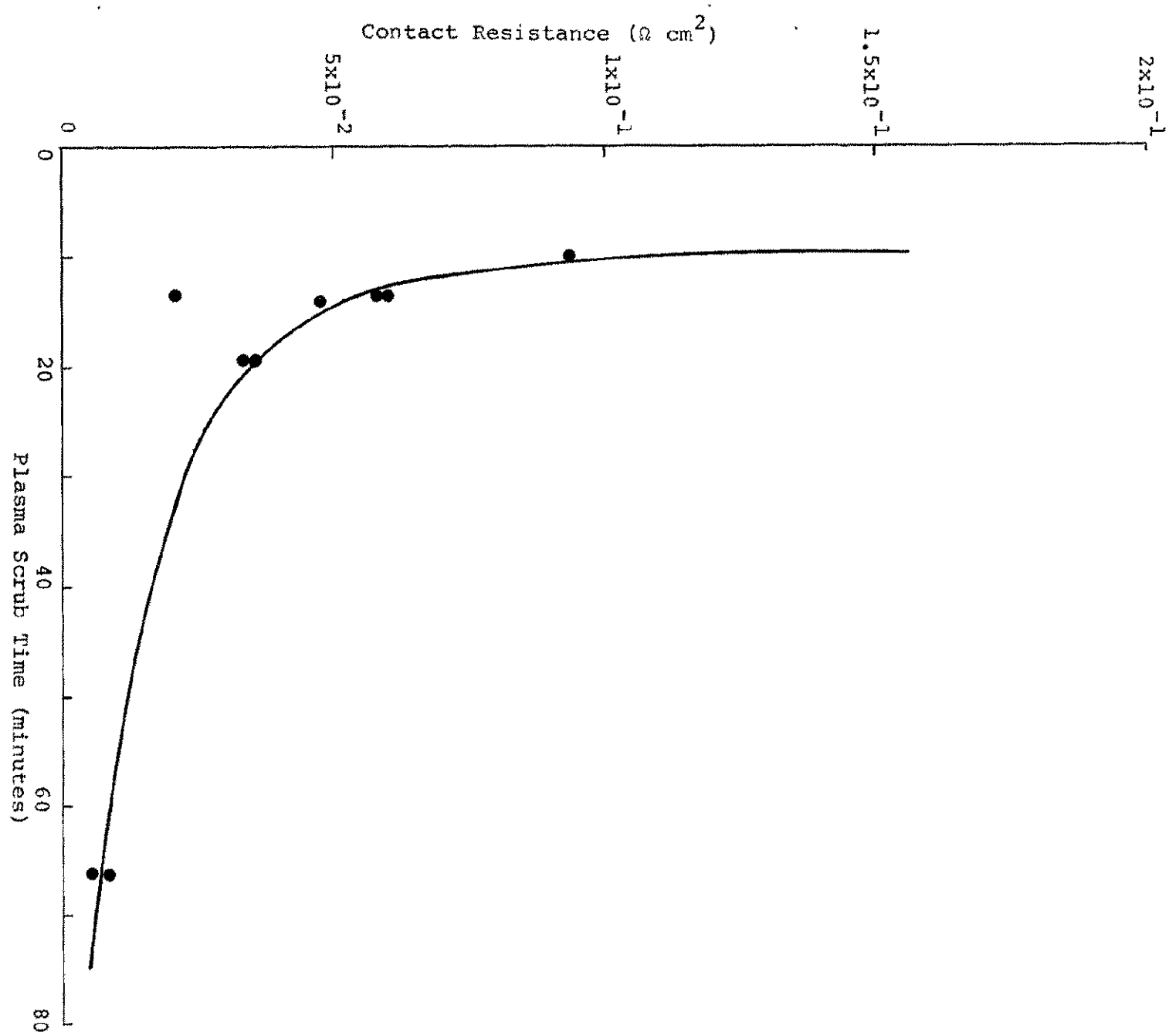

CONTRACT # NAS 5-11595 FINAL REPORT FIG # 4

Contact Resistance of Gold Stripes Versus Plasma Scrub Time

CONTRACT # NAS 5-11585 FINAL REPORT FIG. # 11

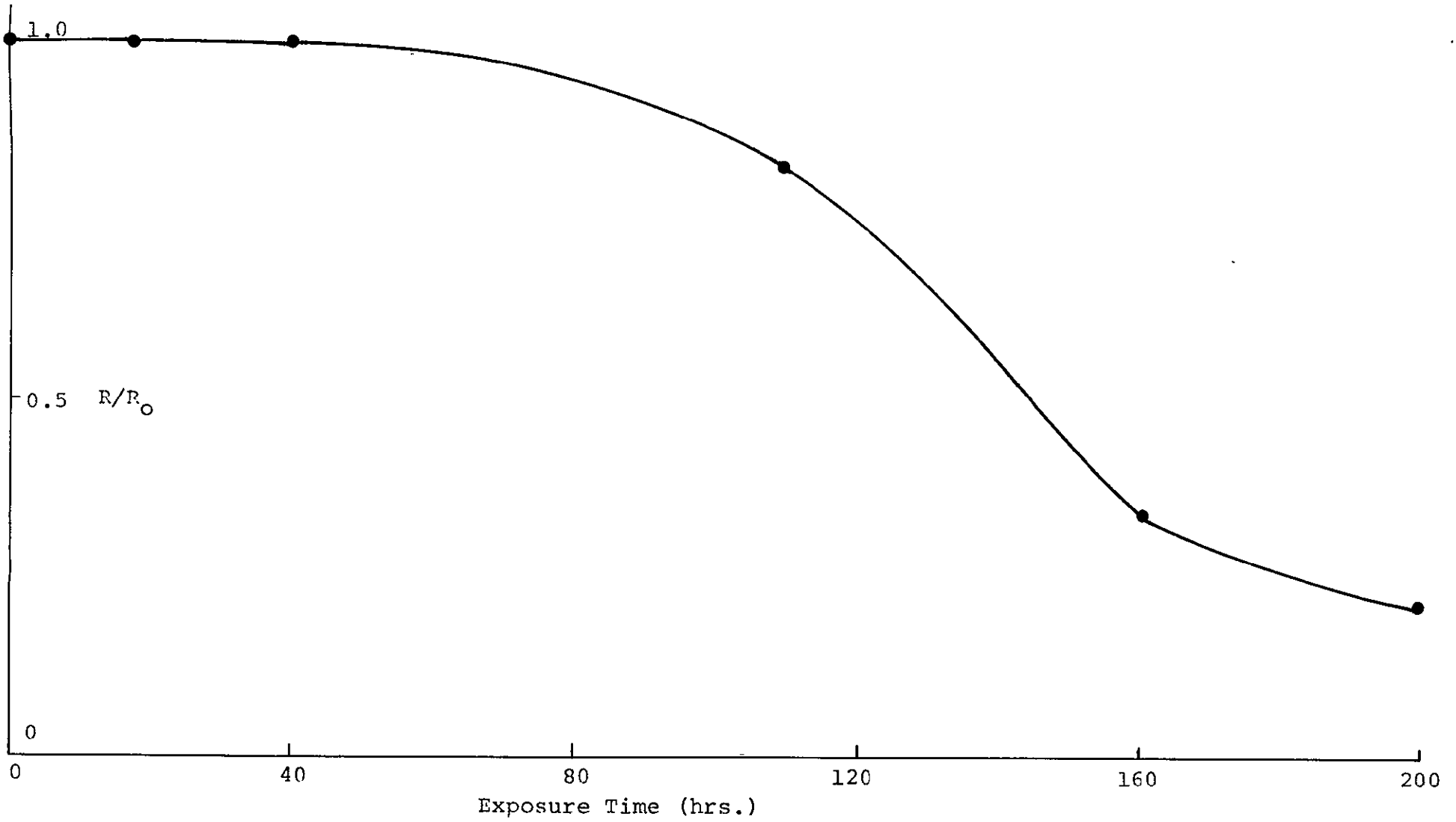

Contract # NAS 5-11595 Final Report - Fig # 5

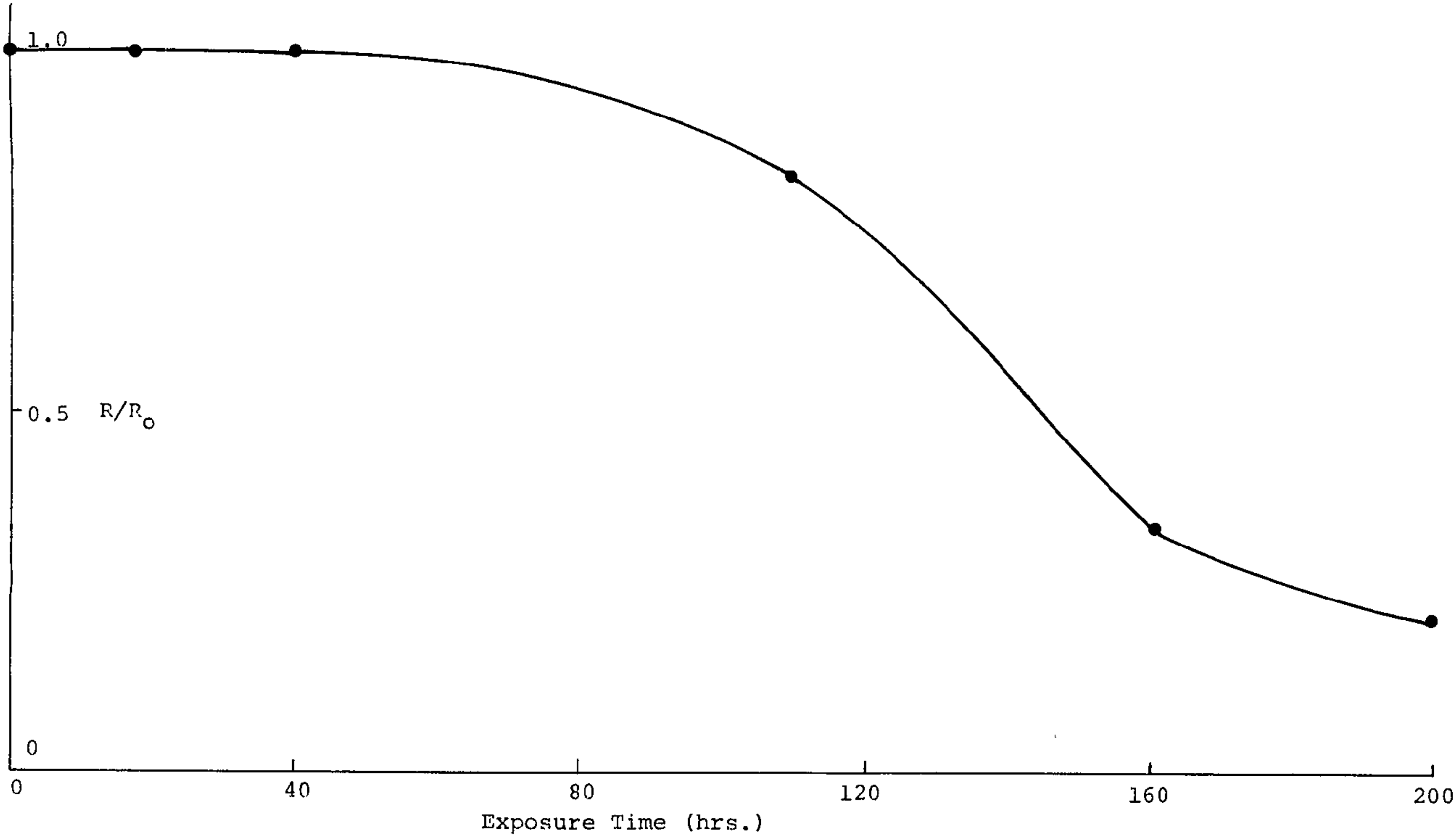
1.0
0.5
R/R_o
0
0
40
80
120
160
200
Exposure Time (hrs.)

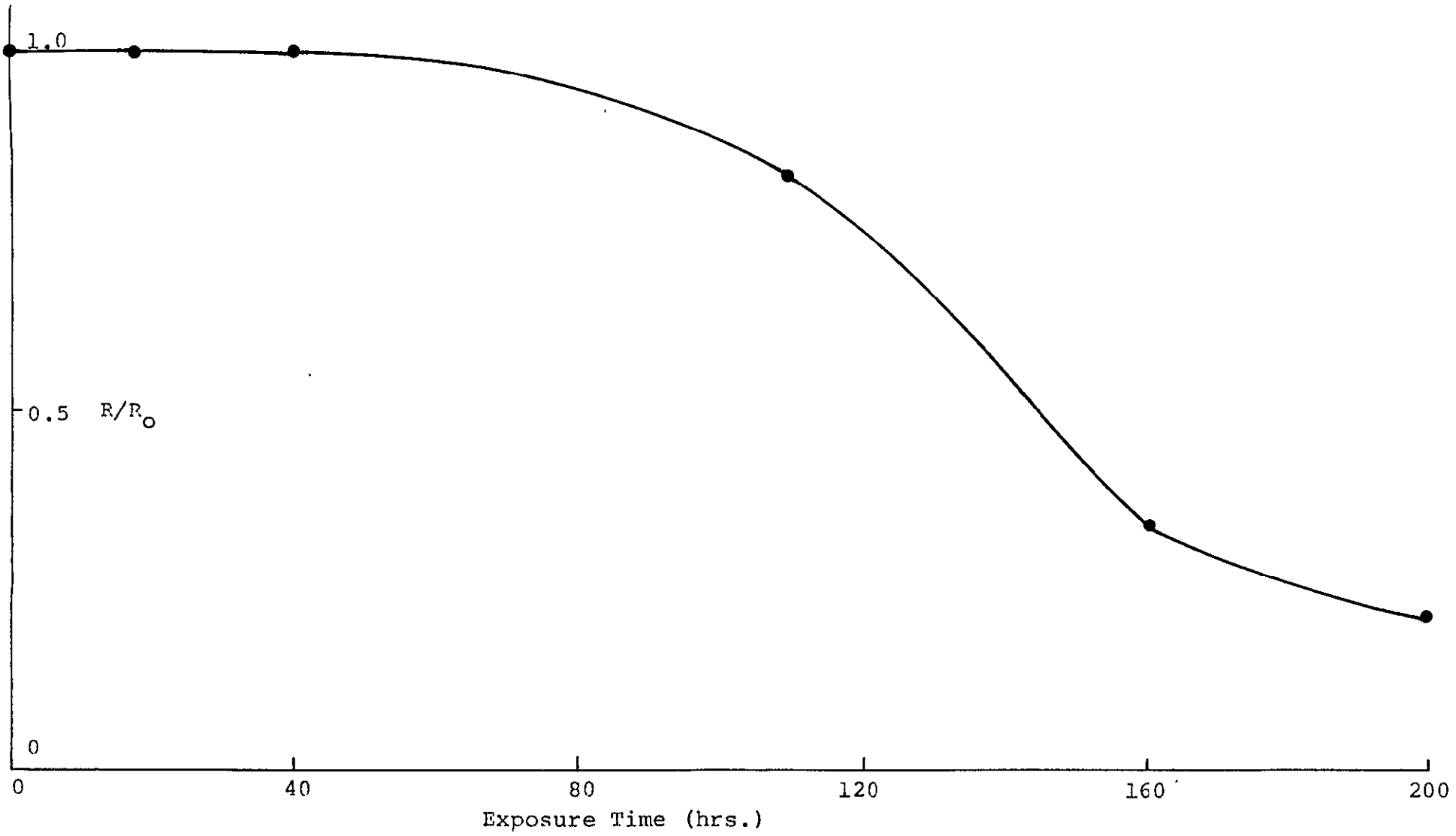

CONTRACT # NAS 5-11525 FINAL REPORT FIG # 5

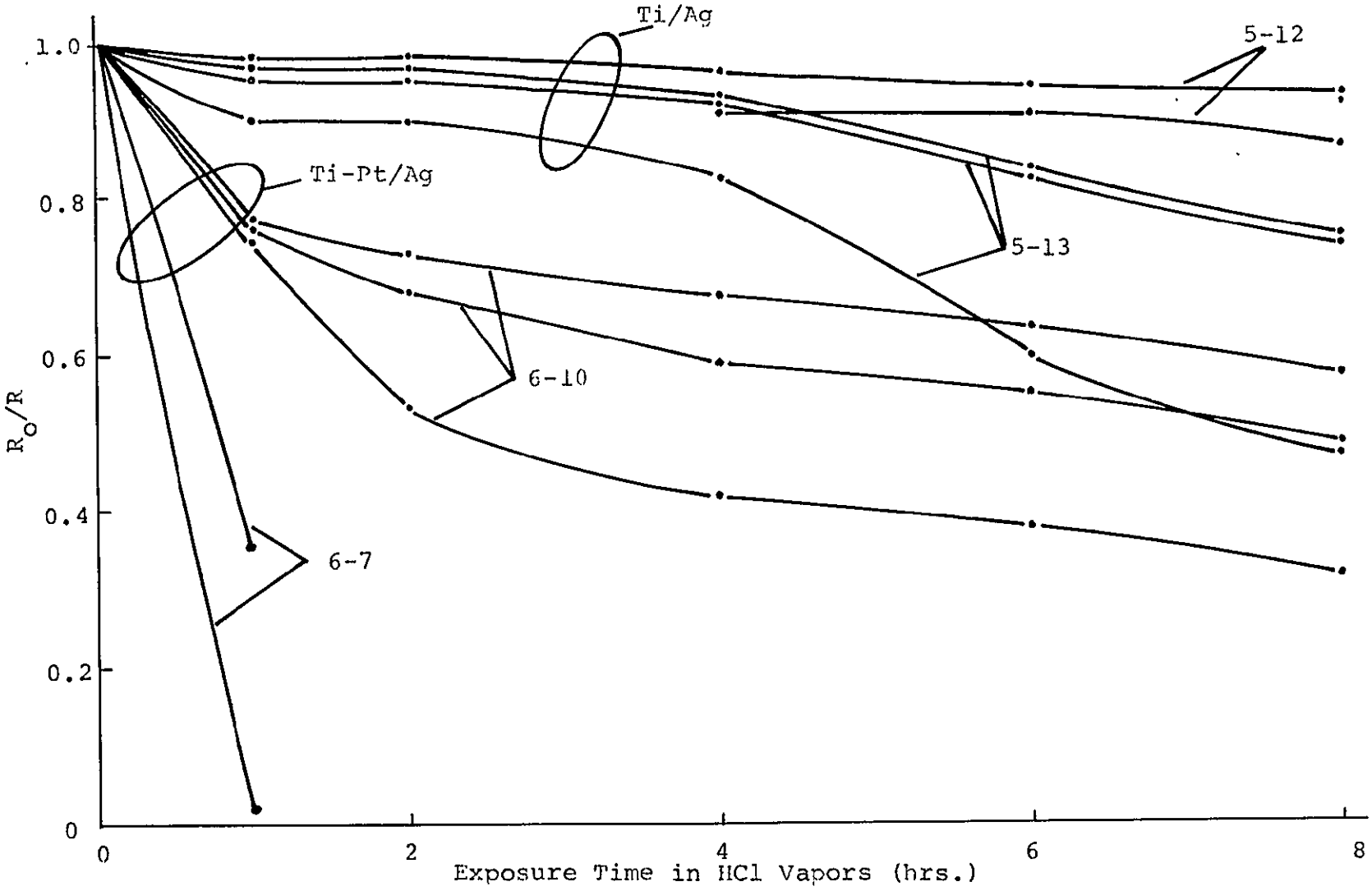

CONTRACT # NAS 5-11595 FINAL REPORT - FIG # 6

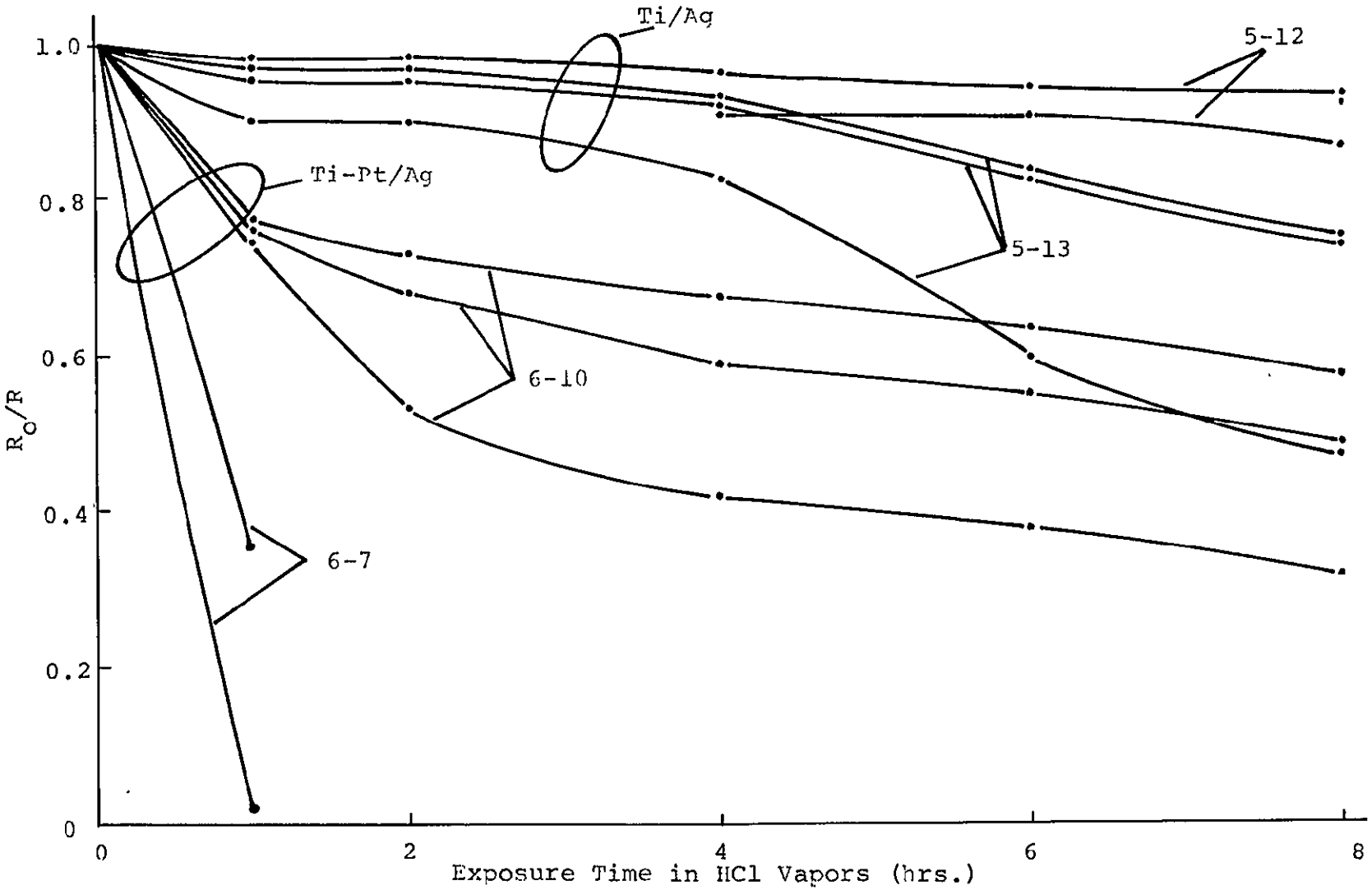

CONTRACT # NAS 5-11595 FINAL REPORT FIG # 6

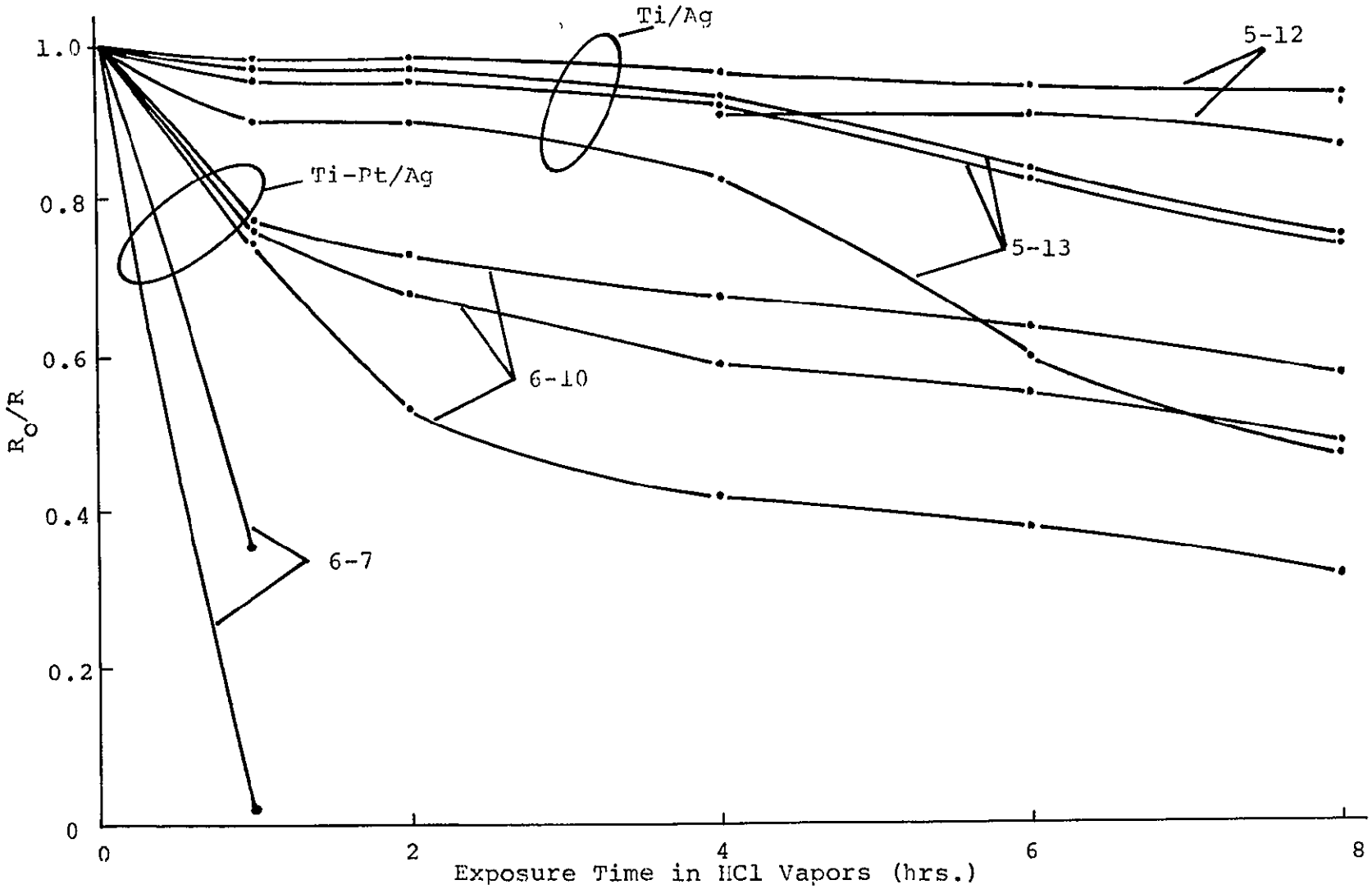

CONTRACT # NAS 5-11595 FINAL REPORT . FIG # 6

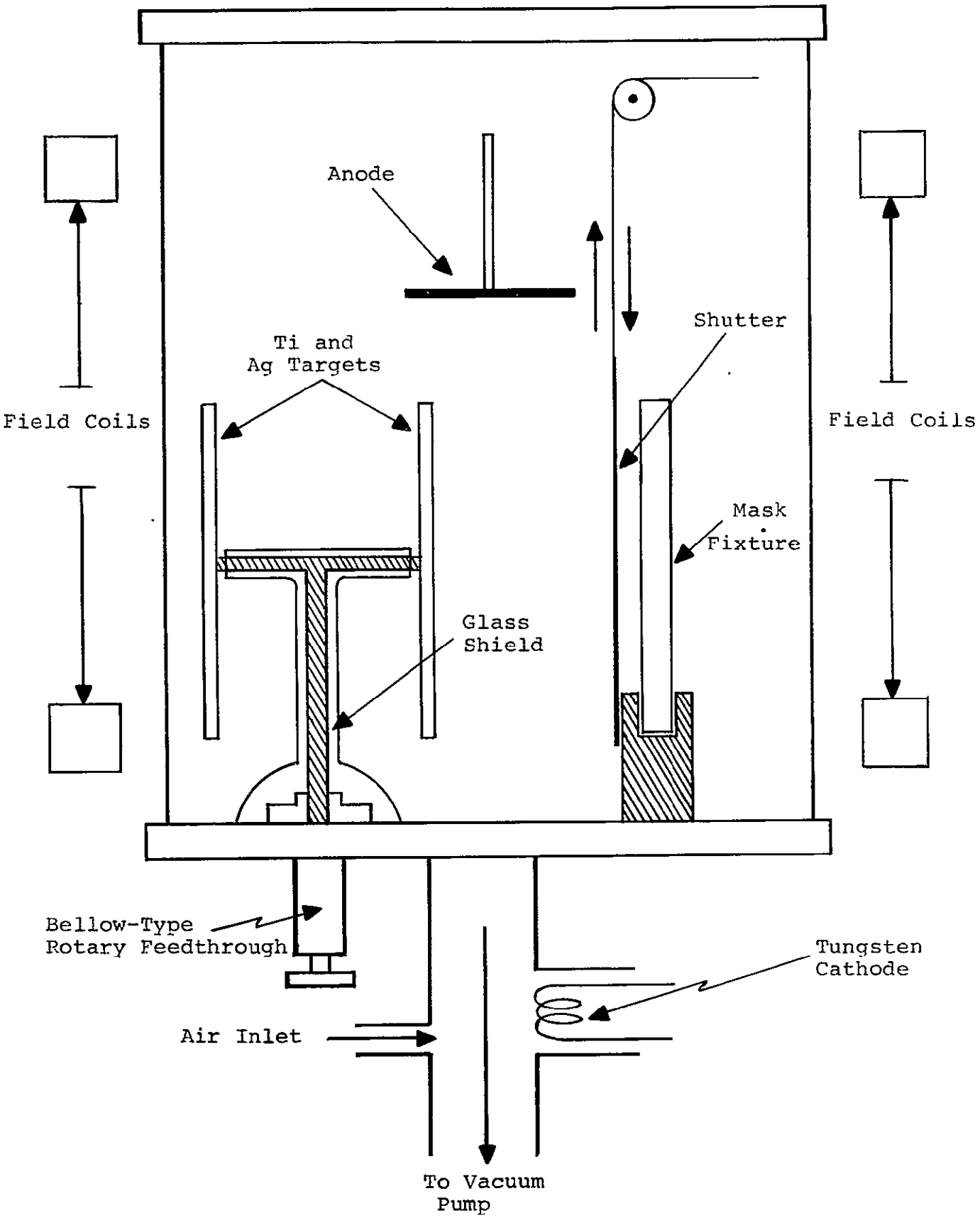

Contract # NAS 5-11595 Final Report Fig # 7

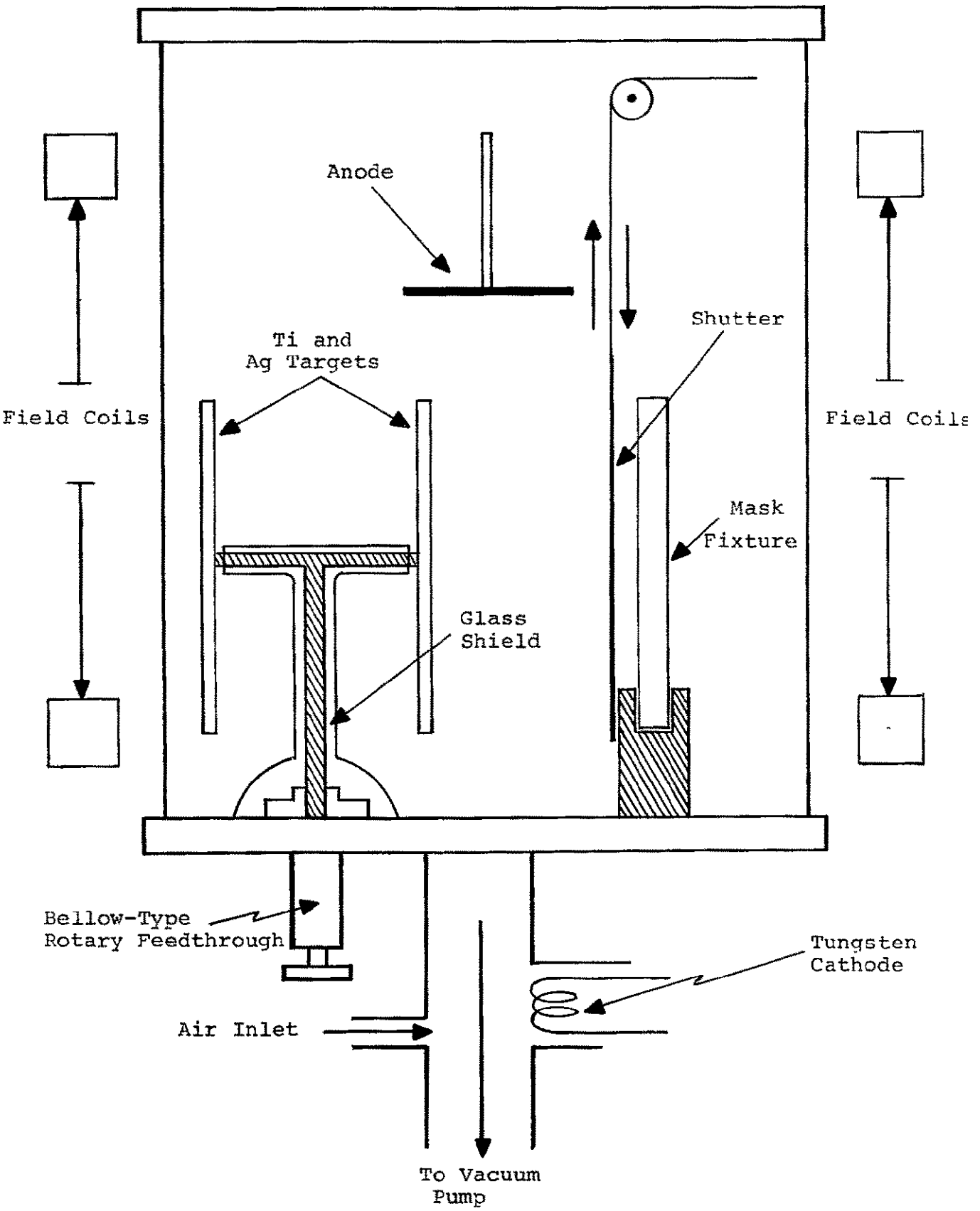
Anode
Shutter
Ti and
Ag Targets
Field Coils
Field Coils
Mask
Fixture
Glass
Shield
Bellow-Type
Rotary Feedthrough
Tungsten
Cathode
Air Inlet
To Vacuum
Pump

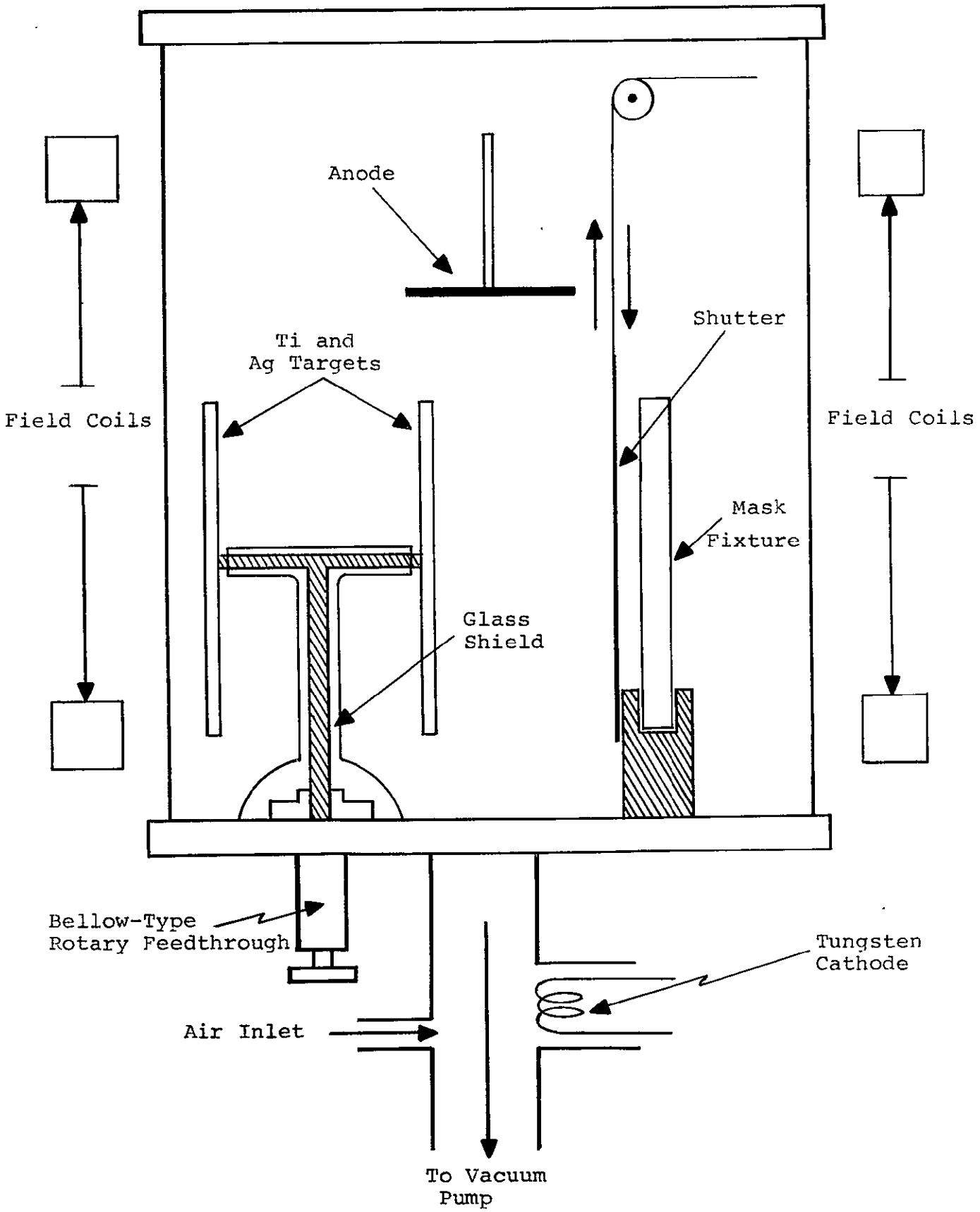
Anode
Shutter
Ti and
Ag Targets
Field Coils
Field Coils
Mask
Fixture
Glass
Shield
Bellow-Type
Rotary Feedthrough
Tungsten
Cathode
Air Inlet
To Vacuum
Pump

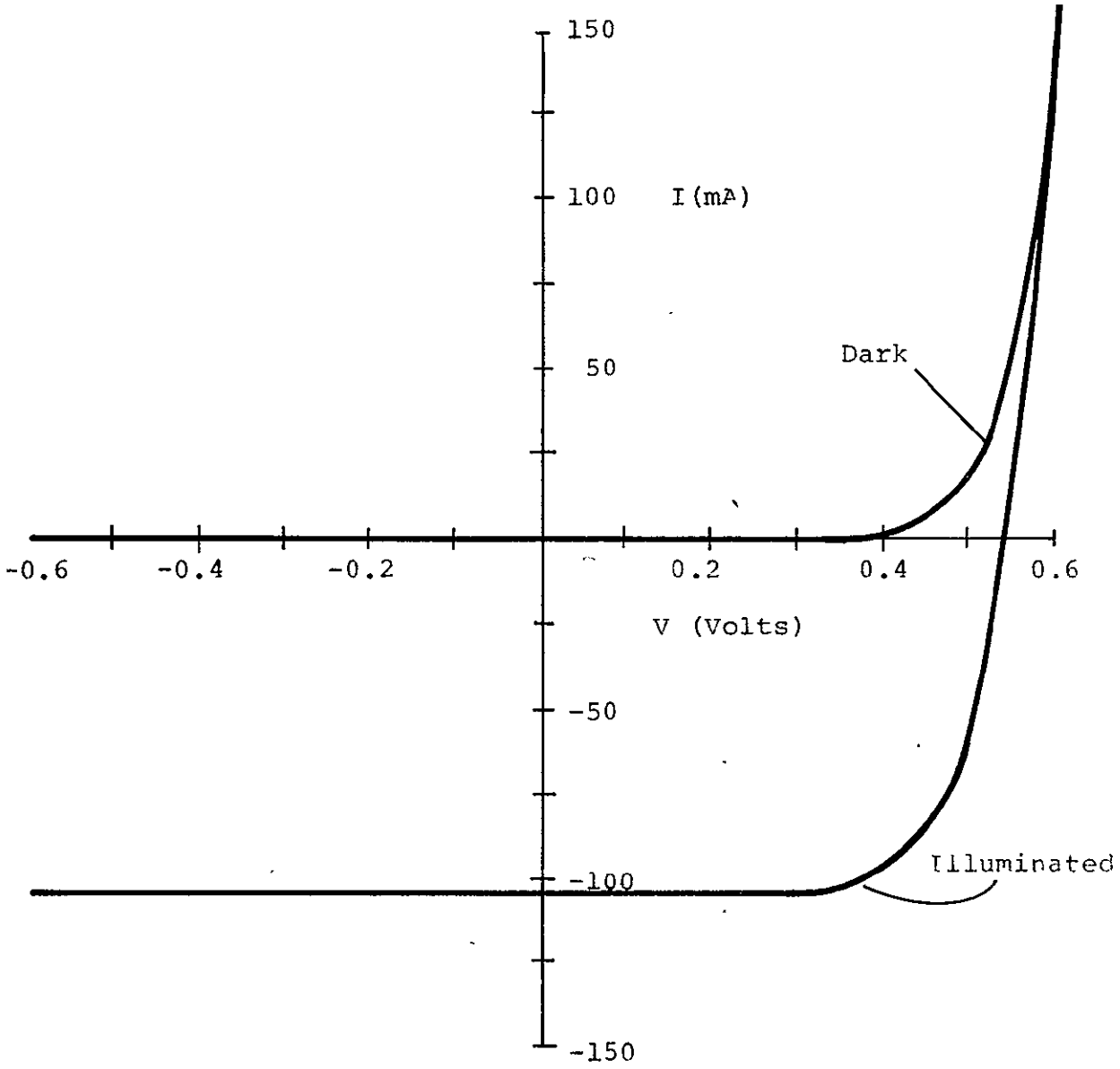

Fig #8A

Final Report

Contract #NAS5-11595

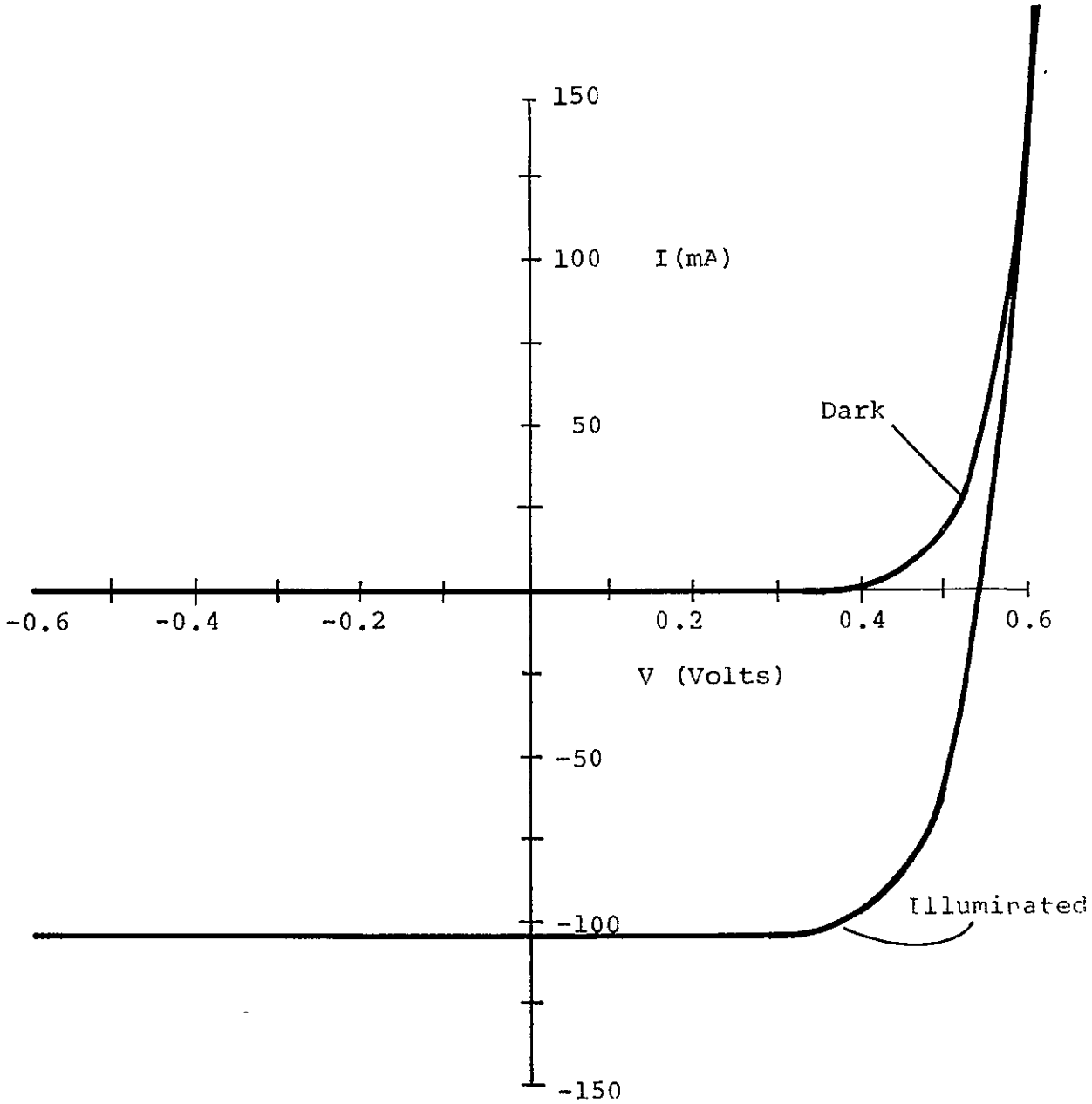
150
100
I(mA)
50
Dark
-0.6
-0.4
-0.2
0.2
0.4
0.6
V (Volts)
-50
-100
Illumirated
-150

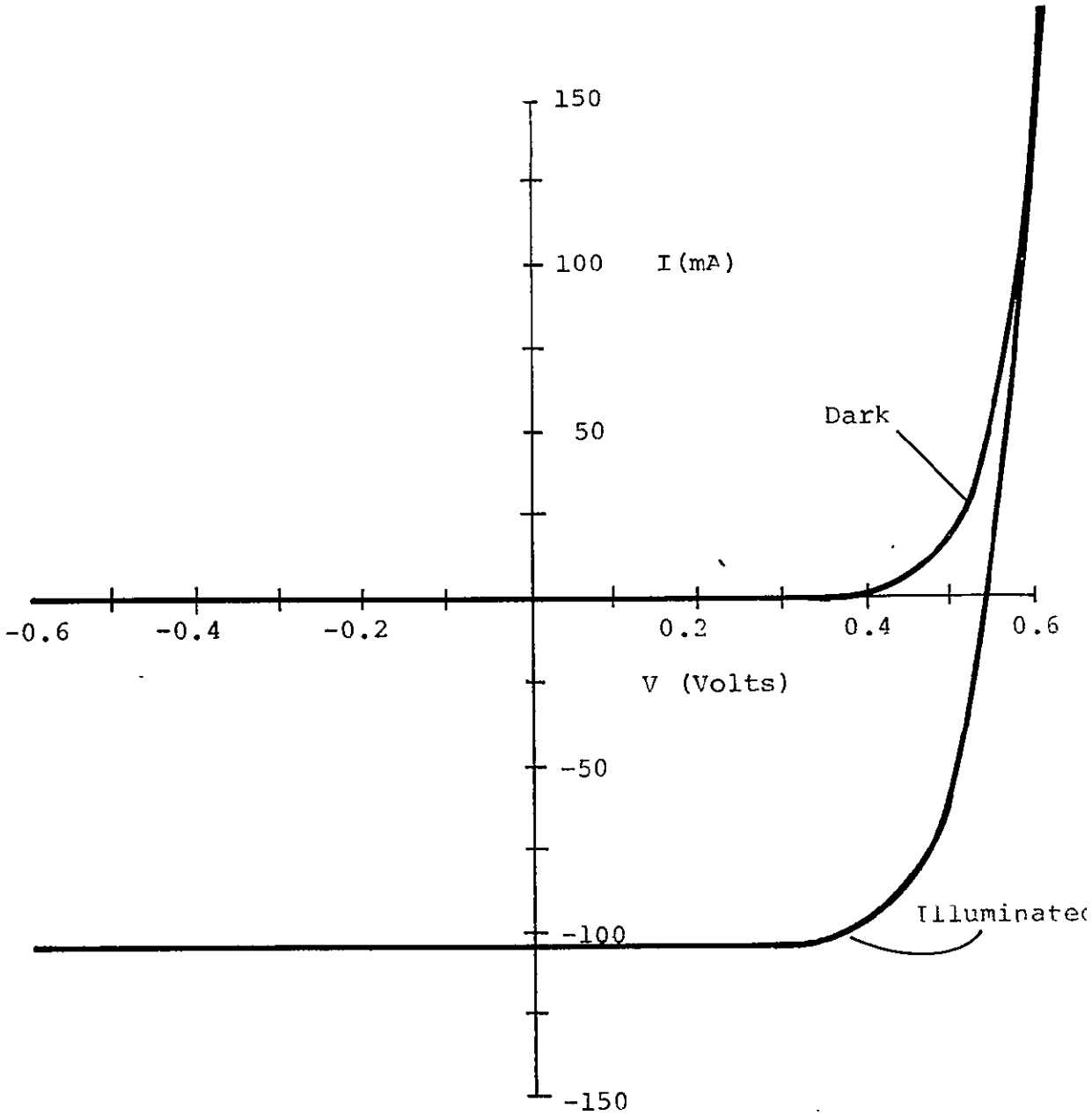
150
100
I(mA)
50
Dark
-0.6
-0.4
-0.2
0.2
0.4
0.6
V (Volts)
-50
-100
Illuminated
-150

Contact # NAS 5-11570 Final Report Fig # 8 B

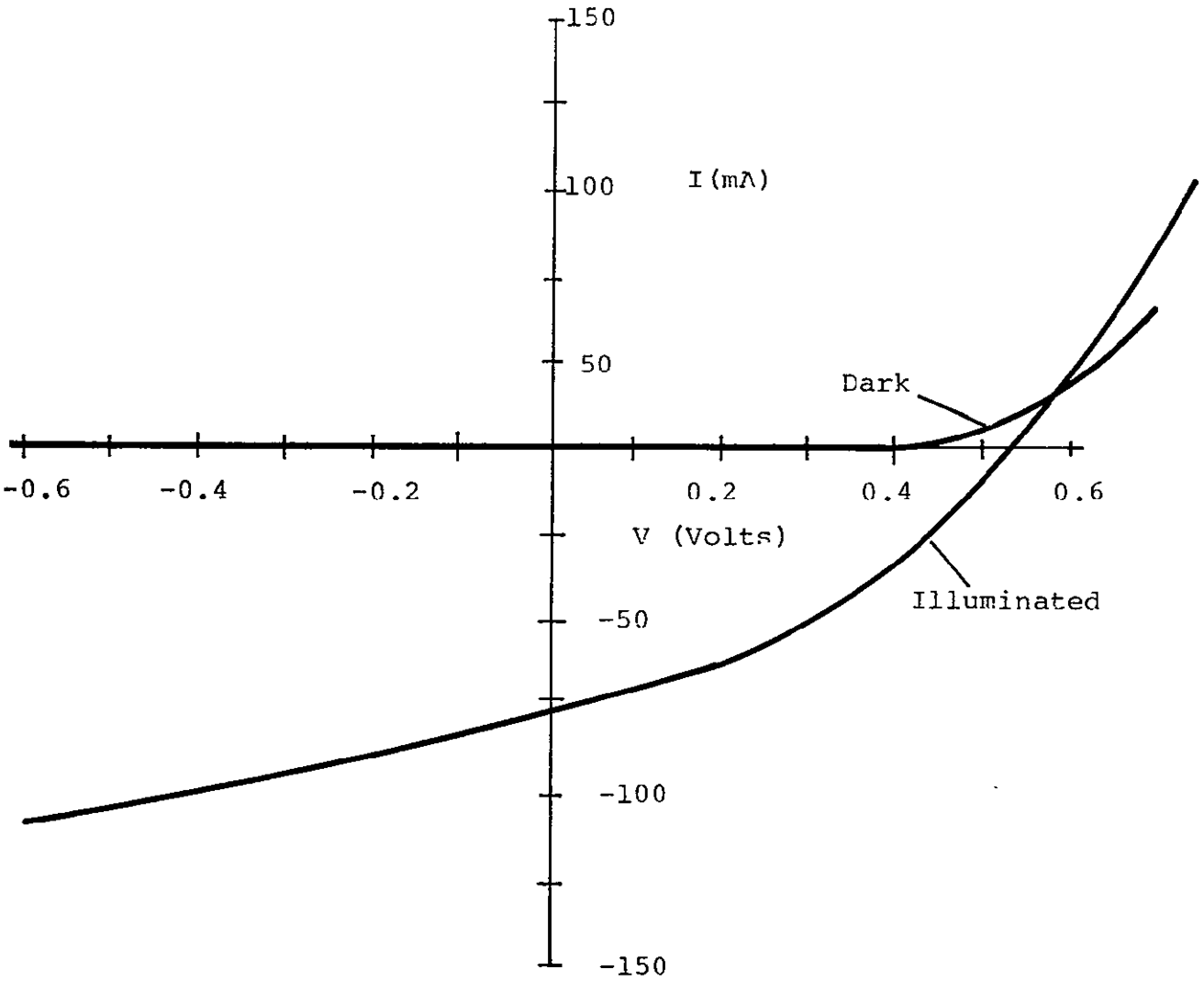
150
100
I(mA)
50
Dark
-0.6
-0.4
-0.2
0.2
0.4
0.6
V (Volts)
Illuminated
-50
-100
-150

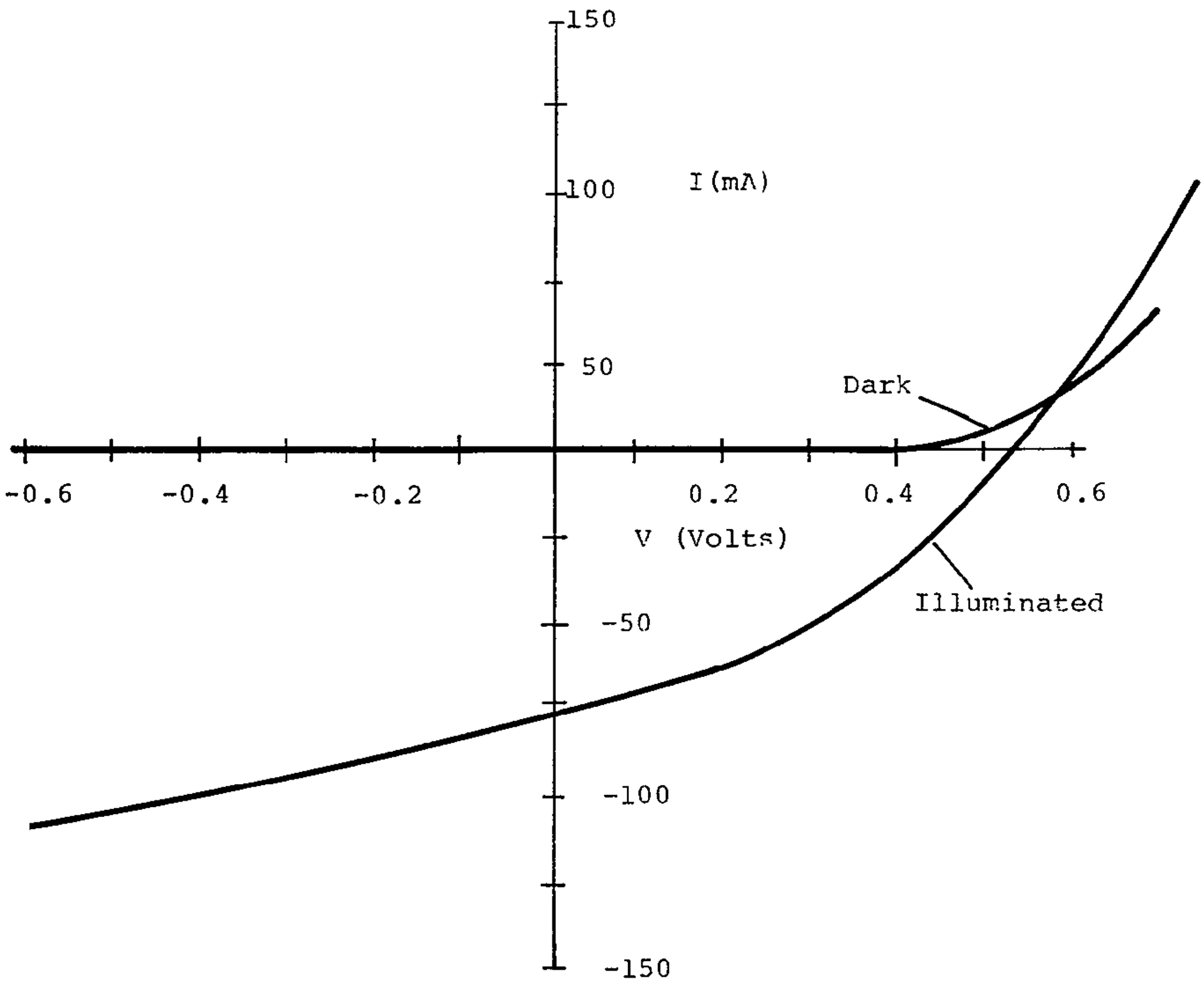

CONTRACT # NAS 5-115[illegible] FINAL REPORT FIG # 8 B

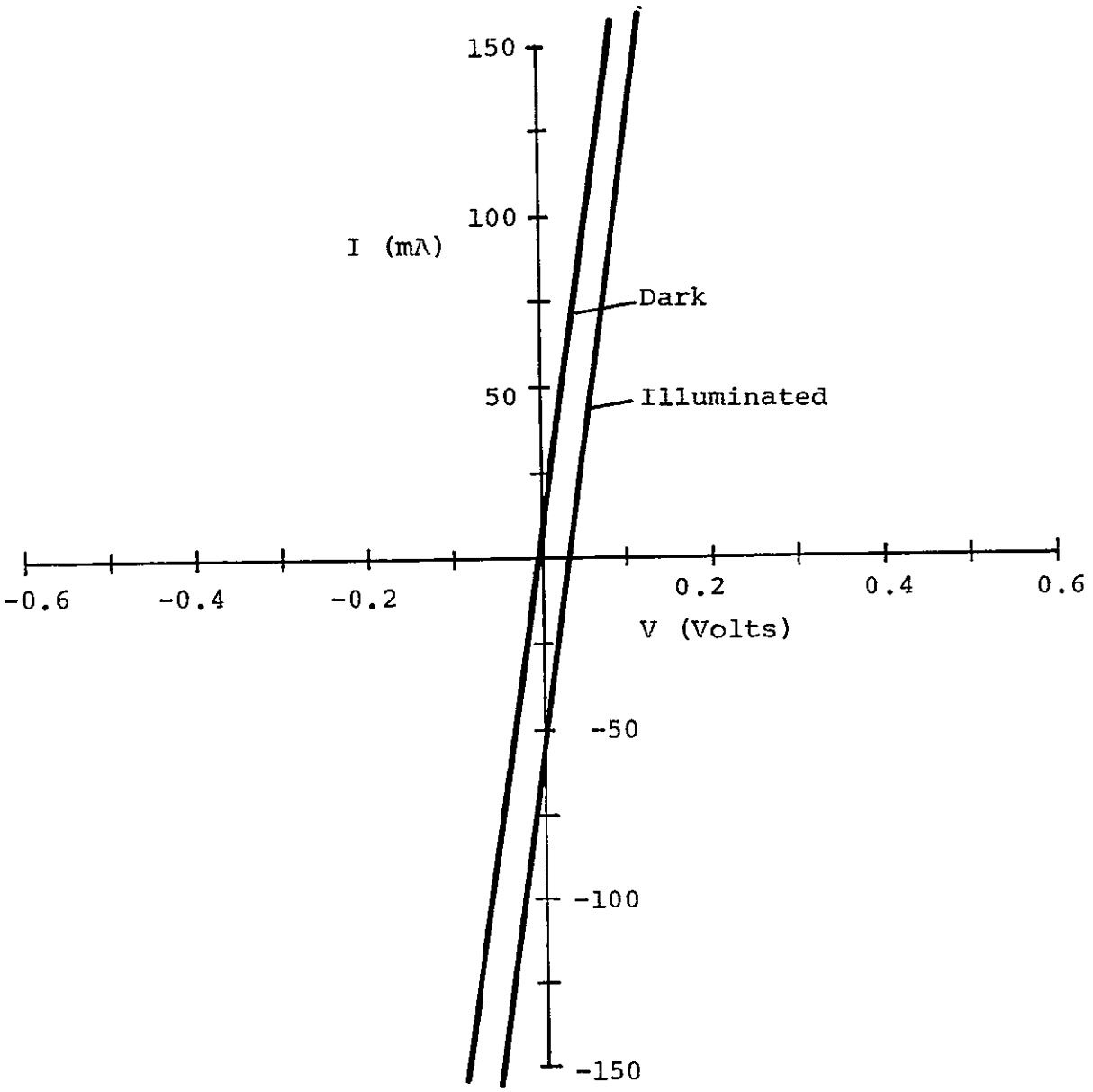

Contract #NAS 5-11532 Final Report Fig #8c

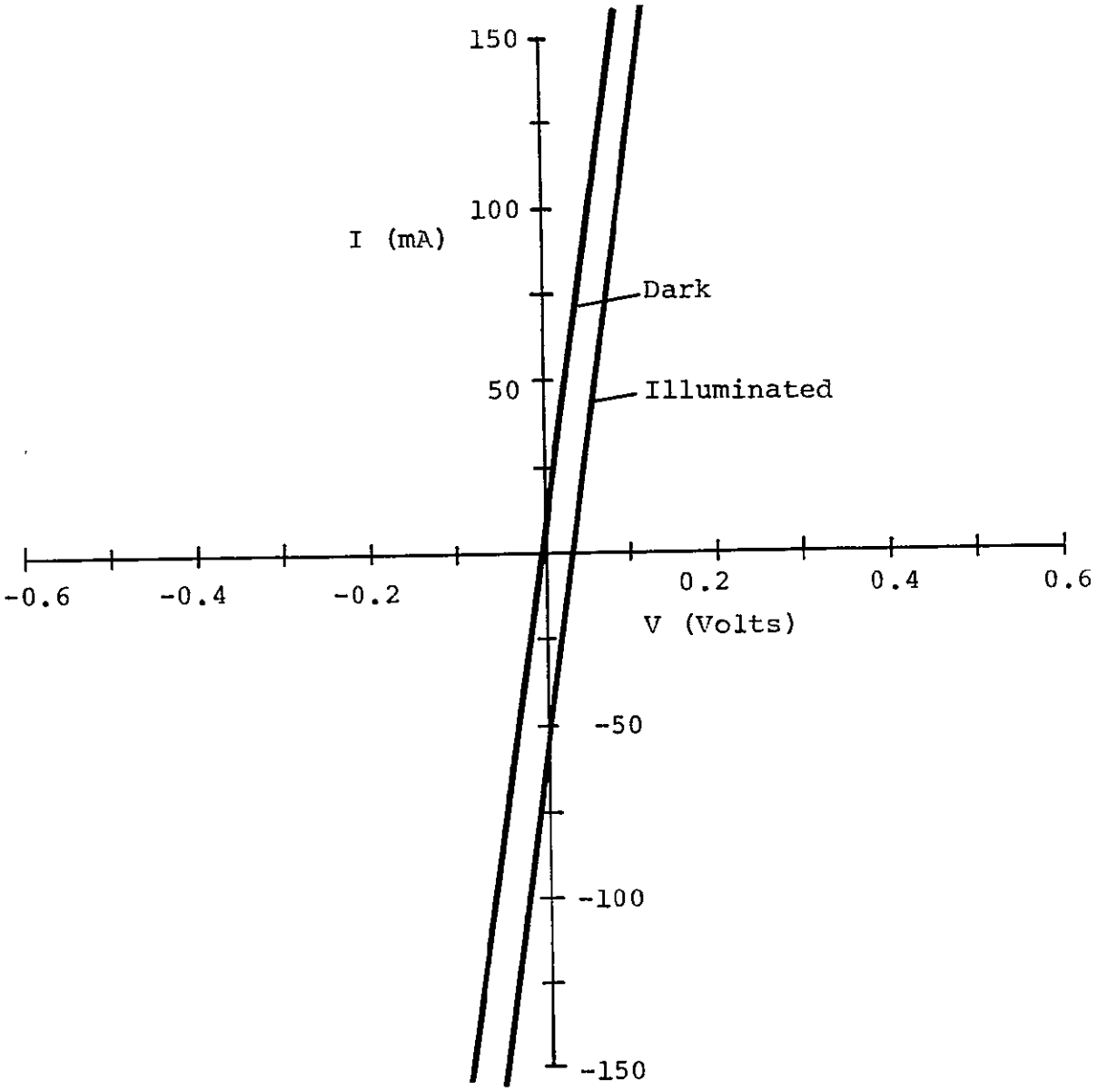
150
100
I (mA)
Dark
50
Illuminated
-0.6
-0.4
-0.2
0.2
0.4
0.6
V (Volts)
-50
-100
-150

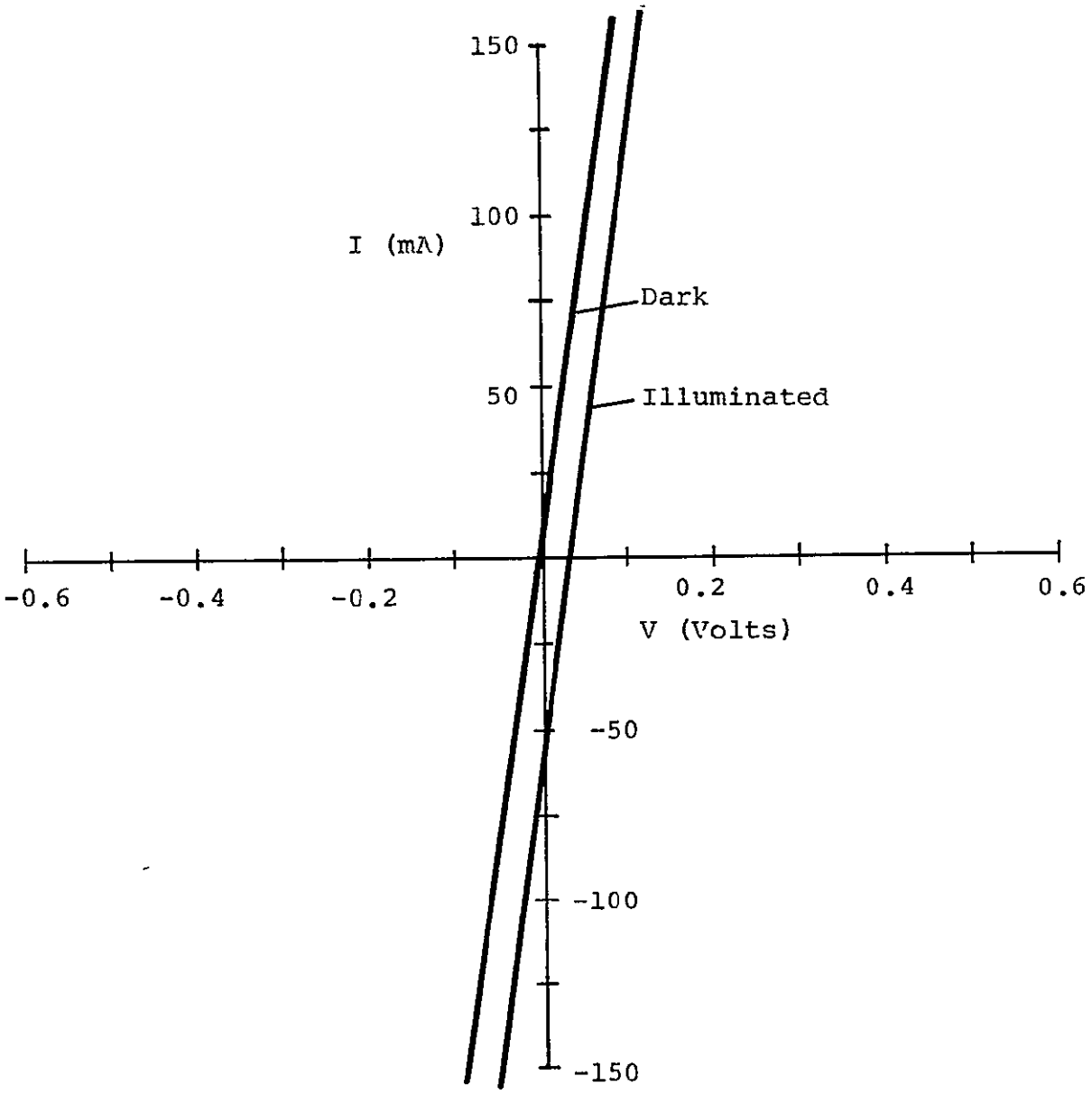

CONTRACT # NAS 5-11585 FINAL REPORT FIG # 8c

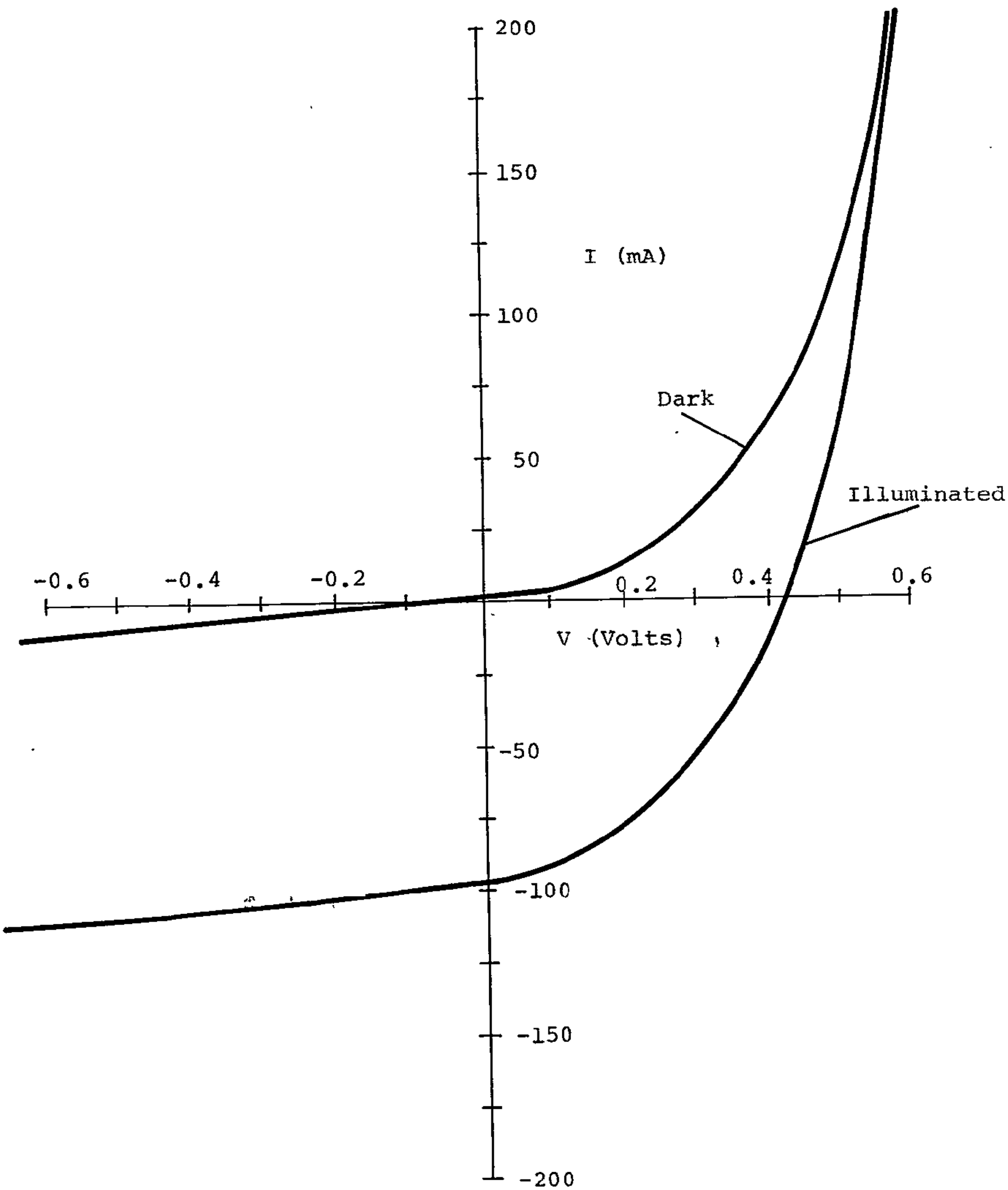

CONTRACT # NAS 5-11595 FINAL REPORT FIG # 9

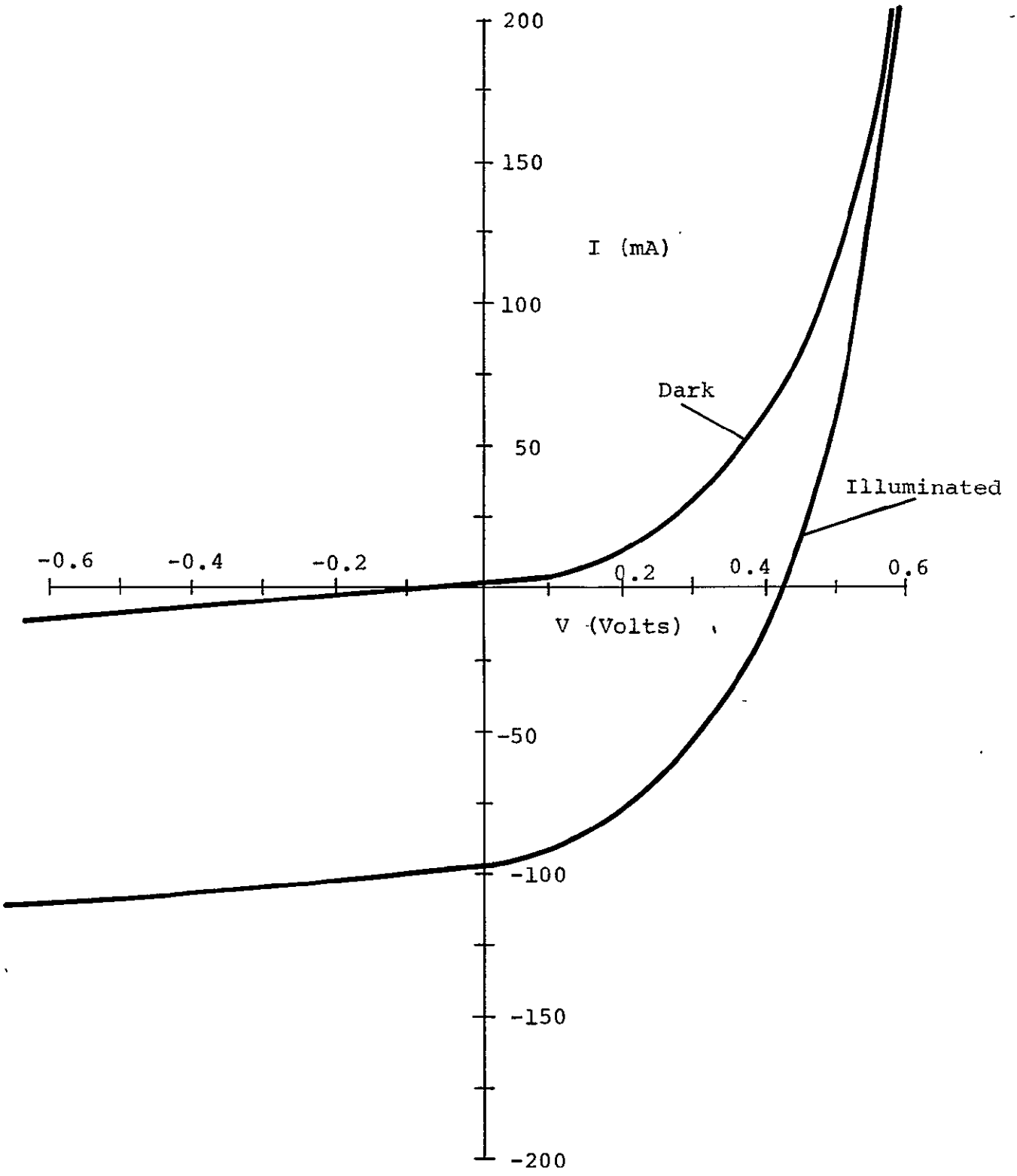

CONTRACT # NAS5-11595 FINAL REPORT FIG #9

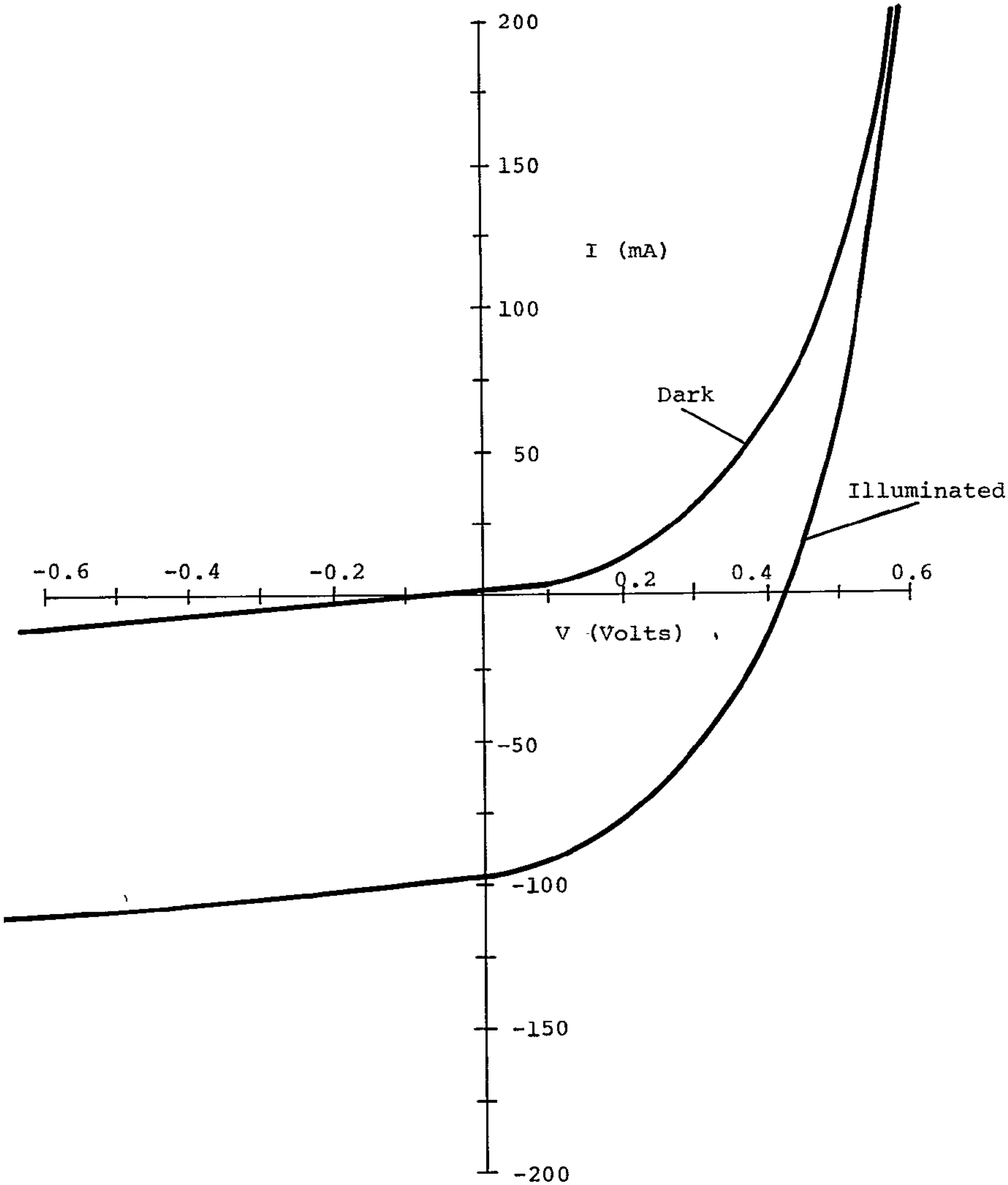

CONTRACT # NAS 5-11585 FINAL REPORT Exhibit 9

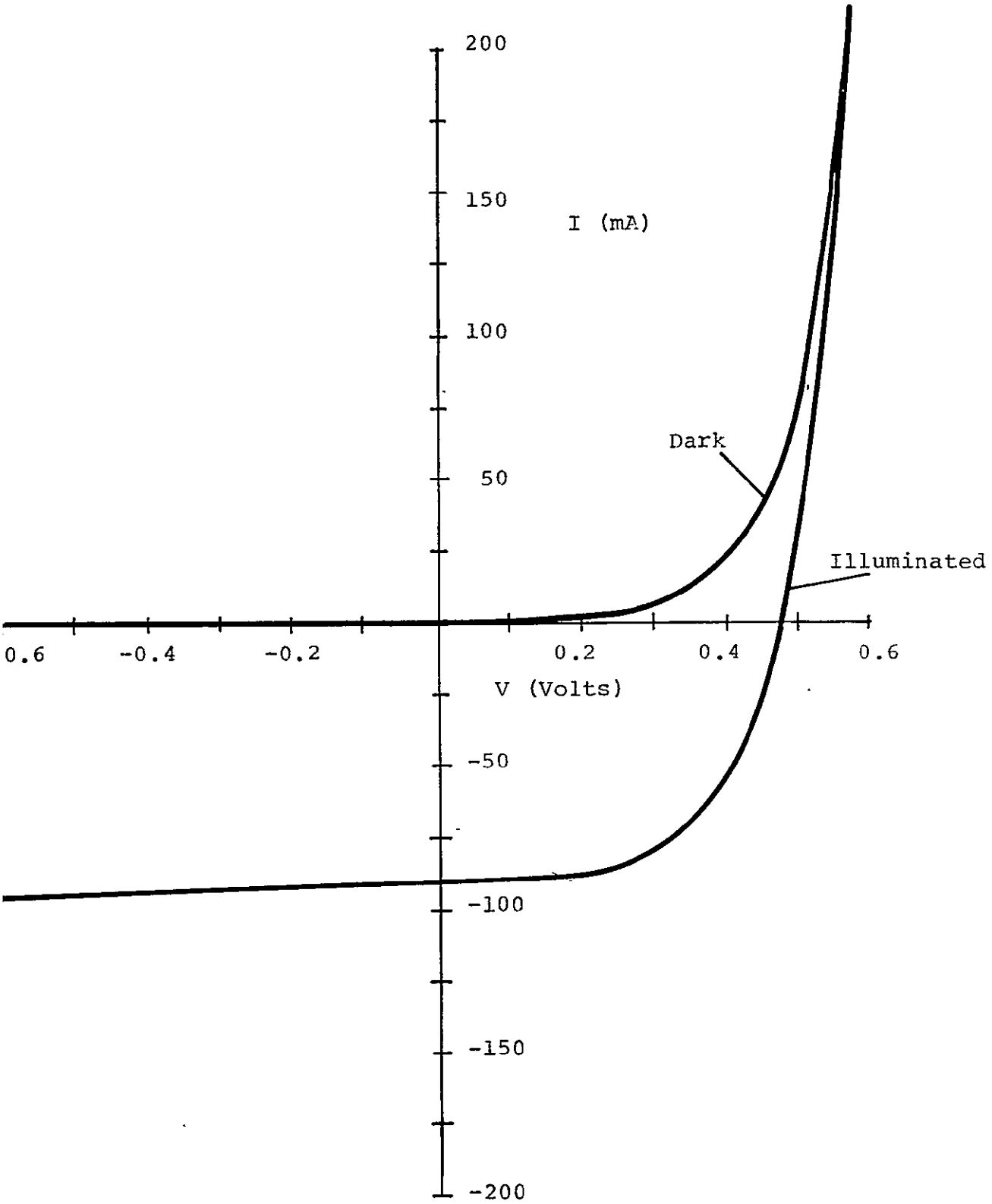

CONTRACT # NAS 3-11535 FINAL REPORT EIC #90

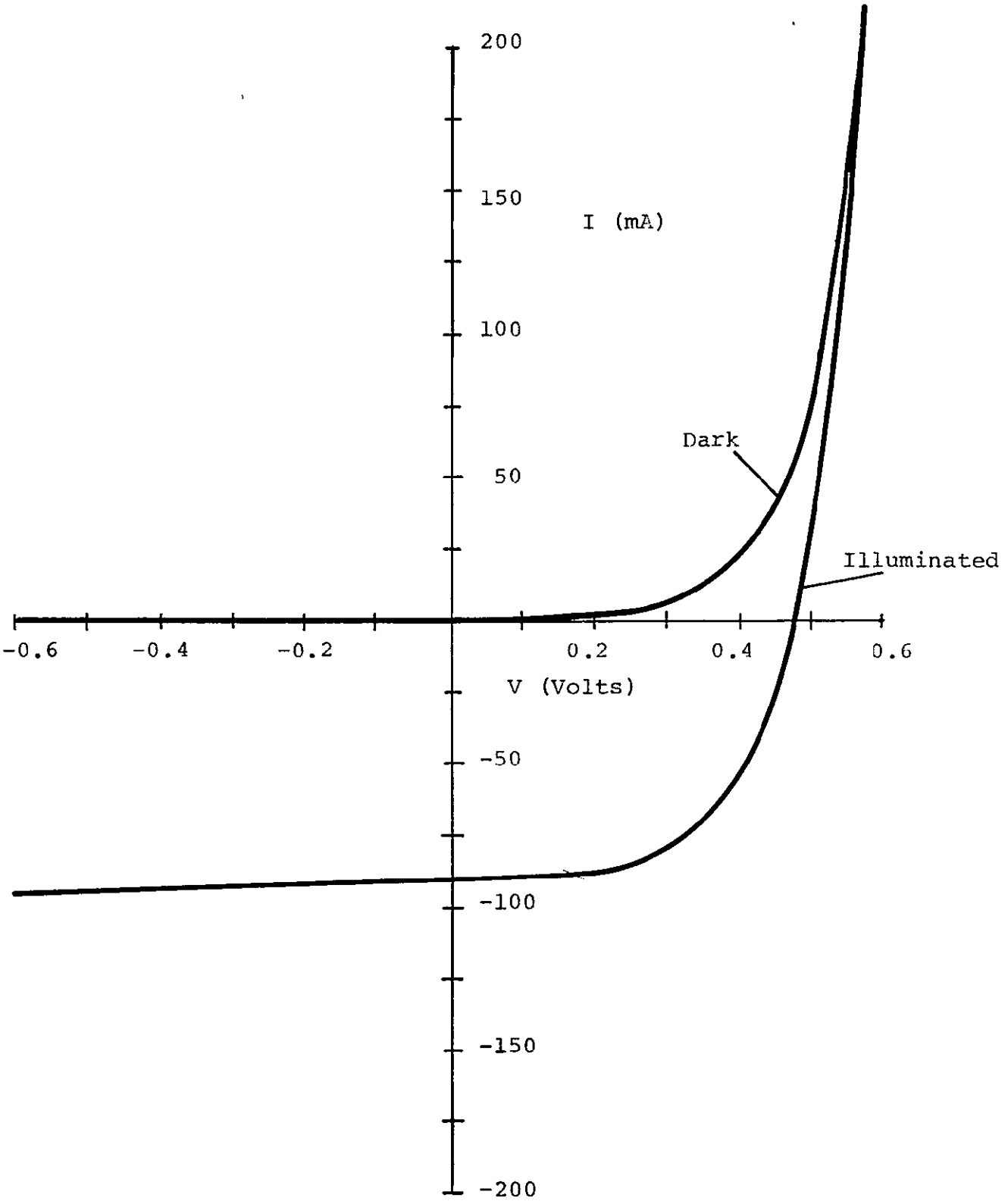
200
150
I (mA)
100
Dark
50
Illuminated
-0.6
-0.4
-0.2
0.2
0.4
0.6
V (Volts)
-50
-100
-150
-200

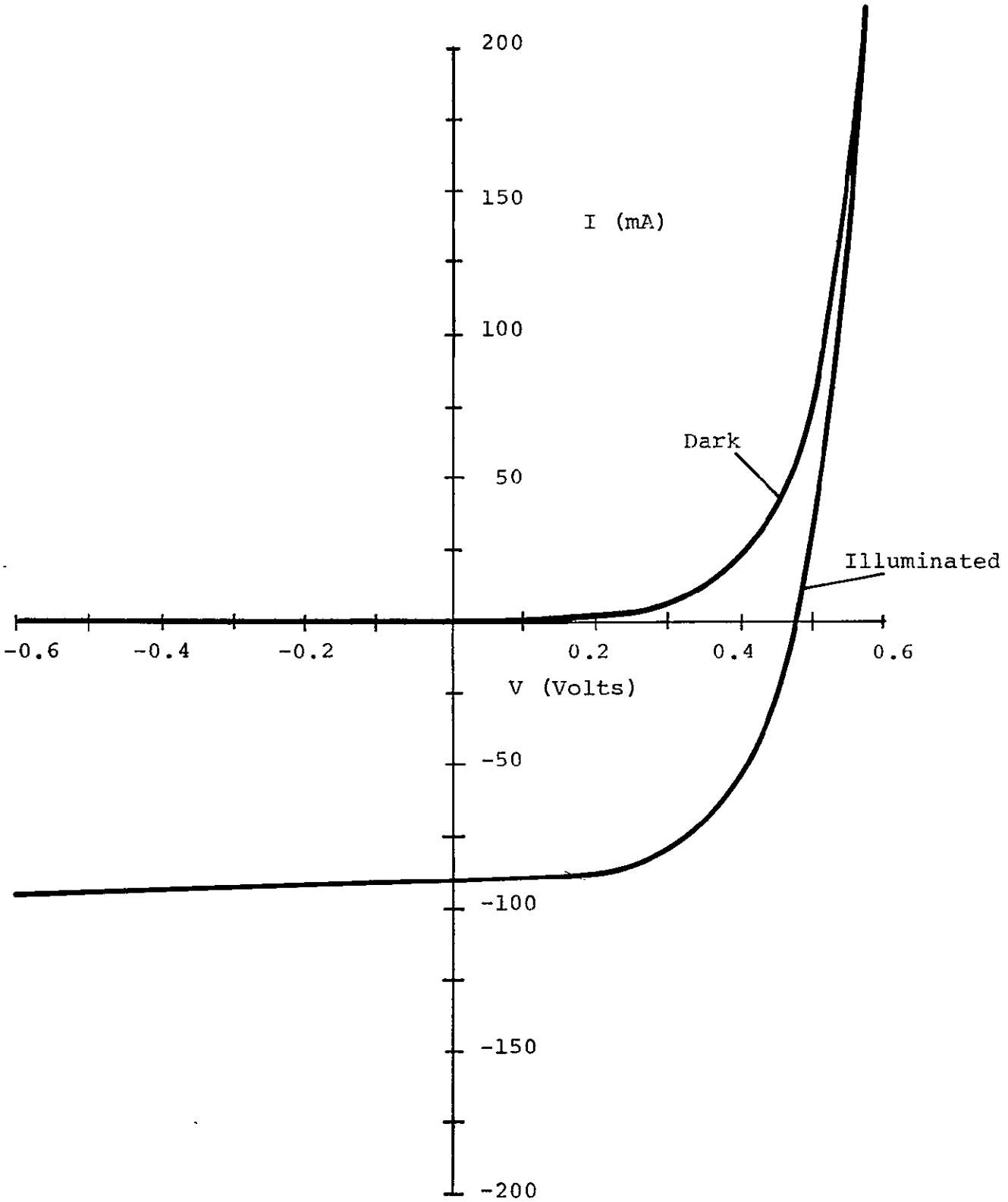
200
150
I (mA)
100
Dark
50
Illuminated
-0.6
-0.4
-0.2
0.2
0.4
0.6
V (Volts)
-50
-100
-150
-200

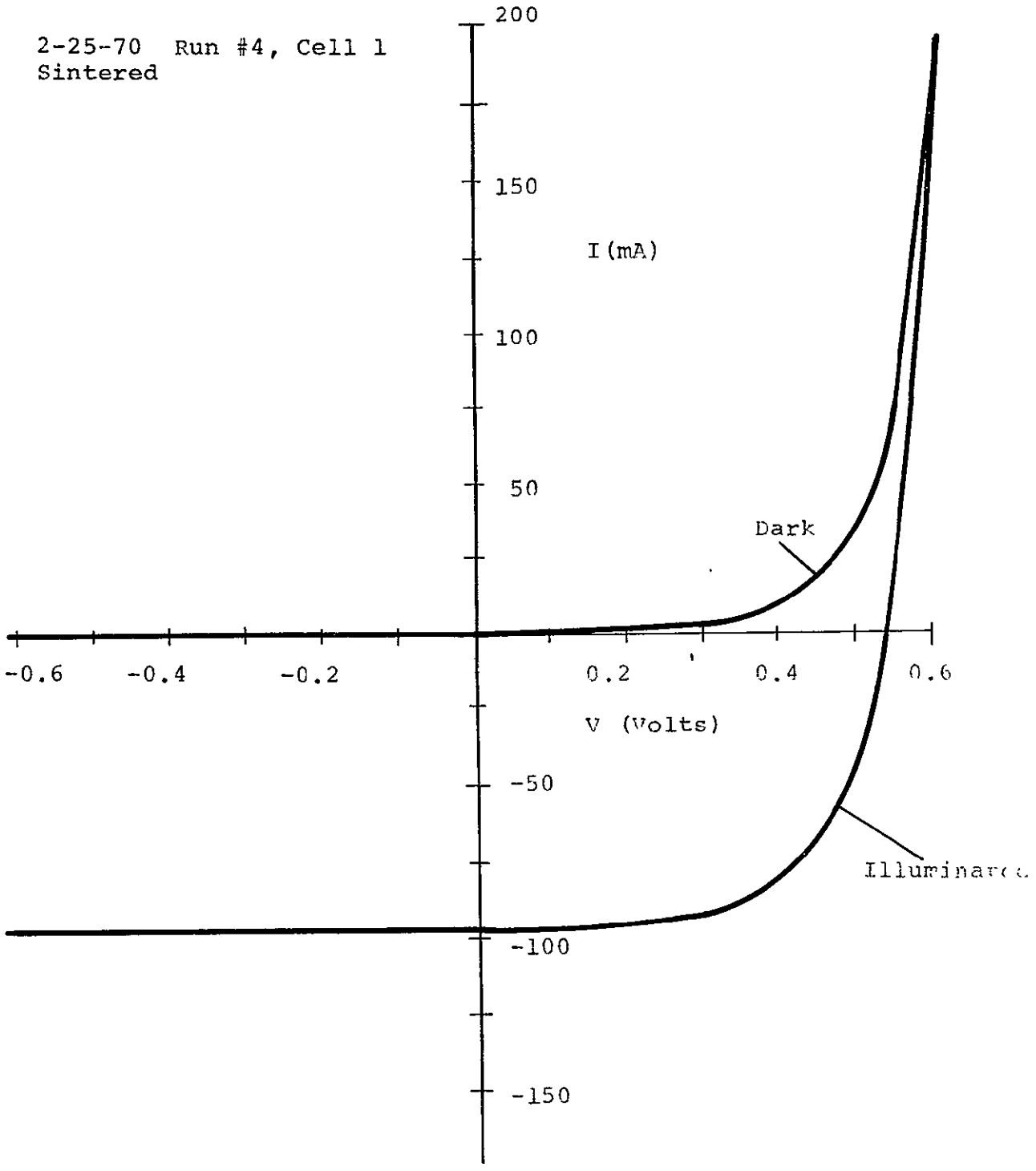
2-25-70 Run #4, Cell 1
Sintered
200
150
I(mA)
100
50
Dark
-0.6
-0.4
-0.2
0.2
0.4
0.6
V (Volts)
-50
Illuminated
-100
-150

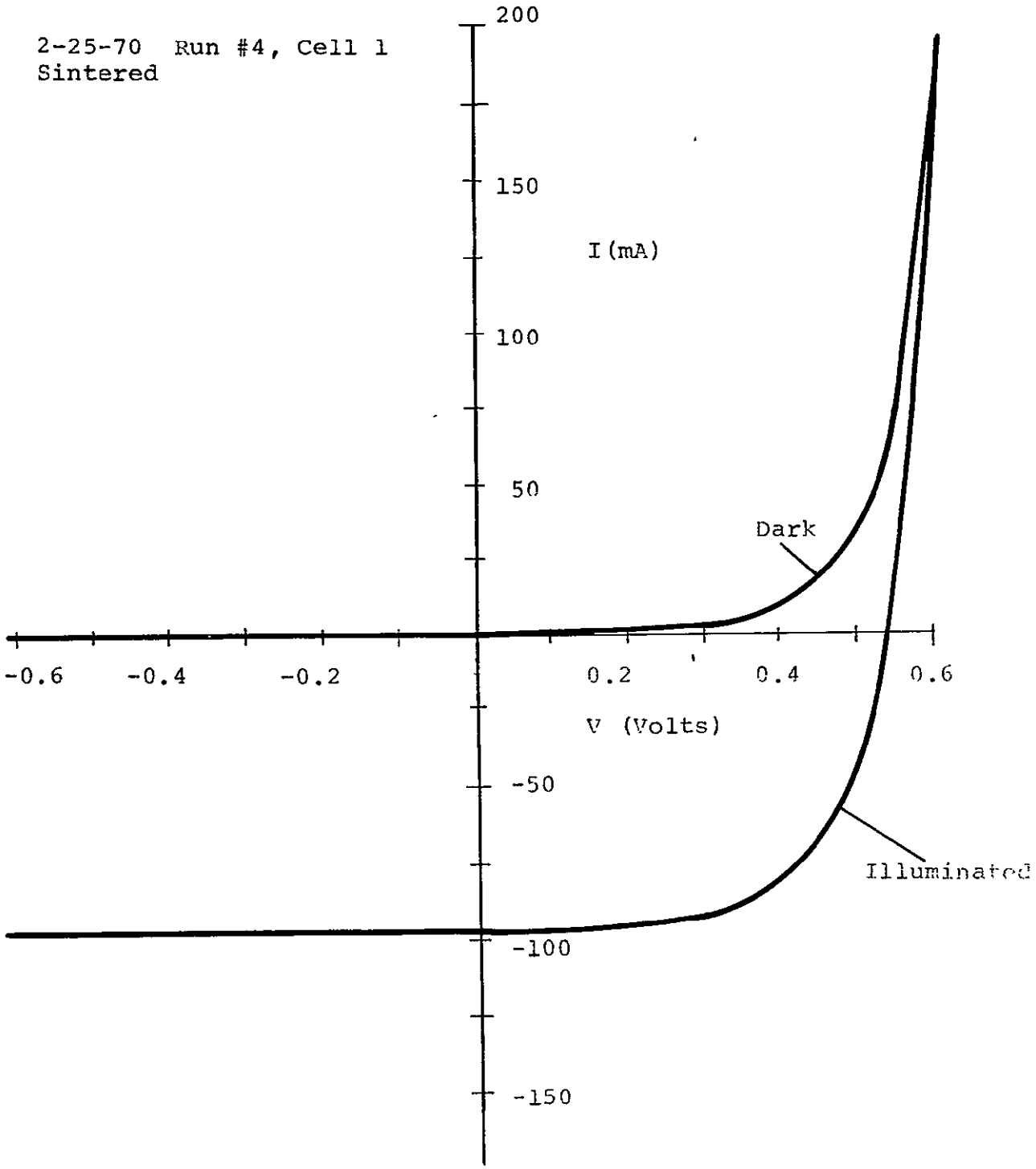

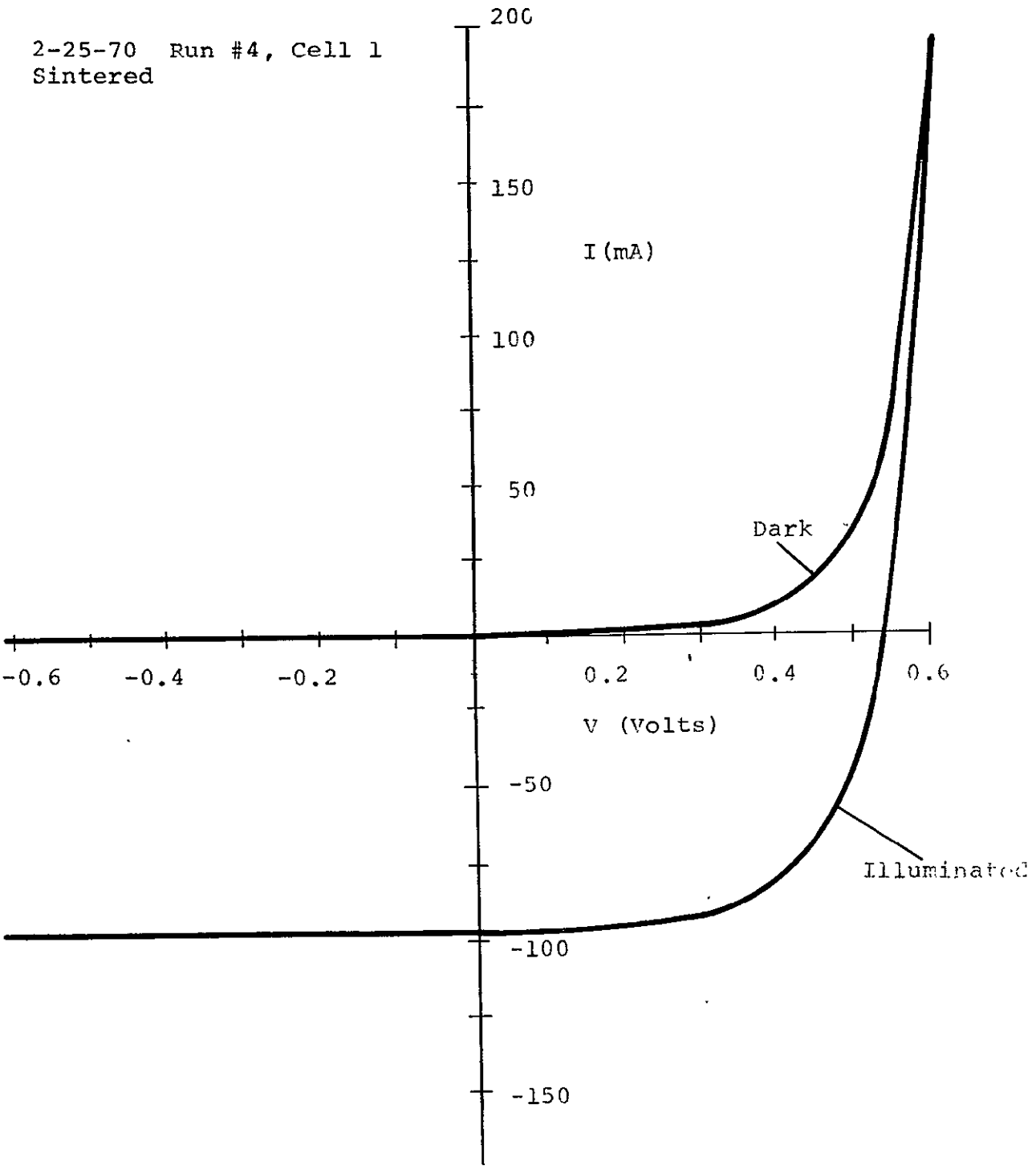

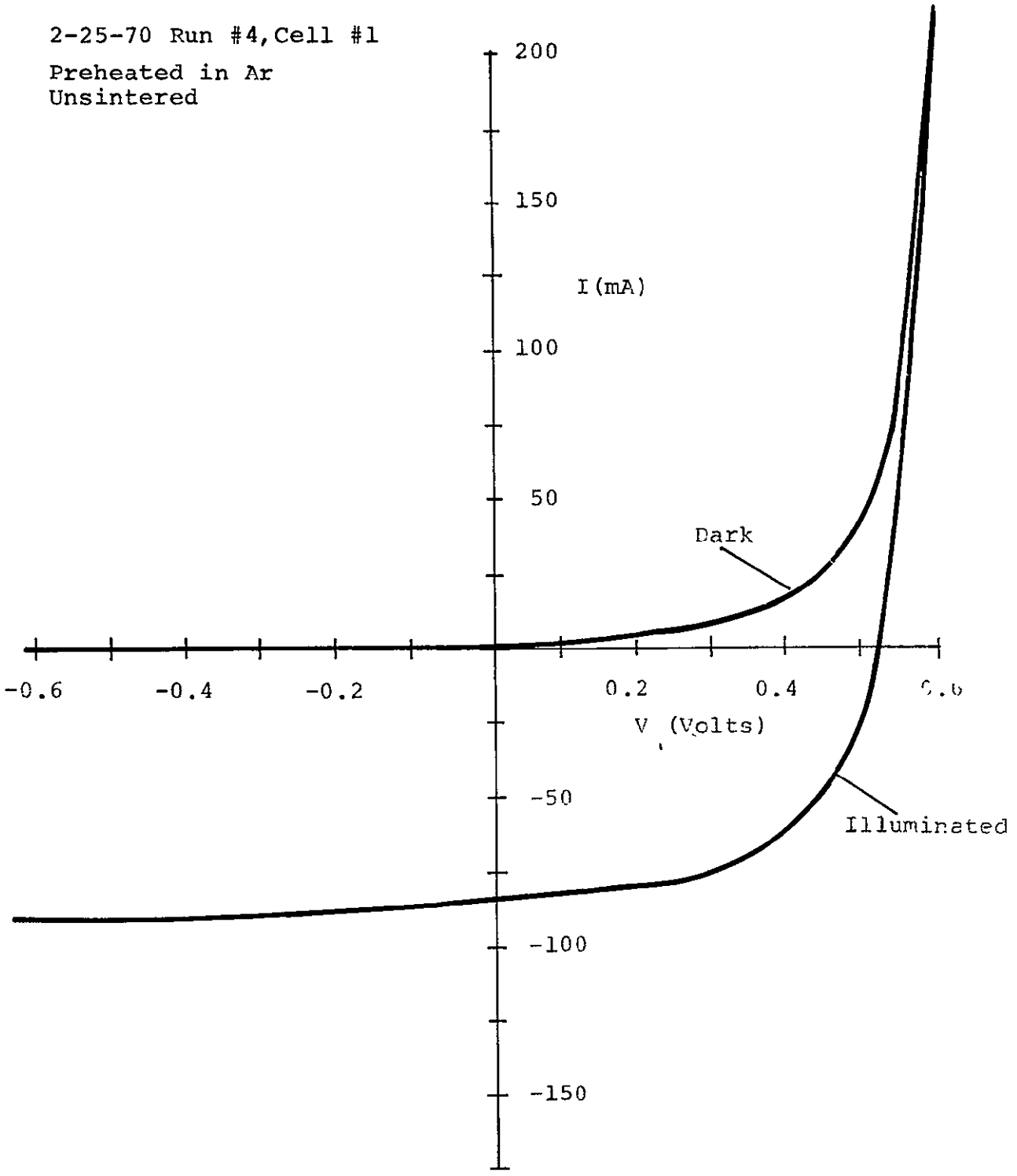
2-25-70 Run #4, Cell #1
Preheated in Ar
Unsintered
200
150
I(mA)
100
50
Dark
-0.6
-0.4
-0.2
0.2
0.4
V (Volts)
-50
Illuminated
-100
-150

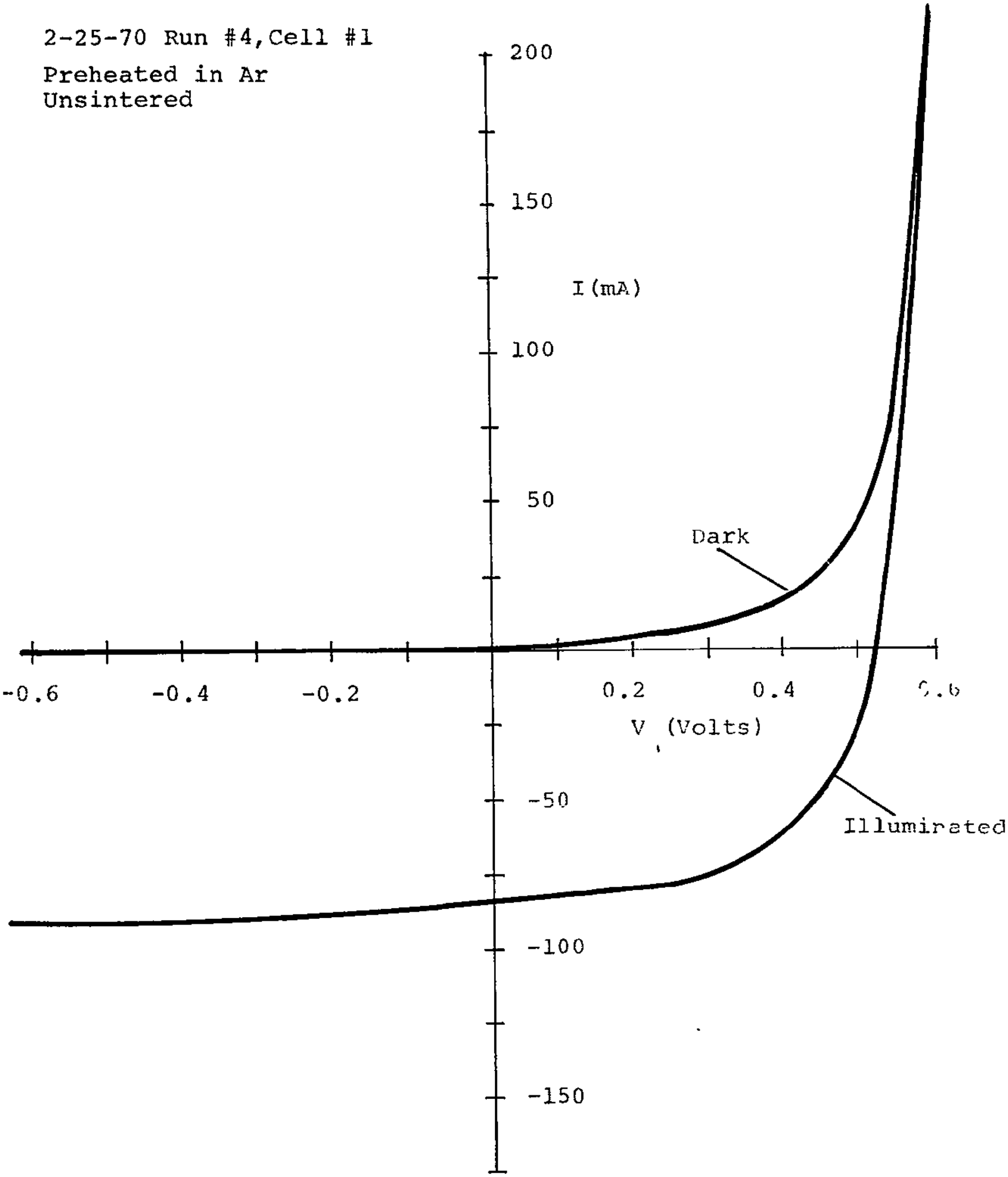

CONTRACT # NAS 5-11595 FINAL REPORT FIG #10A

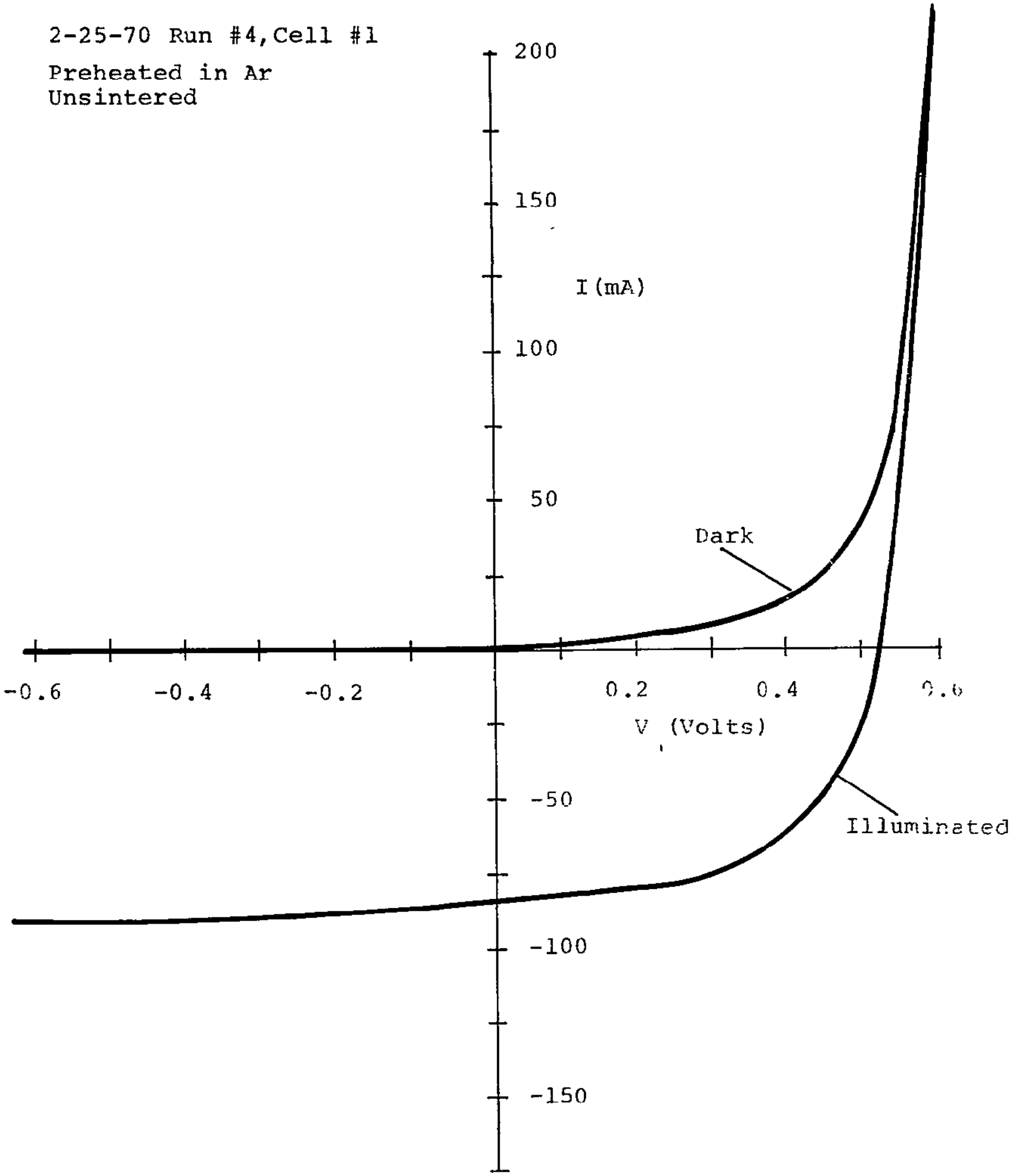

Contract #NAS 5-11595 Final Report Fig #10 A

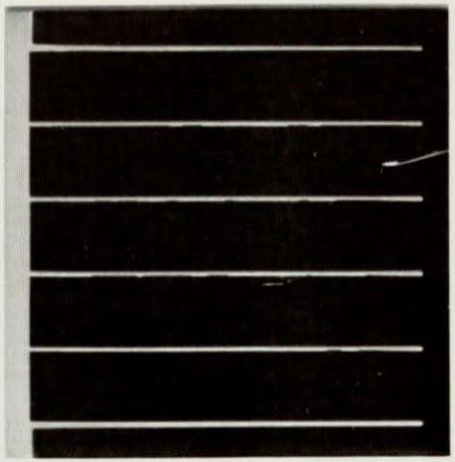

CONTRACT #NAS 5-11595 FINAL REPORT FIG #11

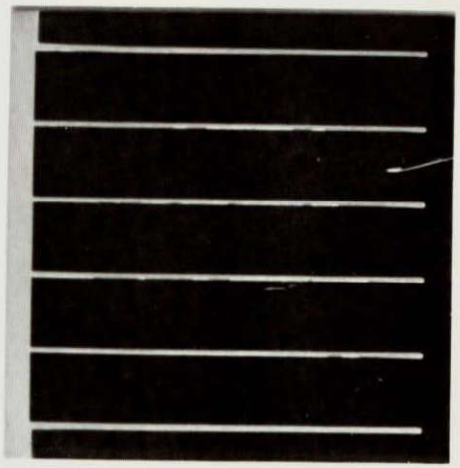

CONTRACT # NAS 5-11595 FINAL REPORT FIG # 11

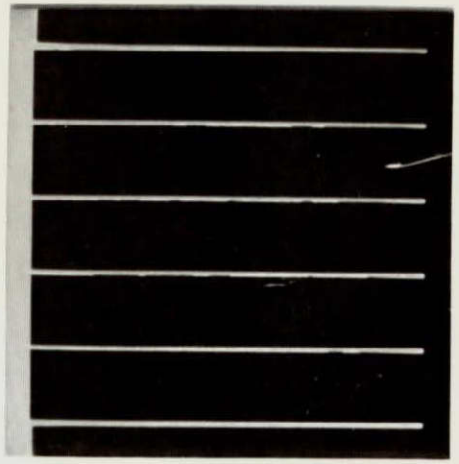

CONTRACT # NAS 5-11595 FINAL REPORT FIG # 11

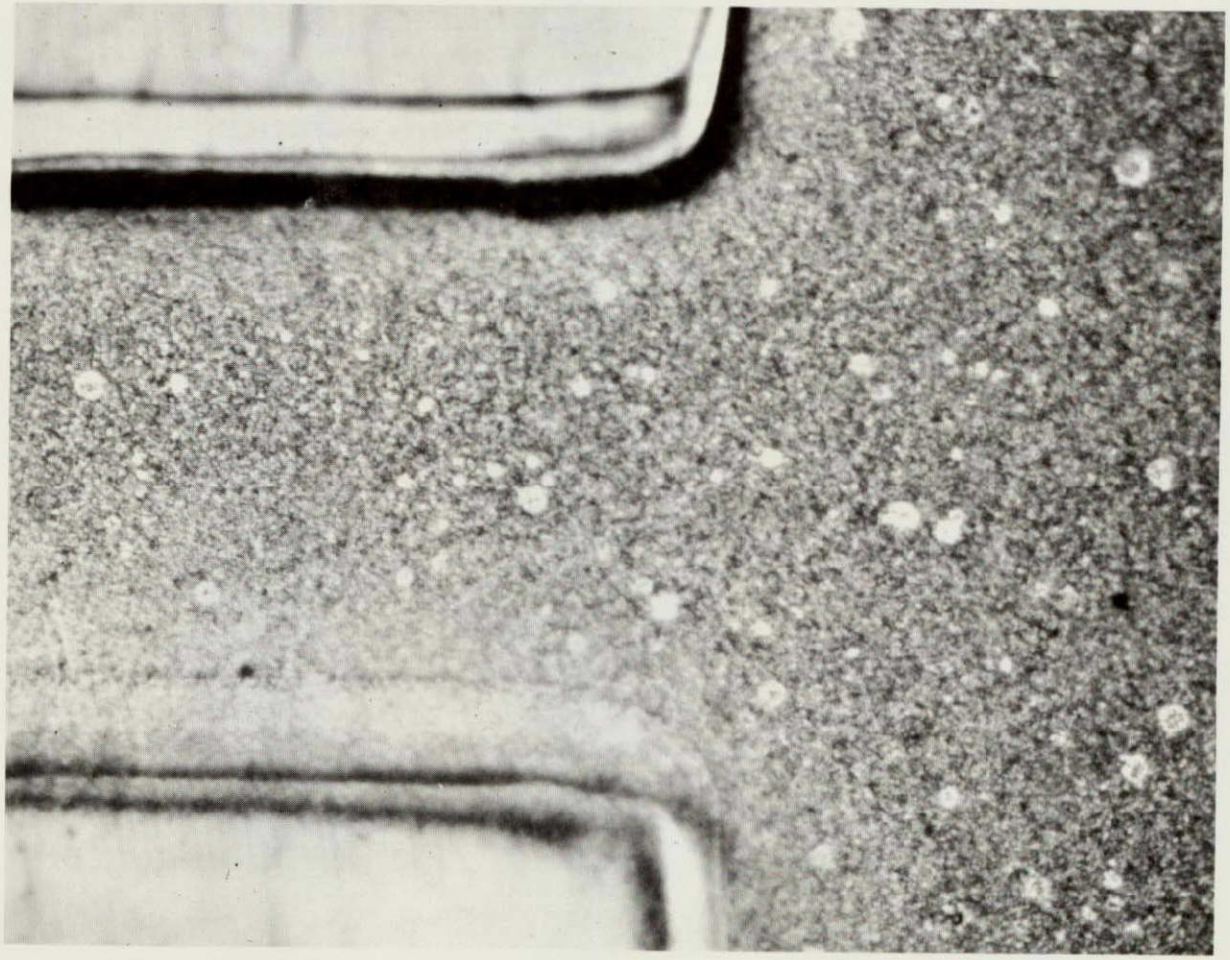

CONTRACT # NAS 5-11595 FINAL REPORT FIG #12

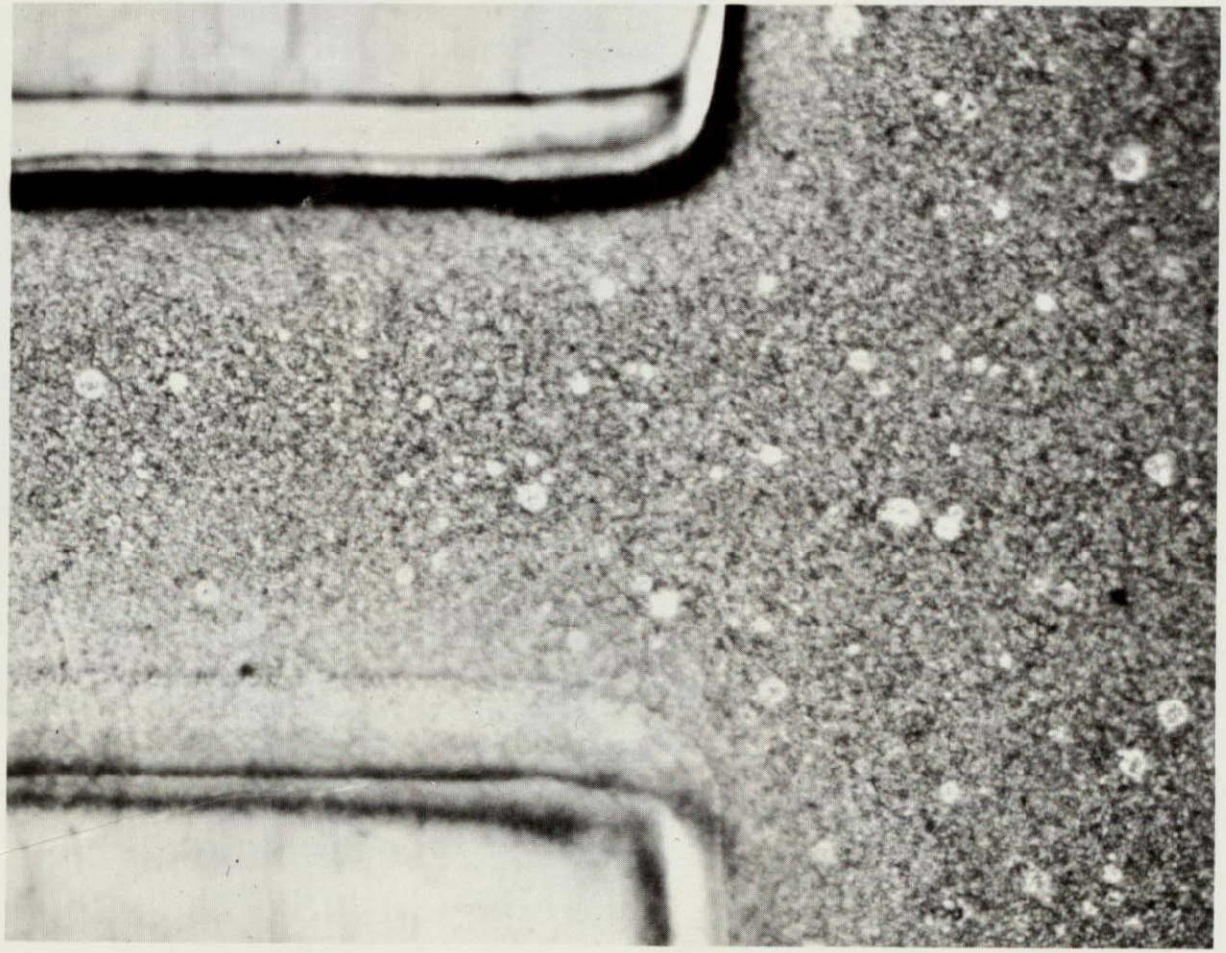

CONTRACT # NAS 5-11595 FINAL REPORT FIG # 12

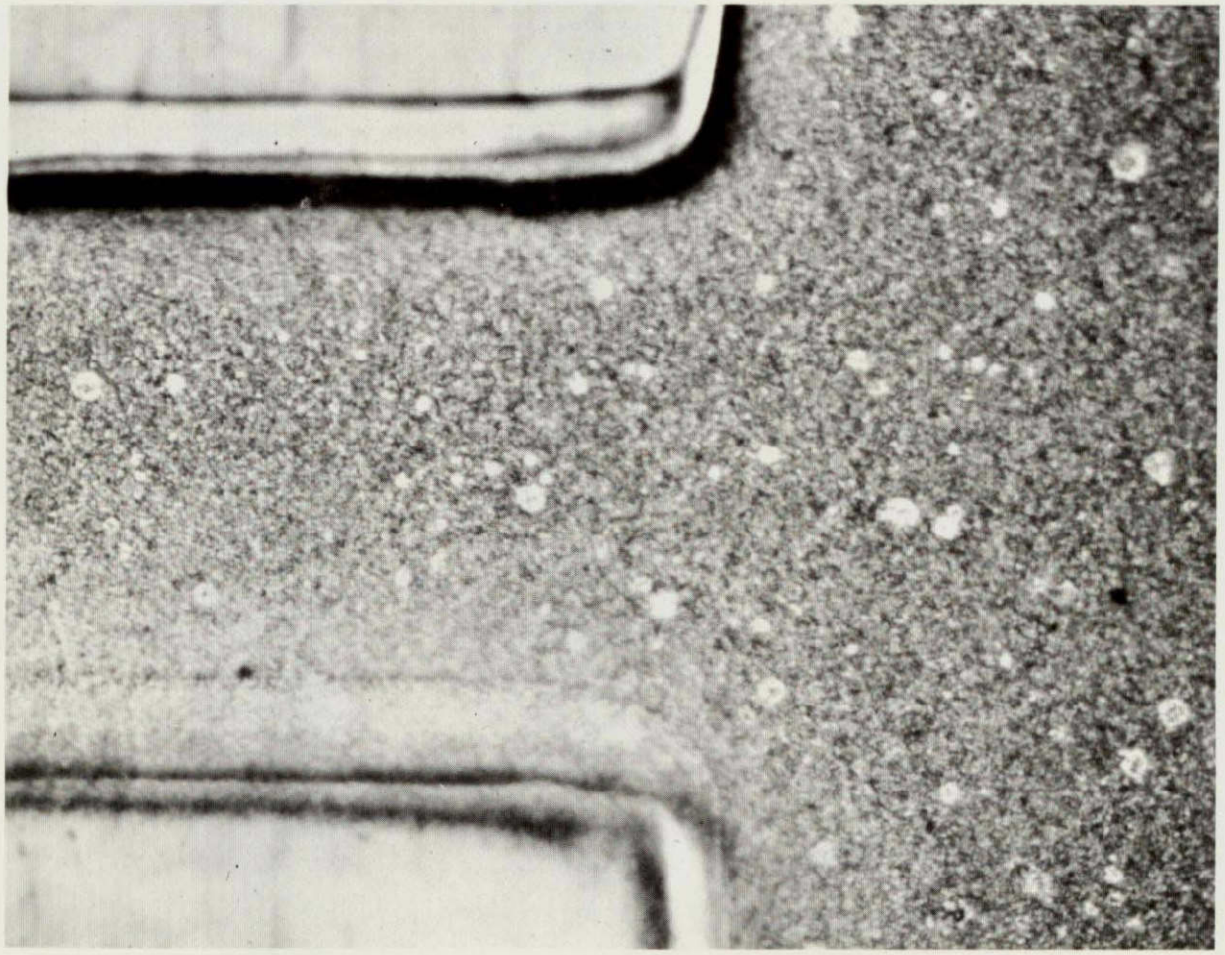

CONTRACT # NAS 5- 11595 FINAL REPORT FIG # 12

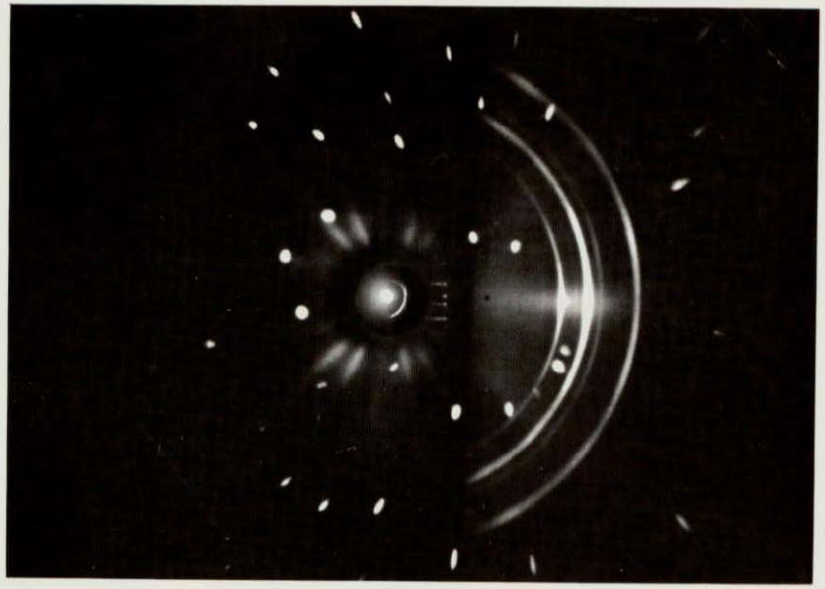

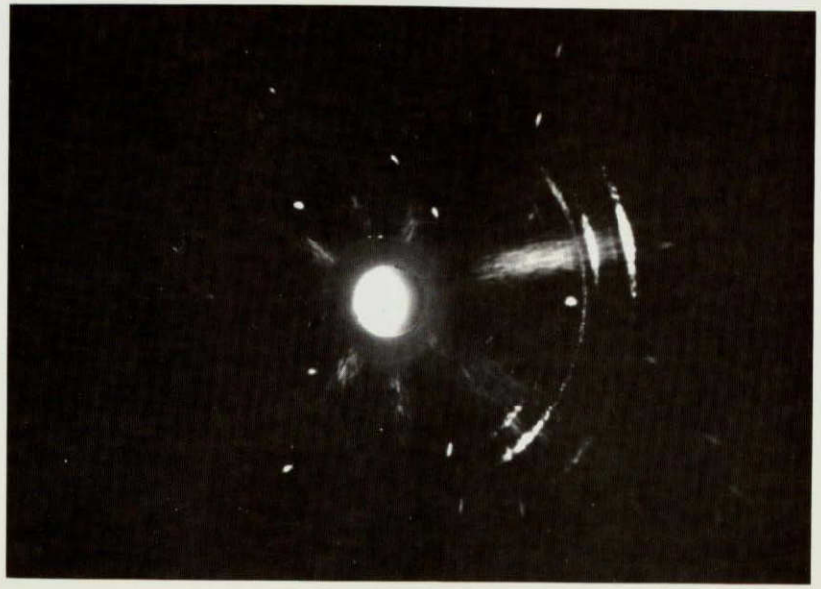

CONTRACT # NAS 5-11595 FINAL REPORT FIG # 13

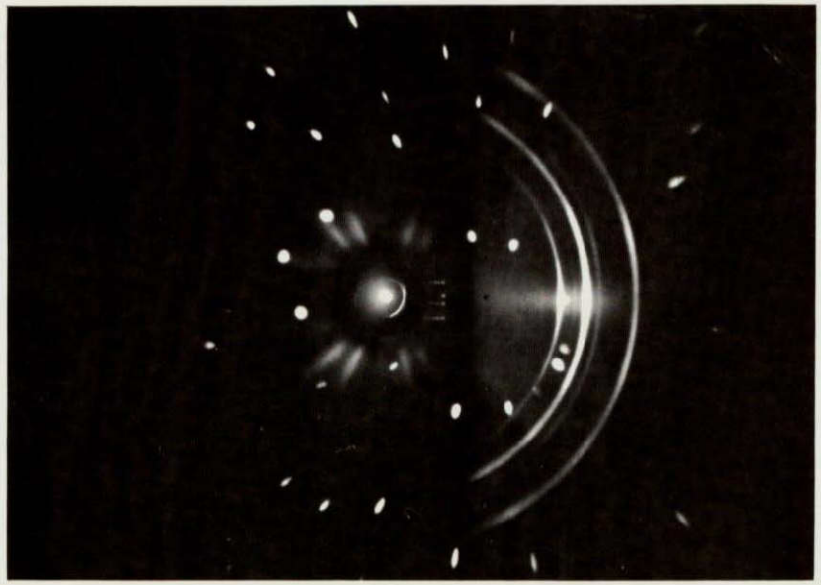

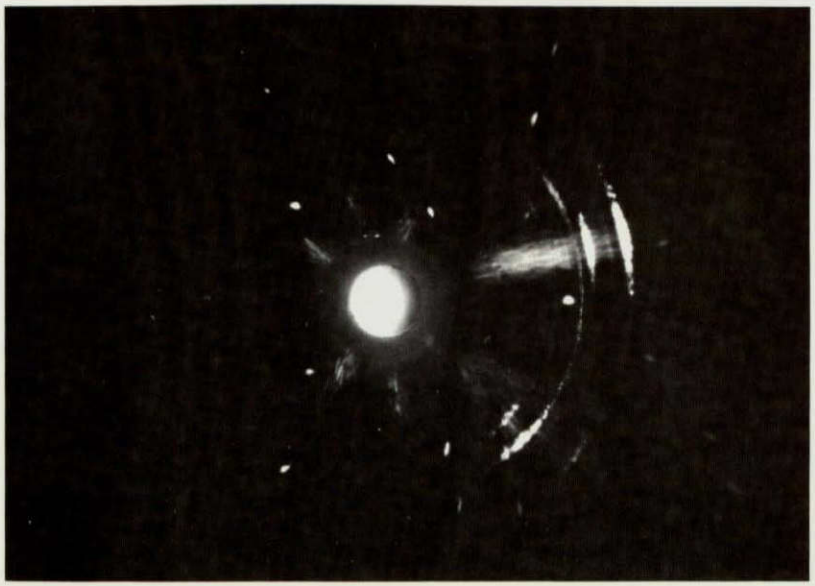

CONTRACT # NAS 5-11595 FINAL REPORT FIG # 13

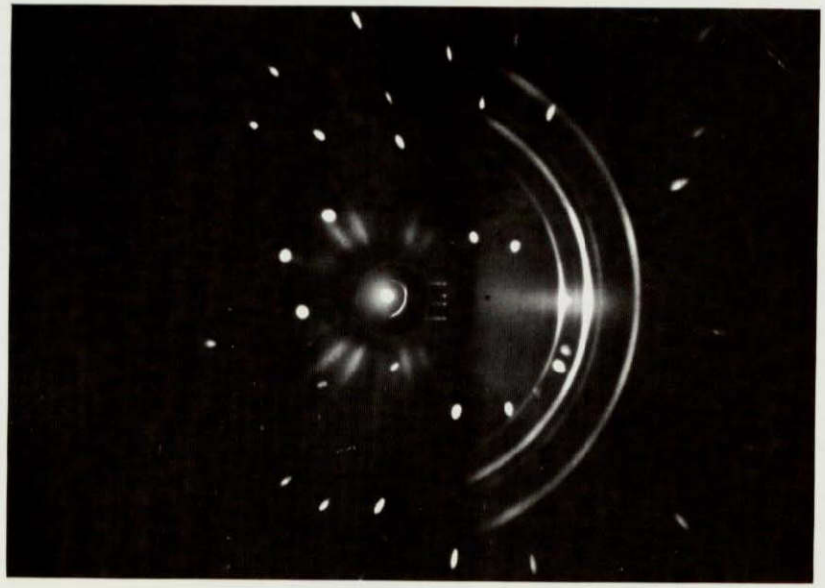

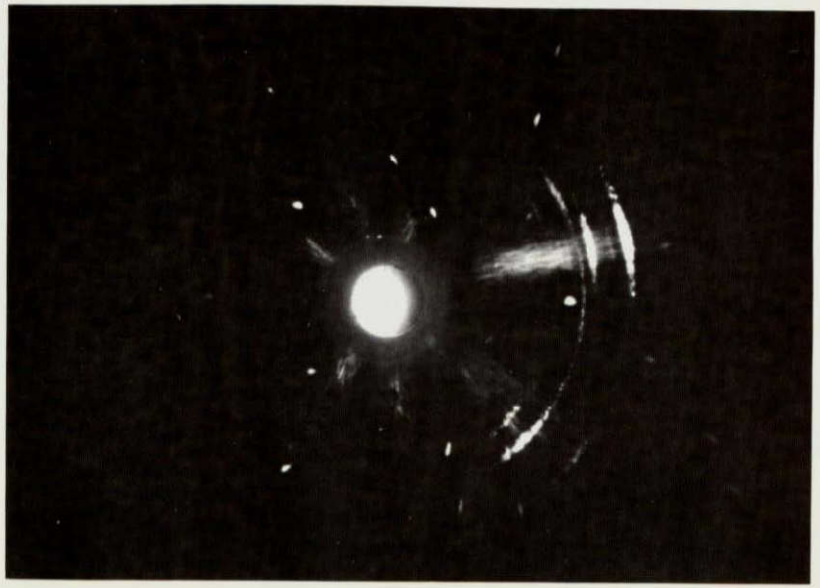

CONTRACT # NAS 5-11595 FINAL REPORT FIG # 13

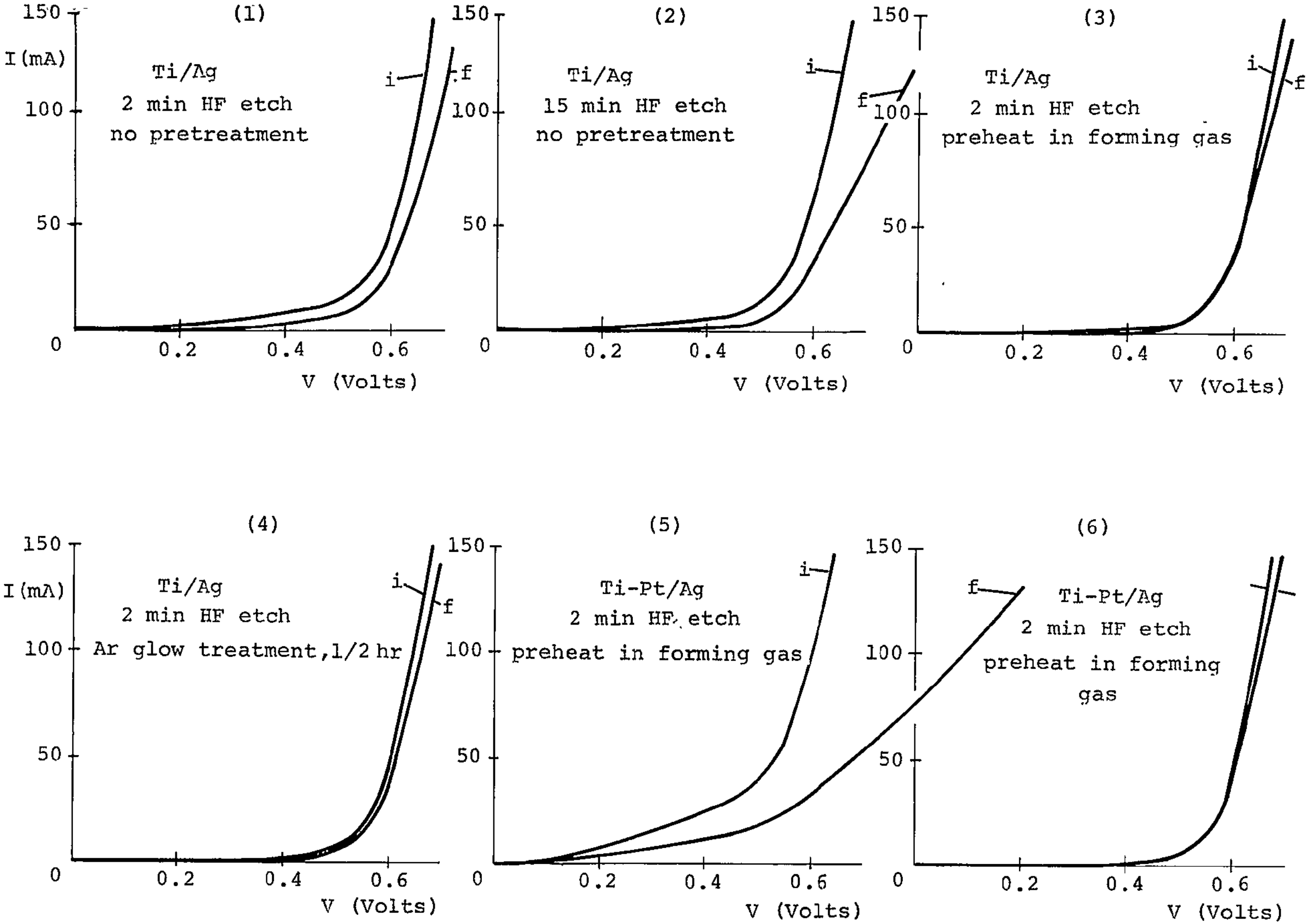

Contract # NAS [illegible] Final Report Fig #14

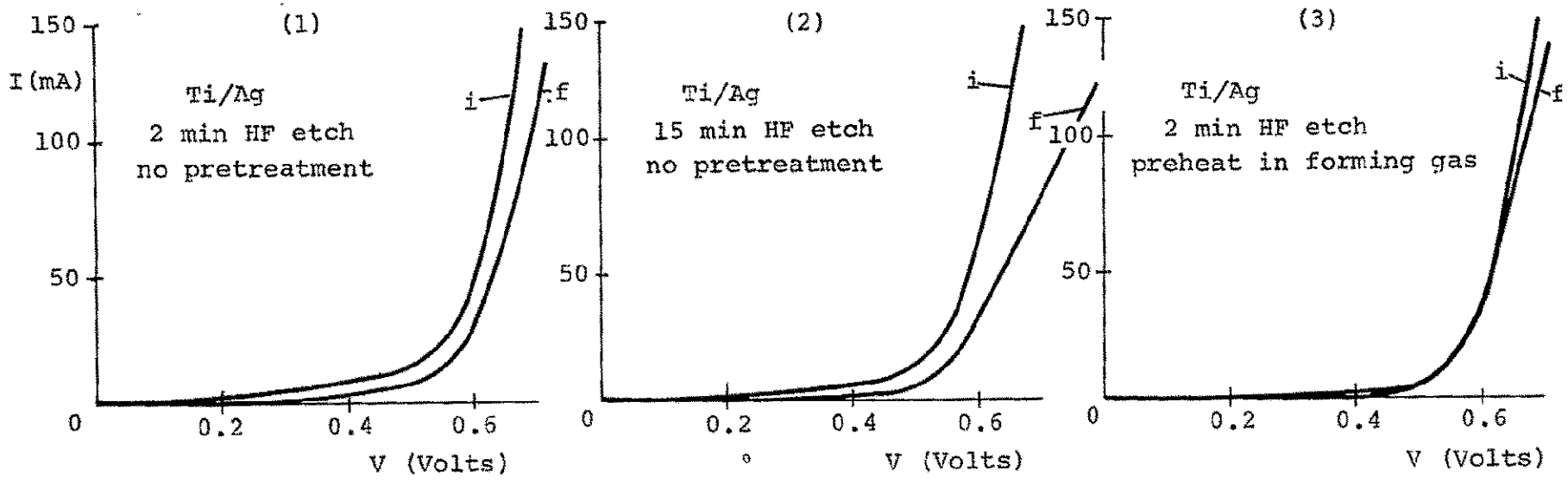

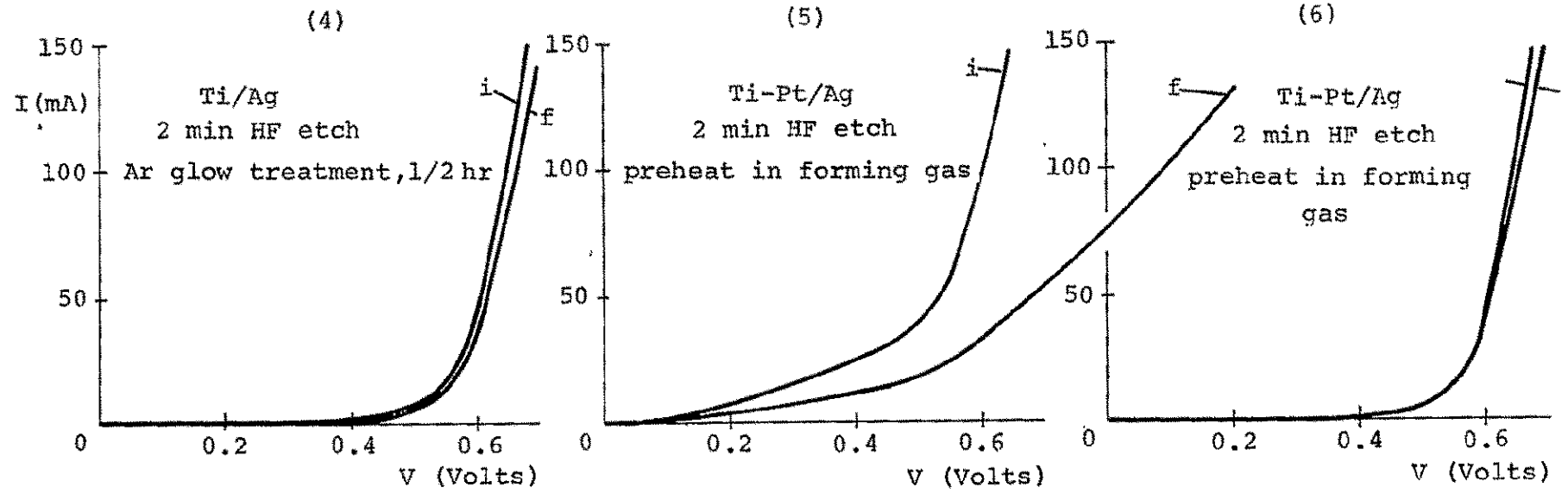

Contract # NAS 5-11595 FINAL REPORT FIG # 14

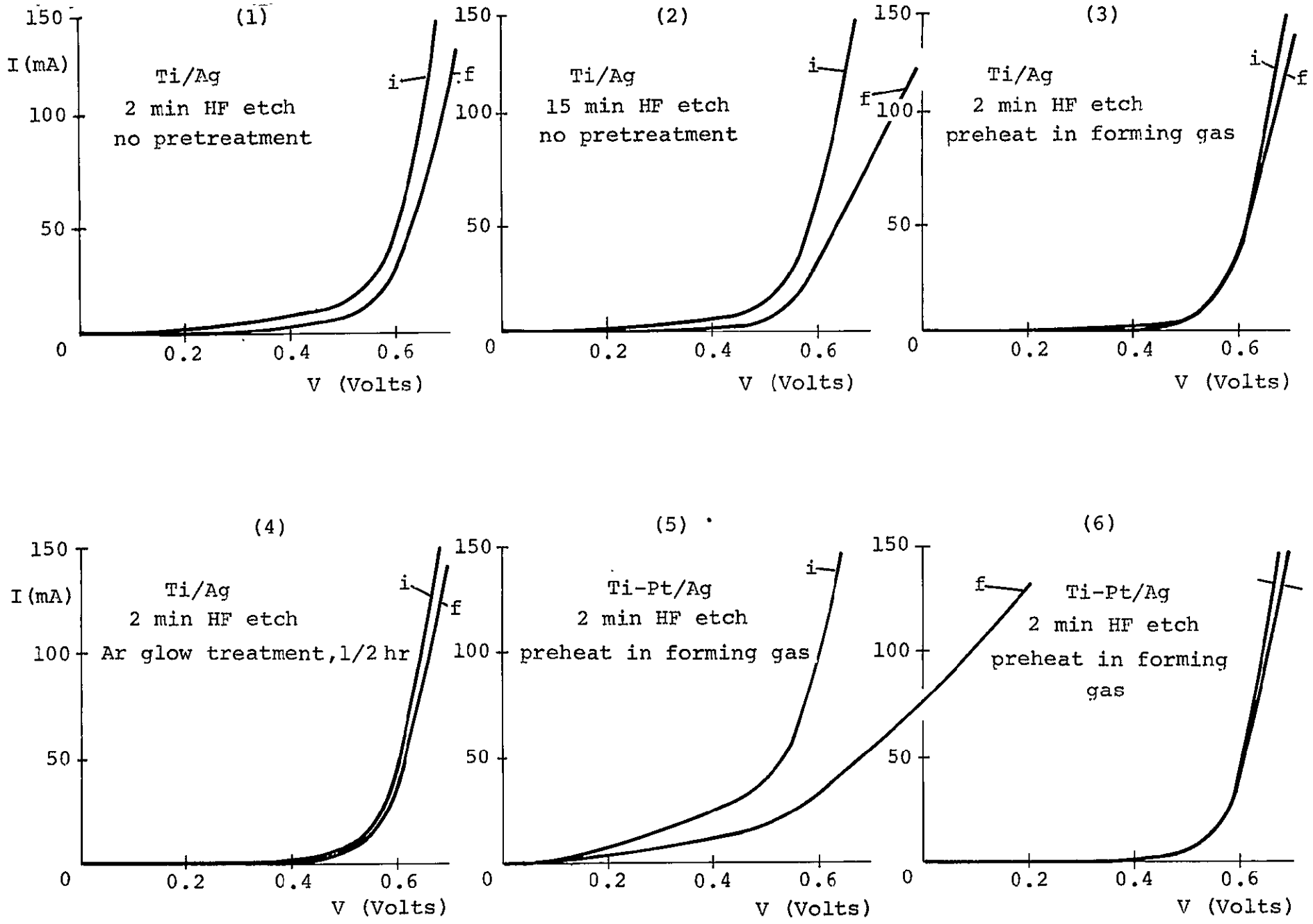

CONTRACT # NAS 5-11595 FINAL REPORT FIG # 14

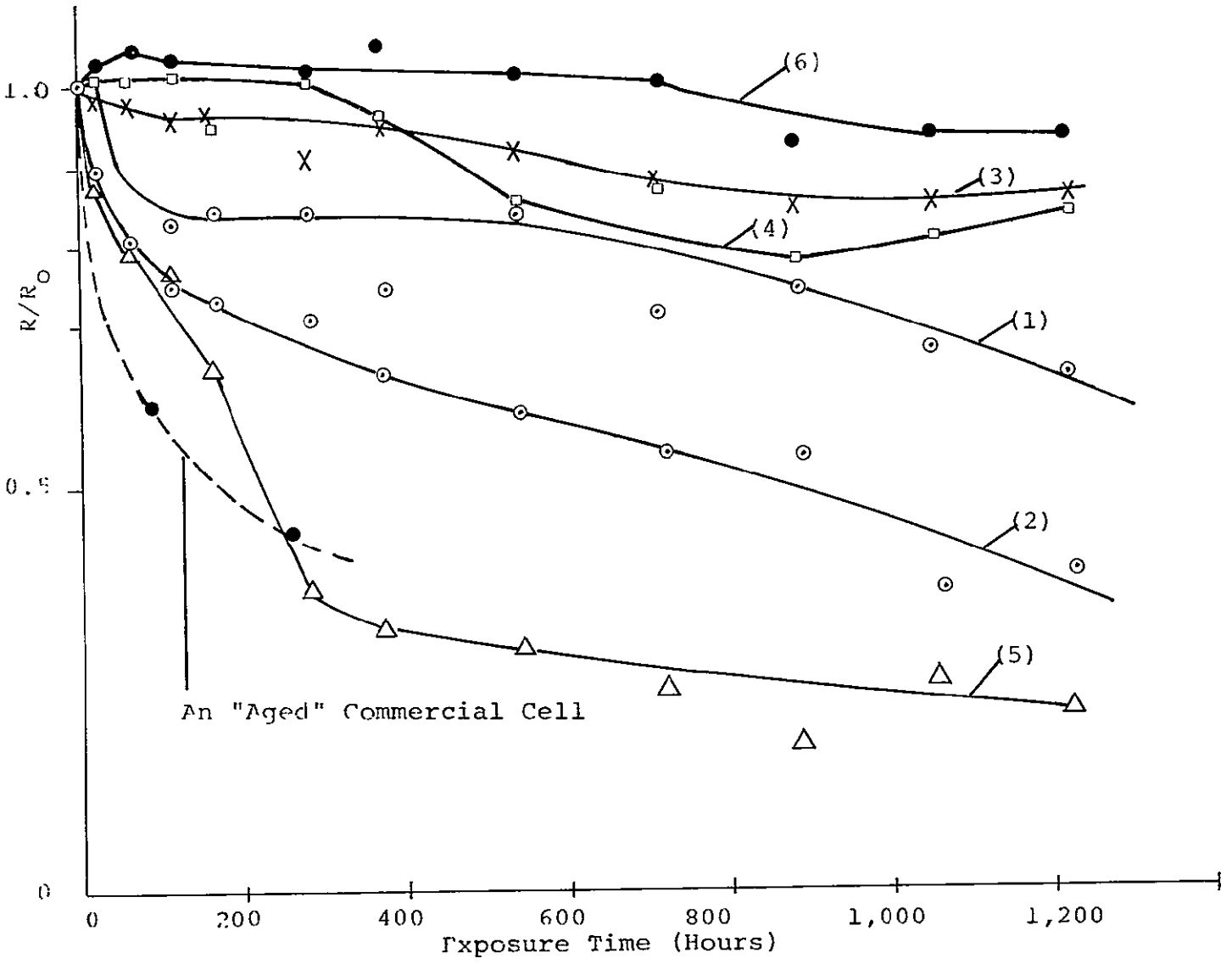

Contract #NAS 5-11595 Final Report Fig #15

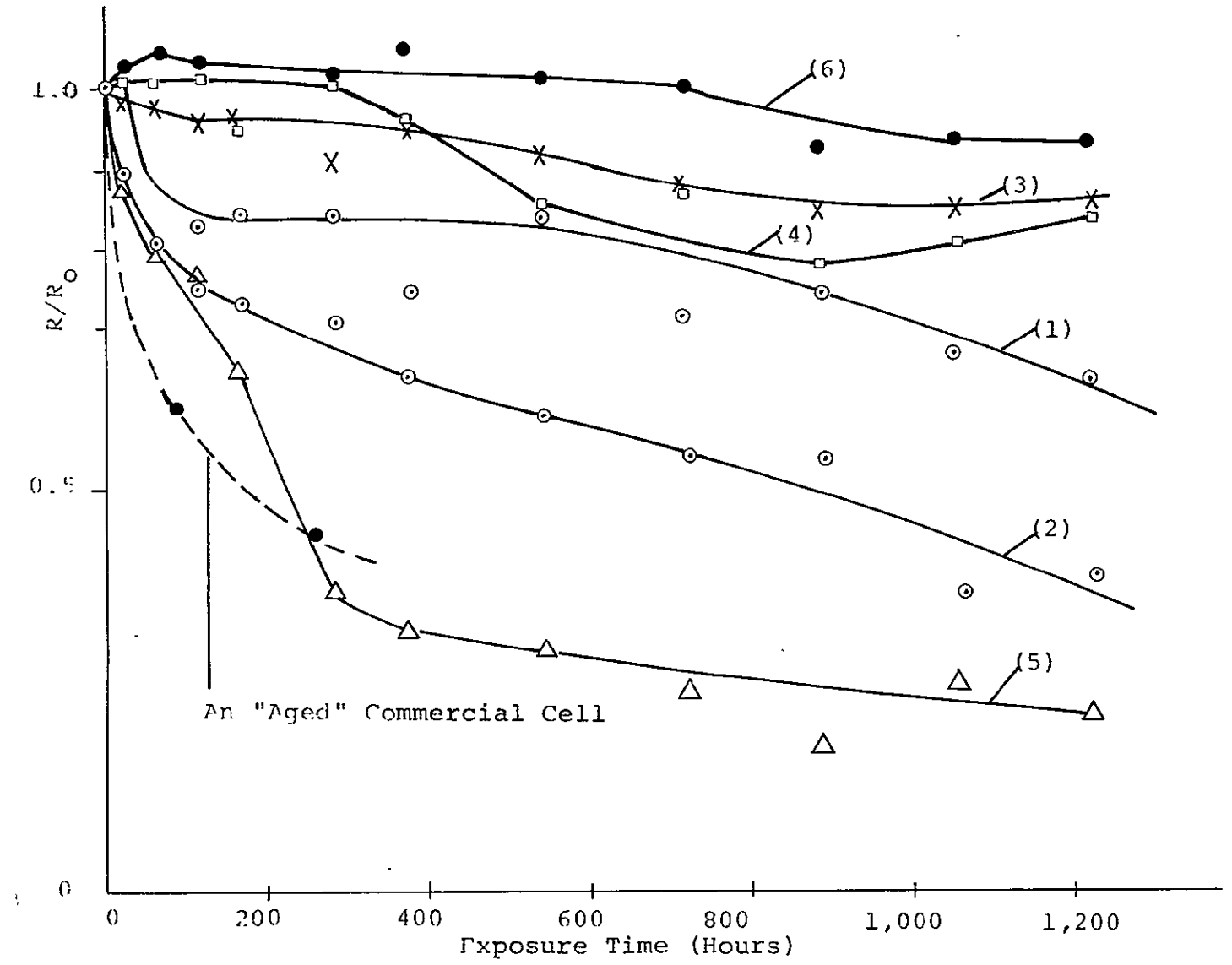

Contract # NAS 3-11585 Final Report Fig. #15

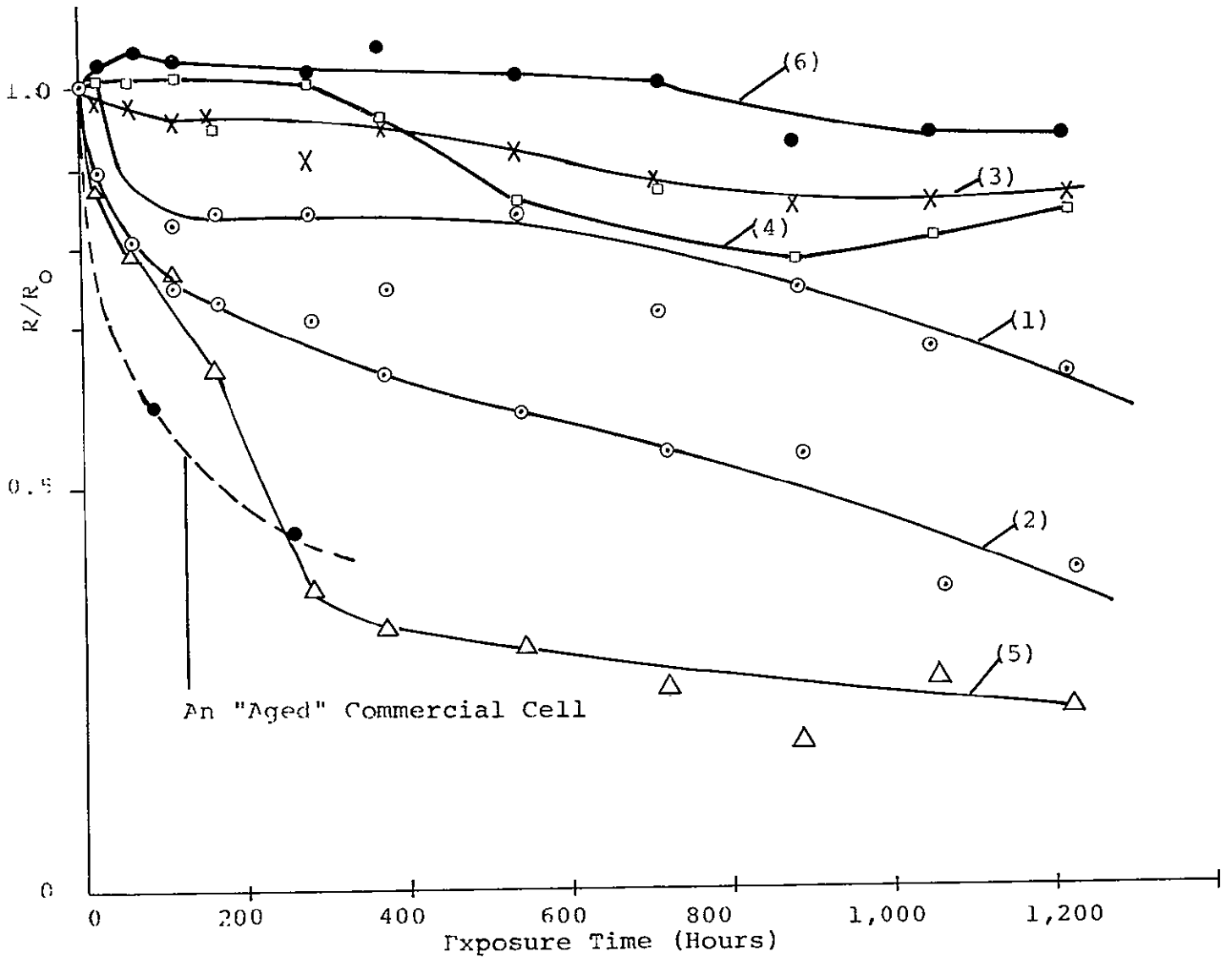

Contract # NAS 5-11585 Final Report Fig. #15